UNDER THE SEA(BED):

SENSITIVITY ANALYSIS OF THE NON-MOBILE REFERENCE LEVEL FOR HIGH-VOLTAGE CABLES IN THE NORTH SEA

MASTER THESIS

M. (Maarten) Verboom
Enschede, November 10, 2024

Supervisors:

Dr. Ir. P.C. (Pieter) Roos	University of Twente
Dr. Ir. J.J. (Jebbe) van der Werf	University of Twente
Dr. Ir. B.J. (Barend) Bentvelsen	TenneT
Ir. D.W. (Wino) Snip	TenneT
MSc. K.J. (Koen) van der Laan	WaterProof

MELODY

WATER PROOF

TenneT

UNIVERSITY OF TWENTE.

Cover picture: Most Recent Seabed level of Dutch North Sea, obtained from Deltares OPeNDAP repository

PREFACE

This thesis marks the end of my MSc in Civil Engineering and Management at the University of Twente in the direction of River and Coastal Engineering. This research was done in collaboration with TenneT and WaterProof within the Melody Research Project to obtain more knowledge about the uncertainties within the method for obtaining the Non-Mobile Reference level. During this thesis project, I learned a lot about every aspect involved in cables and energy from the North Sea.

This all would not have been possible without the help of my supervisors. From TenneT, I want to thank Barend Bentvelsen and Wino Snip, who helped me around within TenneT and helped me with exciting discussions and their expert knowledge in cable installation. Besides helping me with guidance, getting me in touch with the right people, and providing me with helpful feedback, they let me wander into the world of energy transition. They gave me inspiration and motivation to finalise this thesis project. Due to discussions with Barend and Wino, I really obtained the feeling that this research project is an addition.

I also want to thank all the people within WaterProof for their open attitude, help and inspiration. Especially Koen van der Laan and Rinse de Swart helped me understand their method's programming and guided me through all the data involved in this thesis project. They welcomed me within the company and showed me all the exciting projects they were working on during the company's weekly lunch lecture.

I want to thank Pieter Roos and Jebbe van der Werf from the University of Twente for their guidance and support during this thesis. If there were problems, Pieter Roos always made time for me to have a discussion or chat. With all his written feedback, my thesis improved significantly. Jebbe van der Werf gave insightful feedback and let me think twice about what I wrote.

Next to my supervisors, I want to thank all the people/instances involved in this project; there are way too many to name them all. Still, without Arno Meurink from the Dienst der Hydrografie, I would not have been able to obtain high resolution surveys from the source itself. Thank you for that.

Lastly, I want to thank my family and friends. For their support and sometimes distraction, a special thanks to my fellow Civil Engineering students in the basement of the Horst, who motivated me to continue and with whom I could always ask a question or have a chat.

With this sensitivity analysis of the Non-Mobile Reference level for high-voltage cables in the North Sea, I hope that TenneT can improve its understanding of the Non-Mobile Reference level, and the uncertainties involved so that it can reduce societal costs for installing cables under the seabed.

Hopefully, you will enjoy reading this thesis!

Maarten Verboom

Enschede, November 2024

SUMMARY

More and more offshore wind farms are installed in the Dutch North Sea, with plans to expand capacity fifteenfold by 2050. The electricity generated is transmitted to the onshore grid via submarine cables, which are lowered into the seabed to protect them against external threats. To account for seabed mobility, the cables are lowered relative to a Non-Mobile Reference level (NMRL), designed to maintain minimum protective coverage throughout the cable operation phase and minimise life cycle costs, even when the seabed changes due to sand wave migration. However, this 3D reference level involves uncertainties that have previously not been thoroughly evaluated and quantified.

Therefore, this study aimed to evaluate the uncertainties in the Non-Mobile Reference level determined by WaterProof in the offshore seabed of the Dutch North Sea by testing various settings of the method and using various bathymetric inputs. For this, bathymetric data was collected, reprojected, and corrected from four different data sources, of which three were used to establish the NMRL in two different locations. With four tested settings and four tested various methods for handling and using input data, this study tried to evaluate uncertainties within the NMRL.

The NMRL established with WaterProof's method showed sensitivity to parameter setting changes. The most sensitive parameter in WaterProof's method is the percentile setting, selecting the representative per cross-section. WaterProof's method has been shown to be sensitive to the parameters of length of and distance between cross-sections. Varying the period between surveys does slightly have an impact on the NMRL, but since it is easy to implement, it is recommended to include the monthly accuracy of the method as this reduces the uncertainty. During these experiments, it was also found that there is almost no difference in the moving average depth per 5 m or 25 m cable relative to the MRSL and the NMRL. This implies that there is no need to obtain the moving average depth of 5 m; instead, the moving average per 25 m is recommended to be used.

The three different repositories have been utilised to compare the bathymetric data. While publishing the same data, differences were found. A mean difference of up to 21 cm and a shift in the horizontal plane of 29 m were found between the repositories, seriously affecting the Non-Mobile Reference level. Due to the large differences between the bathymetric data of the repositories, it is not possible to combine the different repositories to obtain migration rates and growth rates of sand waves.

Besides using different repositories, the grid resolution and grid origin were varied. Due to the method of comparison, no quantitative conclusions can be drawn. Despite this, the NMRL was shown to be sensitive to data input. During this research, it was also found that the method of interpolation from 2D cross-sections to the 3D NMRL has limiting effects on increasing the resolution of the bathymetric data.

For further research, it is recommended that the most sensitive parameter, the percentile, is further investigated. Also, when using different repositories, the question of whether it would be possible to extrapolate the seabed found in other repositories by using the observed sand wave migration and growth rates rose. The author sees potential in this, but further research should be done to see whether this form of combination between repositories can be made.

TABLE OF CONTENTS

LIST OF SYMBOLS AND ABBREVIATIONS

Abbreviations:

Cable	-	Submarine high-voltage cable bundle with a capacity of up to 2GW
DoC	Depth of Cover	The distance between the seabed and the top of the cable (in m)
DoL	Depth of Lowering	The distance from the NMRL to the top of the cable (in m)
DSL	Dynamic Seabed Level	The variance present in the seabed. Retrieved via subtracting the present seabed by the local mean.
IQR	Interquartile range	The distance between the 1st and 3rd quartile (can be in various dimensions)
KPI	Key Performance Indicator	The indicators on which the differences between the Reference Case and Experiment Cases will be compared on
LAT	Lowest Astronomical Tide	Reference level based on the lowest possible water level under normal weather conditions. In this thesis, the LAT determined in 2018 is used, officially referred to as NLLAT2018 (Ministerie van Defensie, 2020).
MBES	Multi-Beam Echos Sunder	A type of sonar that uses multiple beams to map the seafloor in high resolution across a wide range
MRSL	Most Recent Seabed Level	A combined map containing per grid cell the last observed depth (in LAT)
NLHO	Netherlands Hydrographic Service	Unit within the Royal Netherlands Navy, responsible for surveying and mapping the bathymetry of the Dutch North Sea
NMRL	Non-Mobile Reference Level	The depth of the predicted lowest seabed level over the expected lifespan of a cable system (40-50 year) with a considered acceptable probability of exceedance
NSE	Nash Sutcliff Efficiency	The Nash Sutcliff model efficiency coefficient provides an insight on the coherence between the Reference Case and the Experiment Case
RMSE	Root Mean Square Error	A measure of absolute error between the Reference Case and the Experiment Case
SBES	Single-Beam Echo Sounder	A type of sonar that emits a single beam to measure the depth directly below the survey vessel
TSO	Transmission System Operator	TenneT is the TSO of the Netherlands, and the developer, owner and operator of the cables discussed in this study

Symbols:

$z_{NMRL\ Ref}$	The NMRL of a Reference Case (in m LAT)
$z_{NMRL\ Exp}$	The NMRL of an Experiment Case (in m LAT)
z_{MRSL}	The MRSL of a repository (in m LAT)
$\delta z_{\square}^{Ref}$ and $\delta z_{\square}^{Exp}$	The NMRL of the Reference Case and Experiment Case relative to the MRSL respectively (in m)
Δz	The NMRL of the Experiment Case relative to the Reference Case (in m)
x	Location along cable or cross-section (in m)
$xmin$	Location on cable where Section 1 or Section 2 start (in m)
L	Length of cable used per cable section to calculate the KPIs on (in m)
O	Indicating that surveys from the Deltares OPeNDAP repository were used
E	Indicating that surveys from the EMODnet repository were used
H	Indicating that surveys from the NLHO repository were used
$t1$	Indicating that the surveys from 1999, 2001, 2007,20011, 2012 and 2016 are used
$t2$	Indicating that the surveys from 2007,20011, 2012 and 2016 are used
MA	Moving average depth (in m) per 5 m or (as used in this thesis) 25 m cable

1. INTRODUCTION

1.1. PROBLEM CONTEXT

Over the past few decades, the world has started to switch from fossil fuels to renewable energy. The European Union aims to reduce its emissions via, among others, wind energy (European Commission, 2023). This also applies to the Netherlands. In 2007, the first offshore wind farm (near Egmond aan Zee) went into operation. New windfarms followed, and at the end of 2023, the power production capacity increased to nearly 4 GW (CBS, 2024). In 2023, offshore wind farms produced 9% of the total electricity production in the Netherlands (CBS, 2023, 2024). The government of the Netherlands aims to increase the power capacity to 21 GW in 2030 (Windopzee, 2023) and to 70 GW in 2050 (Jetten, 2022; Rijksoverheid, 2024). The electricity produced by these wind farms needs to be transported to the electricity network on land via export cables[1].

The Netherlands also has connections with other countries around the North Sea (interconnectors) and interconnectors passing through Dutch waters connecting other countries (COGEA, 2014; Noordzeeloket, 2023a); see red cable routes in Figure 1. These trade connections run for example between the Netherlands and the United Kingdom (BritNed) and Denmark (COBRAcable) (BritNed, 2019; TenneT, 2008, 2019a). There are also multiple international connections planned for example from the Netherlands via windfarm Nederwiek 3 to the UK (LionLink) and between Denmark to Belgium (Triton Link) (Elia Group, 2022; NeuConnect, 2023; TenneT, 2023a). This aligns with plans from the European Union to make the power grid of Europe more integrated (European Commission, 2023).

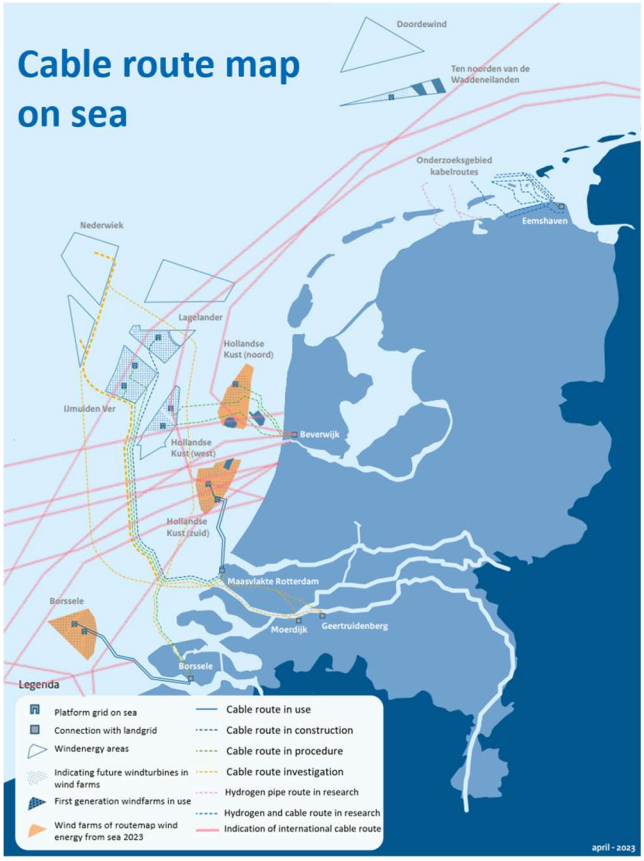

Figure 1: Submarine cable route map with cables from wind farms and between countries. Including current and planned wind farms (COGEA, 2014; Noordzeeloket, 2023b)

[1] The type of submarine cable will be elaborated on in Section 2.1

The costs of disruption of a cable, with the loss of energy production included, are in the order of 100 million euros, assuming a disruption period of 60-70 days and 71.2 euro/MWh (ICPC, 2009; RVO, 2017; TenneT, 2019b). In Europe, one offshore connection fails on average yearly (Paulsen et al., 2016). To prevent disruption by external threats, the offshore connections are installed in the seabed so that it is protected with a layer of soil (CIGRE, 2022; ICPC, 2009). Since seabed on the Netherlands Continental Shelf displays mobile seabed features, the thickness of the sediment cover can decrease (and increase) over the operation period (around 50 years) of such connection and intervention may be needed. Interventions had to be carried out on previously installed connections due to insufficient protection (Jan De Nul, 2021). With the increasingly number of connections in the North Sea, the importance of proper and sustainable cable installation increases as maintenance should be prevented.

1.2. THEORETICAL FRAMEWORK

1.2.1. Mobile seabed features

The sandy seabed in the Dutch North Sea is covered with mobile features such as (mega) ripples, tidal sand waves and sand banks. In Section 2.2.1, the (mega) ripples and sand banks will be discussed.

Sand waves

Tidal sand waves are primarily formed by net tidal currents induced by tidal forces and occur exclusively in sandy shelf seas with strong tidal currents (Hulscher, 1996). Dodd et al. (2003) suggest that depth-averaged tidal currents must exceed 0.5 m/s for tidal sand waves to develop. These waves are composed of sediment, featuring alternating crests and troughs (Hulscher, 1996), and vary in shape, wavelength and amplitude (Dodd et al., 2003; Hulscher, 1996). Typically, tidal sand waves have wavelengths ranging from 100 metres to 1 kilometre, with heights between 1 and 5 meters, and in extreme cases up to 10 meters (Cheng, 2021; Morelissen et al., 2003; van der Meijden et al., 2023). Leenders et al. (2021) state that a sand wave can be up to 20% of the water depth. Research by van Dijk & Kleinhans (2005) and van der Meijden et al. (2023) suggests that nearshore sand waves tend to be lower compared to those offshore.

Sand waves form rhythmic patterns, as noted by Hulscher (1996), Dodd et al. (2003) and Morelissen et al. (2023). Near the coast, the patterns appear more regularly organised in a 2D field, while offshore sand waves are higher and are organised in an irregular 3D field (van der Meijden et al., 2023). In the Dutch North Sea, tidal sand waves often align their crests in a North-West to South-East orientation which is perpendicular to their migration direction (van der Meijden et al., 2023). Sand waves are usually asymmetrical, with a steeper lee side, from crest to nearest trough, compared to the stoss side, from crest to furthest trough as illustrated in Figure 2 (Damen et al., 2018; van Dijk & Kleinhans, 2005).

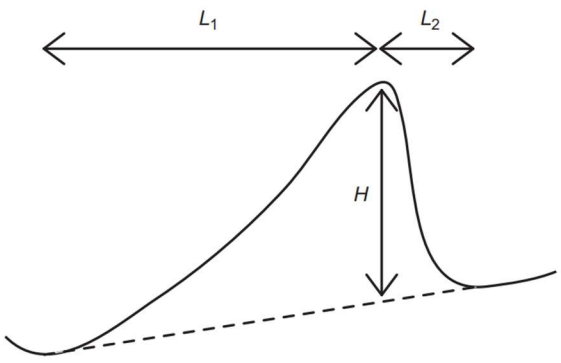

Figure 2: Schematic representation of a sand wave with height H, stoss side (with length L_1) and lee side (with length L_2). A dashed line is drawn between the troughs. The net flow direction of the tide is from left to right, which is also the migration direction. Retrieved from Buijsman & Ridderinkhof (2008).

Research indicates that tidal sand waves are mobile bed forms, typically migrating at rates of meters per year (Morelissen et al., 2003; van der Meijden et al., 2023). Dijk et al. (2011) highlight that there are large differences in migration rates within the Dutch Continental Shelf. The observed average migration rate for sand waves is between 0 to 5 m/year. Migration rates western from Texel are an exception, they can reach up to 19 m/year (van Dijk et al., 2011), the highest migration rates in the Dutch part of the North Sea (van der Meijden et al., 2023). Moreover, as van der Meijden et al. (2023) observed, sand waves in the Dutch North Sea are migrating in various directions, although they generally trend to migrate in the direction around 22 degrees off the North. In addition to migrating, tidal sand waves also exhibit growth over time.

Due to their wavelength and migration rate, sand waves will partially cross the offshore connection over their lifespan, in contrast with mega ripples. Since the height of sand waves is in the order of several metres, their influence on the protection of offshore connections is considered to be significant as the burial depth is also in the order of metres (see Section 2.1).

1.2.2. Non-Mobile Reference Level

To reach a sufficient layer of sediment above the cable (see Section 2.1), the cable can be lowered into the seabed from various reference levels; from the original current seabed or from a created 3D level. As explained in Section 1.2.1, the mobile seabed is dynamic, and the present mobile seabed features change in shape and move over time. Therefore, using the current (original) seabed as the reference level for cable burial over a cable's lifespan is not preferred since this would result in a compromised cover on the cable where erosion occurs. It is recommended by the International Council on Large Electric Systems (CIGRE) and TenneT to have a reference level at the level of the seabed's lowest point during the lifespan of the cable, termed the Non-Mobile Reference Level (NMRL) (CIGRE, 2022; L. Perk et al., personal communication, Feb. 2024; D. W. Snip & D. Liefferink, personal communication, Dec 2023). This NMRL is a 3D surface.

Despite that the term NMRL is used in the Waterwet permits issued for the installation and operation of the Net op zee cables over the past years as a reference level, it is a relatively new term (CIGRE, 2022; Rijkswaterstaat Zee en Delta, 2021a). There are not many methods for establishing this reference level. TenneT's current approach is to create a NMRL based on the observed movement of sand waves; this is has been done via the data-driven probabilistic method developed by WaterProof (a specialised consultancy firm for the marine sector). Other consulting engineering companies have developed other methods to engineer a NMRL, as for instance Deltares and Svašek. This method predicts the seabed mobility over a cable's lifespan and establishes the Non-Mobile Reference Level.

Relation between Depth of Cover and Non-Mobile Reference Level

In the literature, different definitions for cable installation burial related parameters are used.. The recommended definitions by the International Council on Large Electric Systems (CIGRE) are used in this thesis (see Figure 3). In this, the **Depth of Lowering (DoL)** is the distance between the NMRL and the top of the cable. The **Depth of Cover (DoC)** is the distance between the seabed and the top of the cable system. It is assumed that the last executed survey campaign displays the present seabed, the **Most Recent Seabed Level (MRSL)**. The DoL and the DoC may be equal, but due to the installation of the cable, a trench is formed and therefore. The cable is buried into the **Original Seabed Level (OSL)** at the **Depth of Burial (DoB)** depth. Confusion exists in with regard to the term "Depth of Burial" which can be perceived as the cover on a cable or as the depth of the cable below surrounding seabed (CIGRE, 2022). To prevent misunderstanding, the DoB will not be used in this thesis.

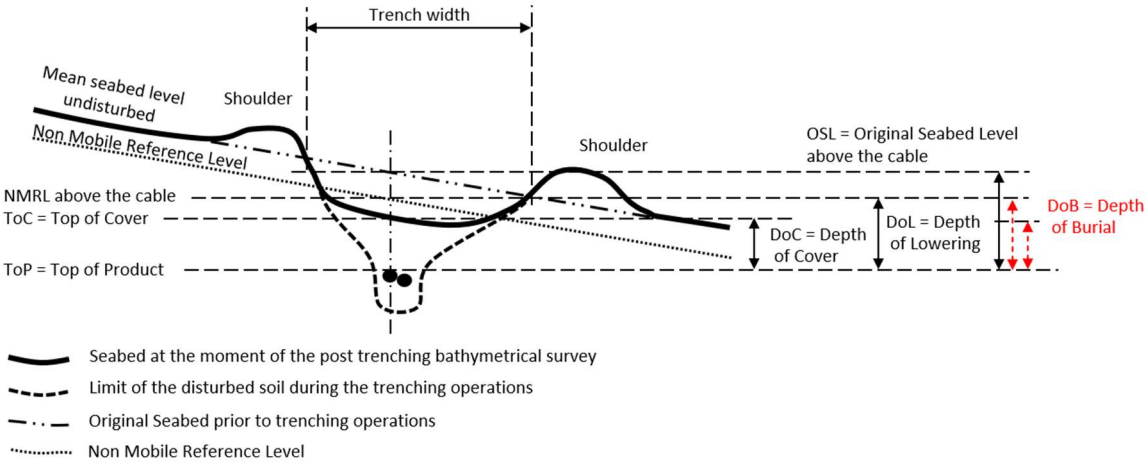

Figure 3: Schematic sketch of the cable cross-section lowered into the seabed with a trench. The cable burial-related levels and depths are shown, adjusted from CIGRE (2022).

The chosen minimal DoC should always be maintained (see Section 2.1) and depends on the DoL, the trench's recovery rate and other seabed mobility such as sandwaves.

There are uncertainties surrounding the method developed by WaterProof for determining the NMRL. These are two types of uncertainties: (i) related to model assumptions and (ii) caused by input data (bathymetric surveys). Currently, the uncertainties in bathymetric surveys, tectonic subsidence and the amplitude of (mega) ripples are accounted for by lowering the NMRL with an additional 25 cm (de Swart & van der Laan, 2024).

1.3. KNOWLEDGE GAPS

The uncertainties presented in the method of WaterProof for establishing the NMRL as discussed in Section 1.2.2 are currently compensated by lowering the NMRL by 25 cm (de Swart & van der Laan, 2024). It is not known whether this 25 cm compensation is sufficient, as little research has been done on the uncertainties in WaterProof's method.

In a recent study, carried out by de Swart & van der Laan (2024), it was found that there are large differences between data sources containing similar survey data. According to de Swart and van der Laan (2024), the differences should be due to the difference in processing of the bathymetric datasets before publishing the sets. It is not known what the effect would be of using different repositories for compiling the NMRL.

Due to its probabilistic approach, the NMRL changes when new data is provided (de Swart & van der Laan, 2024). A new NMRL could be used to assess potential undershoot of the DoC and predict when such undershoot may occur. With this insight, TenneT could strategically plan reburial operations to maintain the minimal DoC, allowing interventions to be scheduled at more convenient times, thus lowering operational costs. However, the feasibility of using this approach could not be found in earlier research.

1.4. RESEARCH AIM

This study aims **to evaluate the uncertainties in the NMRL[1] determined by the method developed by WaterProof[2] in the offshore seabed of the Dutch North Sea[3], by testing various settings of the method[4] and using various bathymetric input[5]**.

[1] The Non-Mobile Reference Level (NMRL) is a 3D model of an expected lowest seabed level over the expected lifespan of a cable system with an acceptable probability of exceedance. For this acceptable probability of exceedance TenneT currently uses 25%, based on a merely qualitative assessment of the life cycle impact on society of the protection by burial of the cables (Laan et al., 2023). In this study, the NMRL will be projected for the year 2078, aligned with the expiration of TenneT's permit for the cable system as will be explained in Section 2.2.

[2] This study uses the probabilistic method developed by WaterProof Marine Consultancy & Services BV (WaterProof) for determining the NMRL (Laan et al., 2023). The method uses historic bathymetric surveys to estimate migration and growth rates and extrapolates the MRSL to the desired period. Section 3.2 describes the method in detail.

[3] This study focuses on the lower-offshore seabed in the Dutch North Sea (-25 up to -18 m LAT). The lower shoreface is between the inner shelf and the upper shoreface (Anthony & Aagaard, 2020). This zone features mobile bedforms, and tidal currents primarily drive the movement of the present tidal sand waves (Anthony & Aagaard, 2020; Knaapen, 2005; van der Spek et al., 2022). The reason for choosing this region can be found in Section 2.2.

[4] This study tests the impact of four settings within WaterProof's method on the NMRL, namely (i) the percentile, (ii) the length and (iii) spacing of cross-sections and (iv) the period between surveys, as will be explained in Section 3.5.

[5] The various bathymetric inputs used in this study are obtained from TenneT, Deltares OPeNDAP, EMODnet and the Hydrographic Service of the Royal Netherlands Navy. The input varied by excluding surveys and varying the resolution and repository. This is described in Section 3.6 in more detail.

1.5. RESEARCH QUESTIONS

To achieve the research aim, two research questions (RQs) are formulated:

RQ1: What is the sensitivity of the parameter settings in WaterProof's method on the Non-Mobile Reference level?

RQ2: To what extent is the Non-Mobile Reference Level, as determined by WaterProof's method, sensitive to handling and selection of input data?

1.6. RESEARCH SCOPE

This study focuses on the uncertainties in the NMRL caused by four method settings and the four variations on handling and using input data in the lower offshore seabed of the Dutch North Sea. This means that the outcomes of this research apply to this region but cannot be directly translated to other regions.

Since WaterProof's method is purely data-driven, it does not involve the physical parameters of sediment transport. Therefore, the focus of this study is predicting the NMRL up to the year 2078 with earlier obtained bathymetric data. This implies that (planned) interventions within the North Sea, such as dredging/sediment dumping, cannot be included. It is assumed that the seabed will not change due to human intervention but only due to sand waves' (historically observed) mobility. Due to this approach, climate change effects are not incorporated.

1.7. THESIS OUTLINE

Chapter 2 explains the study area and provides the background of this thesis. In particular, the requirements around cable installation. Chapter 3 explains the research method by first discussing the bathymetric data available and the pre-processing of this bathymetric data before explaining

WaterProof's method for determining the NMRL. Also, the method for each research question is elaborated here. Chapter 4 presents the results in the order of the research questions. This is followed by Chapter 5 with a discussion about WaterProof's method and the limitations of this thesis. Within Chapter 6 conclusions are presented answering the research questions. The thesis ends with further research recommendations and recommendations for establishing the NMRL.

2. BACKGROUND

2.1. SUBMARINE HIGH-VOLTAGE POWER CABLES

The offshore produced and traded electricity needs to be transferred; this is done via submarine high-voltage cables. The newly proposed standard for submarine high-voltage power cables for projects by TenneT is a 525-kV direct current (DC) 2 GW capacity cable bundle consisting of four cables (Prysmian Group, 2019; TenneT, 2023c). The plus, minus, metallic return (to allow for the transport of the imbalance energy between the plus and the minus pole, resulting from an imbalanced load from the wind turbine fields into the offshore AD/DC converter, and as well for redundancy), and a glass fibre cable (for communication between land, the offshore station and the wind turbines) are often bundled into one single cable bundle (1x4 configuration) (Pondera & Arcadis, 2023; TenneT, 2019b). For brevity, this thesis refers to a submarine cable bundle with a capacity of up to 2 GW and operating at 525 kV DC simply as 'cable'.

Multiple parties are involved in installing and operating offshore connections in the Dutch North Sea. The Ministry of Economic Affairs and Climate Policy, “Klimaat en Groene Groei” since the last change of government, gives the commission for cable installation. The future owner and operator of the cable is the Transmission System Operator (TSO). In the Netherlands TenneT is the only TSO for the high voltage (110 kV or more) network, with as the only shareholder the government of the Netherlands. As TSO, TenneT is responsible for maintaining a balance in supply and demand on the 25,000 km high-voltage network in the Netherlands and a large part of Germany (TenneT, 2023b).

2.1.1. Cable Protection Requirements

The consequence of a submarine power cable being cut through would be a (direct) monetary cost; a (partly) disruption of a submarine cable does not cause danger to people or nature (E-Connection, 2001). The loss due to that the electricity from the windfarms cannot be delivered to shore are not paid for by TenneT, this loss is for the owners of the windfarms. The repair is paid by the owner and operator of the cable (TenneT) and the insurance companies. Since TenneT's only shareholder is the government of the Netherlands (TenneT, 2024), repair costs can be seen as societal costs.

Therefore, both TenneT’s internal asset management (from the perspective of asset safety) and the permit issued by Rijkswaterstaat (from the perspective of the considered nautical safety), with the authority of the Ministry of Infrastructure and Water Management, require a minimal depth of cover (DoC) above the cable. TenneT’s internal asset management draws up the first requirements, following TenneT’s aim to ensure grid stability and safety against the lowest possible lifecycle costs to society (impact on the environment, disturbance of other users of the sea and financial costs). To obtain a ‘bury like you want to and would like to forget’ depth, TenneT has developed a minimal DoC tailored to each cable route section to protect the cable system. This approach employs probabilistic modelling, where the DoC is determined based on the acceptable probability of failure per kilometre and year, the protecting soil(type), tension on the cable due to hydrodynamics, and the likelihood and impact of a threat posed by activities near the cable, such as fishing and anchoring of ships (ACRB, 2022; CIGRE, 2022; ICPC, 2009; Noordzeeloket, 2023a; D. W. Snip & D. Liefferink, personal communication, 21 December 2023). This also results in a minimal distance between parallel cables (around 200 m), relating to minimising the probability of joint failure of more than one cable system as the result of external threats (for instance a sinking vessel). The minimal required DoC for IJmuiden Ver and Nederwiek offshore connections, which is similar for other cable connections, varies according to TenneT’s internal asset management between 0.5 and 2.0 metres (ACRB, 2022).

The permit sets a minimal DoC of 1.0 metre outside shipping areas and 1.5 metres inside shipping areas offshore, with certain exceptions, for example, near busy waterways such as the Eurogeul near the

Maasvlakte II (Rijkswaterstaat Zee en Delta, 2021a). The expected lifespan of a cable is 40 years; however, additional time is included in the permit to accommodate the construction and decommissioning phases of the cable. The permit imposes strict requirements for maintaining the minimum DoC for 50 years (Rijkswaterstaat Zee en Delta, 2021a, 2021b).

2.1.2. Cable Installation

Placing the cable on top of the seabed and burying it with sand is not viable. Within a matter of weeks, the sand would be eroded (Voet & Moes, 2005). Besides this would have more impact since the sand would be brought in. Therefore, most of the cables are lowered into the seabed by a trencher, which can lower a cable several metres into the seabed without removing soil. For deeper cable burial first a dredger lowers the seabed ('pre sweeping') by dredging the mobile seabed features (from ripples up to sand waves) before a trencher lowers the cable into the lowered seabed (Van Oord, 2020). After lowering the cable into the seabed, the cable is only protected by the sand above the cable (CIGRE, 2022).

Lowering the cable deeper in the seabed would result in a thicker sediment cover, providing more safety from external threats. However, a deeper cable is more expensive for two reasons. Firstly, lowering a cable deeper in the seabed may require pre-dredging ('pre-sweeping'). The increase in dredging volume is more substantial than the proportional growth in depth. This non-linear relationship between depth and volume makes deeper cable lowering, beyond the penetration depth of cable trenchers, expensive, and initially, a larger permissible dredging volume needs to be requested in the permit (Rijkswaterstaat Zee en Delta, 2022). For example, Van Oord's new trencher can now lower a cable up to 5.8 metres and weighs 125 tonnes; technically, larger trenchers could be created when necessary (Van Oord, 2020).The second reason for a potential increase in cost for deeper cable lowering is that the thermal properties of the cover layer are an important design parameter for the submarine cable (CIGRE, 2022). A power cable produces heat due to resistance by the electricity in the cable. If a cable becomes too hot (typically above 70-90 degrees Celsius), the cable fails (Zhang et al., 2020). The created heat is transferred from the cable through the cover layer to the relatively cool water (Olijve, 2019). To reduce the resistance and thus heat production, the core (conductor) of the cable can be made thicker or made from different materials, making it more expensive (Boone & Sonderen, 2015; Prysmian Group, 2019). As the cover layer acts like a blanket, the thicker the cover layer, the harder it is to transfer the heat to the water; thus, the less heat the cable must produce and the more expensive the cable becomes. This is particularly important at locations where mud and clay are present due to their lower thermal conductivity compared to sand (Usbeck et al., 2023).

The increase in safety against external threats by lowering the cable deeper into the seabed than the minimal DoC as determined by TenneT, does not weigh against the increase in costs, effort and environmental impact due to the effects of dredging.

2.1.3. Reburial of Export Cables During Operation

Currently, periodic surveys, at intervals as stated in the permit or as dictated by the operation policies of TenneT, are executed above existing cables during the cable's lifespan. When the minimal required DoC is not present, the cable is not immediately endangered, nor will it fail. Despite this, the cable needs to be lowered as soon as feasible to comply with the guidelines set by TenneT's asset management or as set by the permit (Rijkswaterstaat Zee en Delta, 2021a, 2021b; TenneT, 2019b). This lowering does happen several times yearly on the currently installed cable systems (W. Snip & D. Liefferink, personal communication, 2023), as a consequence of; less successful initial burial, as the result of unexpected seabed mobility or because the cable could not be buried deep enough during

installation because of permit limitations to for instance dredging operations preceding the installation (D. W. Snip, personal communication, 18 October 2024).

2.2. STUDY AREA

This thesis study focused on the cable routes from the offshore wind farm Hollandse Kust (zuid), about 20 kilometres offshore between The Hague and Zandvoort, towards the northwestern corner of Maasvlakte I (Hellenic Cables, 2022).

The study area is intensively used by maritime activities, and mainly therefore, the area has been surveyed repeatedly since 1969 (Dienst der Hydrografie, 2022; van der Meijden et al., 2023). Due to the fact that the seabed is in the lower shoreface zone and features mobile tidal sand waves, the cables should be lowered relative to an NMRL to obtain sufficient protection against external threats (see Section 1.2.2). This made the area interesting to study.

The two present platforms in the wind farm, Alpha and Beta, have an individual capacity of 1400MW. Both platforms have two 220 kV 350 MW AC cable connections with the onshore grid. The four cable systems and a 66 kV interlink cable between the platforms are run parallel to each other and have been in operation since 2022 and are displayed in Figure 4 (TenneT, 2023d).

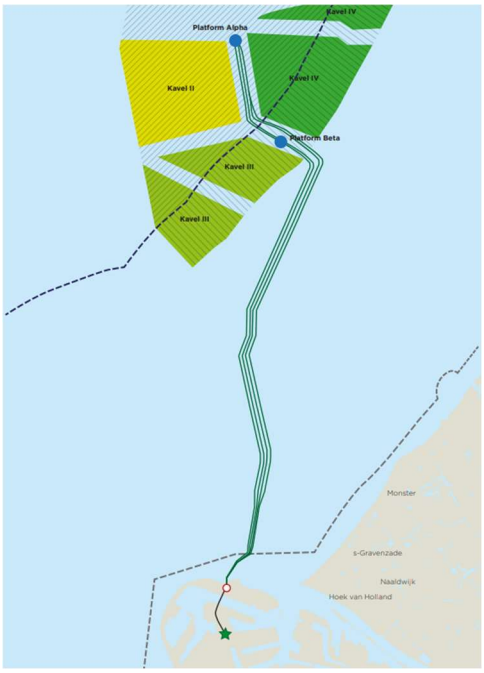

Figure 4: Hollandse Kust (zuid) wind farm and its cable connections (Hellenic Cables, 2022), the green lines indicate the four cable systems, the dots the platforms and the coloured areas are the parcels ('kavels') within the Hollandse Kust (zuid) wind farm.

For this thesis, one cable system was investigated, Alpha 1. The permit for the operational use of the cable is provided till 2055 (Rijkswaterstaat Zee en Delta, 2018). More recently issued permits for wind farm IJmuiden Ver (connections from platforms Alpha, Beta and Gamma with the onshore grid) have a more extended operational period, namely up to 2073, including the removal period (Rijkswaterstaat Zee en Delta, 2021a, 2021b, 2022). In NMRL studies executed for those cable connections, the NMRL was determined for the period between 2022 (the last survey) and 2078 (de Swart & van der Laan, 2024; Laan et al., 2023). Therefore, the NMRL on the Alpha 1 cable for the period till 2078 was also determined.

2.2.1. Mobile seabed features besides sand waves

Besides sand waves, the Dutch Continental Shelf has other mobile bed features, namely ripples, mega ripples, and tidal sandbanks.

Mega Ripples

Mega ripples are present in this study area. Mega ripples are seabed features which have a wavelength in the order of several metres and an amplitude in the order of 20 centimetres (Dodd et al., 2003; Hulscher, 1996; Knaapen, 2005). They have a migration rate in the order of 100 m/year up to 1 m/day (Dodd et al., 2003; Knaapen, 2005). Due to this, they will cross a connection several times during the operation period. Therefore, the height of the complete mega ripples cannot be included as protecting height, the troughs of mega ripples will walk over the cable multiple times. Thus, the NMRL should be located below the mega ripples.

Tidal Sandbanks

Besides the sand waves, larger bed features are present in the study area, namely tidal sandbanks. Tidal sandbanks have wavelengths of 5 up to 80 kilometres and hardly move (Hulscher, 1996; Morelissen et al., 2003; The Open University, 1999). They migrate but have a temporal scale that spans decades to millennia. Additionally, their heights can reach up to tens of meters (The Open University, 1999). Tidal sandbanks are among the largest mobile seabed features on the Dutch Continental shelf. Due to their low migration rate, they do not significantly affect the protection layer during the operating system's lifespan.

3. RESEARCH METHOD

To answer the research questions, the following method was used to eventually satisfy the research aim. First, the method for obtaining, selecting, and pre-processing the bathymetric datasets is described. This is followed by the method for establishing the NMRL, as proposed by WaterProof, as this is the foundation for the methods for answering the research questions. Each research question is split into different parameters and datasets and requires a different method; thus, the method is split into separate sections. As the Alpha 1 cable system is the area of interest, the year of extrapolation needed for the NMRL determination is similar to the year of the permit, and the NMRL is determined up to the year 2078 (see Section 2.2).

3.1. BATHYMETRIC DATA

The Hydrographic Service ('Dienst der Hydrografie') (NLHO) is a unit within the Royal Netherlands Navy, responsible for surveying and mapping the bathymetry of the Dutch North Sea (Ministerie van Defensie, 2018). They perform surveys according to the International Hydrographic Organization (IHO) standards, at the moment IHO S44 6th edition (Rijkswaterstaat Zee en Delta, 2022). The surveys executed by NLHO are not openly available but can be requested. The processed surveys of the NLHO are openly available in other repositories: Deltares' OPeNDAP repository and the European Marine Observation and Data Network (EMODnet). Both repositories cover a larger area than the study area but have temporal gaps of several years and form a patchwork of surveyed sections. The bathymetric data of TenneT, Deltares OPeNDAP and EMODnet were collected at the beginning of the preparation phase of this study. The bathymetric data of the NLHO was collected during the thesis project.

3.1.1. Coordinate system

The coordinate system used in this thesis is EPSG:25831. EPSG:25831 refers to the coordinate reference system used within UTM Zone 31N with the ETRS89 datum (Stal et al., 2022). This system is part of the European Terrestrial Reference System 1989 (ETRS89), which is a geodetic datum. The Universal Transverse Mercator (UTM) is a map projection that divides the world into a series of zones. Zone 31N indicates the projection to areas between 3°E and 9°E longitude in the Northern Hemisphere. The coordinates are provided in meters.

The vertical elevation is relative to the Lowest Astronomical Tide of 2018 (LAT) in meters as defined by the Ministry of Defence and is officially referred to as NLLAT2018 (Ministerie van Defensie, 2020). This is different than in which several surveys have been collected before 2018 (for example, in NLLAT2016) (Ministerie van Defensie, 2020). All surveys obtained are in NLLAT2018, and thus, surveys before 2018 should be corrected towards this height. However, it is not certain whether this has always properly been done since there are no descriptions about changing the reference level. Despite uncertainties caused by the LAT, there is a preference for using an ellipsoidal height, the surveys of TenneT are also referenced to the GRS80 ellipsoidal height (Ministerie van Defensie, 2023; A. Wolowicz-Trouwborst, personal communication, 12 March 2024). The obtained datasets are provided in NLLAT2018 and thus this vertical coordinate system is used, abbreviated to LAT. The positive z-direction points upwards, so the location of the seabed is always a negative value.

3.1.1. Hydrographic Service

For this thesis, the surveys between 1969 and 2022 were requested and obtained from the NLHO for the area of interest on the Alpha 1 cable (Dienst der Hydrografie, 2022). For the survey campaigns, the metadata, such as method of gathering, was also obtained (see Appendix A).

The surveys received from NLHO were not all on the same coordinate system, surveys before 2015 were provided in the EPSG:4258 coordinate system, this means that the x- and y-direction are in degrees. These surveys needed to be reprojected to the same coordinate system in this thesis. Some surveys only contain data points in the travel direction of the surveying vessel. Some of the datasets from 2007 onwards were gathered with a Multi-Beam Echosounder (MBES) and thus are already on a structured grid. The resolution differs per survey due to different sampling and the used coordinate system but are, after reprojecting, 3x5m (2007, 2010, 2011, and 2012) or the unchanged in EPSG:25831 2x2m (2016 and 2022). These surveys were resampled to a 5x5m grid using QGIS. See Appendix A.2 for more information about the interpolation and resampling procedure for the data from the NLHO repository.

3.1.2. Deltares OPeNDAP

Deltares published bathymetric data from 1967 till, at the moment of writing, 2016 in their repository with a resolution of 25x25m (Deltares, 2020). The data is in the same coordinate system (EPSG:25831) and are displayed relative to NLLAT2018. From these datasets, it is known that inverse distance weighted interpolation is carried out to process the NLHO surveys for the datasets published on the repository (T. Vermaas, personal communication, 5 July 2024). For this interpolation, all points within a 100 m radius distance are used (Vermaas, 2017). In Figure 5, the Most Recent Seabed Level (MRSL) of the Deltares repository can be seen.

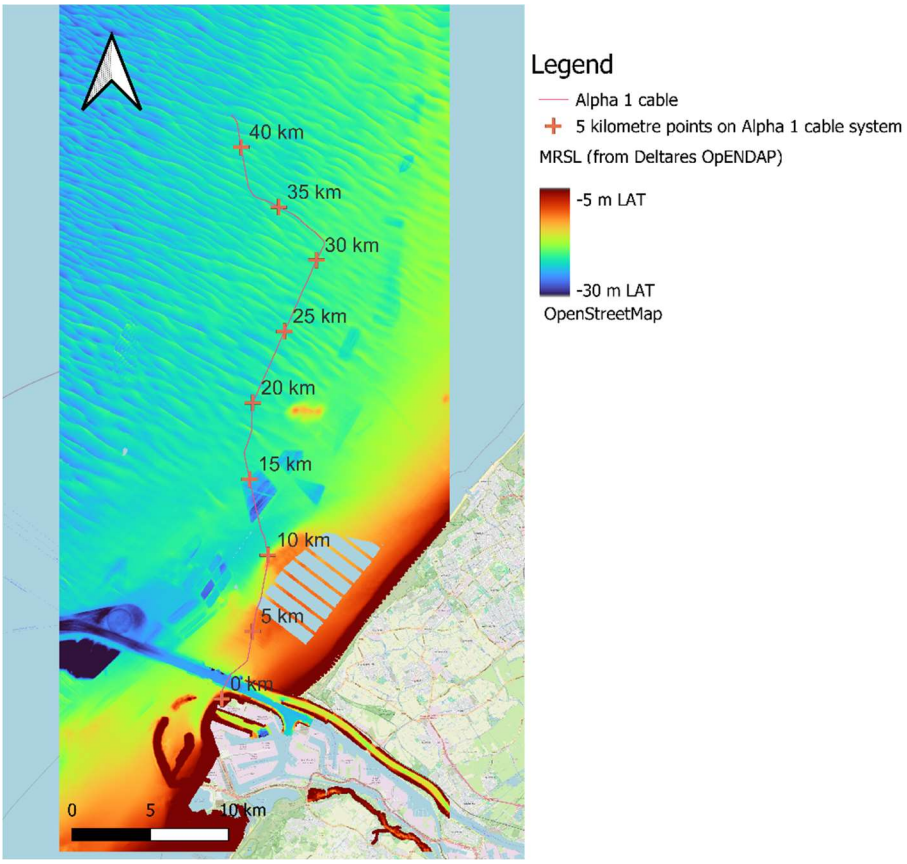

Figure 5: MRSL according to Deltares OPeNDAP repository, including Alpha 1 cable system

Since the coordinate system, resolution and reference level in OPeNDAP are consistent with those used in this thesis, no-preprocessing is required for the surveys in the OPeNDAP repository.

3.1.3. EMODnet

EMODnet has published data from 1969 up to 2023, at the time of writing, with a resolution of 20x20m. From these datasets, it is unknown what interpolation method was applied to the NLHO surveys. The same datasets (excluding the 1999 survey) as in the Deltares OPeNDAP repository were obtained.

For EMODnet, only a change in the coordinate system and resolution had to be executed. The datasets on the EMODnet repository were converted to the same coordinate system (EPSG:25831) and resolution (25x25m) as the Deltares OPeNDAP (see Appendix D.1).

3.1.4. TenneT

For this thesis, TenneT provided three high-resolution (0.3 by 0.3 metres) sets of bathymetrical data, gathered during survey campaigns of the Hollandse Kust (zuid) project. These high-resolution surveys were executed with a Multi-Beam Echosounder (MBES) over a period of less than 4.5 years. The first survey (June 2017) was carried out before the construction of the connection between the Maasvlakte I and the area Hollandse Kust (zuid) (offshore wind farm area to the North of the Maasvlakte I, see Figure 4) and has a coverage of around 800 metres in width over the whole cable route. The second survey (May 2020) was held to assess the construction process, and the third survey (November 2021) was carried out after finalising the construction. The last survey has the smallest coverage, approximately 100 metres wide along the cables. In this last survey, the trench of approximately 25 metres in width formed during the installation of the cable is visible (see Figure E.1).

3.1.5. Selecting Bathymetric Data

As shown in Figure 5, the seabed around the Alpha 1 cable system not only contains sand waves as described in Section 1.2.1 in the whole domain, but also the seabed is also dredged in some areas, especially the Maasgeul/Eurogeul, up to -40 m LAT. Dredging influences the movement of sand waves (Campmans et al., 2021; Krabbendam et al., 2022; Stive et al., 1998). Therefore, the area of interest is narrowed to the northern part of the cable system to limit the effect of dredging on the NMRL.

Some survey campaigns, mostly before 2000 but also the surveys in 2015, have been executed with a Single-Beam Echosounder (SBES) by the NLHO and thus consists of sailed paths with data points. Deltares pre-processed these data points obtained by NLHO before publishing them in the Deltares OPeNDAP repository. Prior to 1999, the survey sail paths exhibited widespread sampling, with sail paths spaced at least 125 meters apart. While interpolation was used by Deltares to fill these gaps, these surveys have been excluded from this research, as the method may not accurately account for such large distances. In Appendix C, the excluded surveys of the Deltares OPeNDAP repository can be seen. Since NLHO provided the survey data for OPeNDAP and EMODnet, the same surveys have been excluded from these repositories.

After excluding these datasets, two locations along the cable route were found where; (i) multiple surveys are available, (ii) the distance from dredged areas is at least 3km and (iii) the time between the first and last available surveys is 10 years or more. The Alpha 1 cable does not completely cross the most Northern location. To include a larger part of the 2007 survey in this thesis, the Alpha 1 cable has imaginarily been increased in length to cover a larger part of the 2007 survey by 3.7km in the North direction. With this, two Cable Sections were found suitable for determining the NMRL projected on the cable. From here on these are referred to as (cable) Section 1 (from 25 to 31 km) and (cable) Section 2 (from 40 to 45 km) (Figure 6). Appendix B shows the number of surveys in the study area and overlaying the cable.

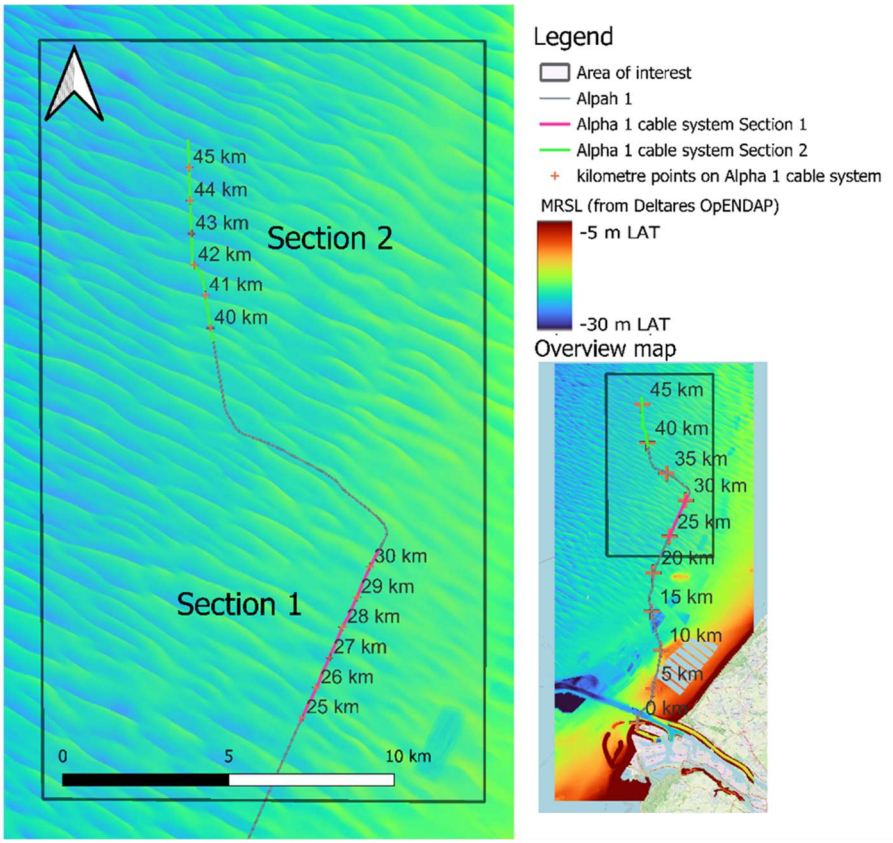

Figure 6: Cable sections which contain sufficient data in the Deltares OPeNDAP repository for establishing the NMRL.

3.1.6. Differences between repositories

Despite receiving the same data from NLHO, Deltares and EMODnet publish different depths. To illustrate this Figure 7, shows a constant shift in height between the different repositories. Also, the down-sampled by mean to 25m resolution datasets of NLHO and TenneT show a less smooth seabed profile than the surveys from the Deltares OPeNDAP and EMODnet repositories.

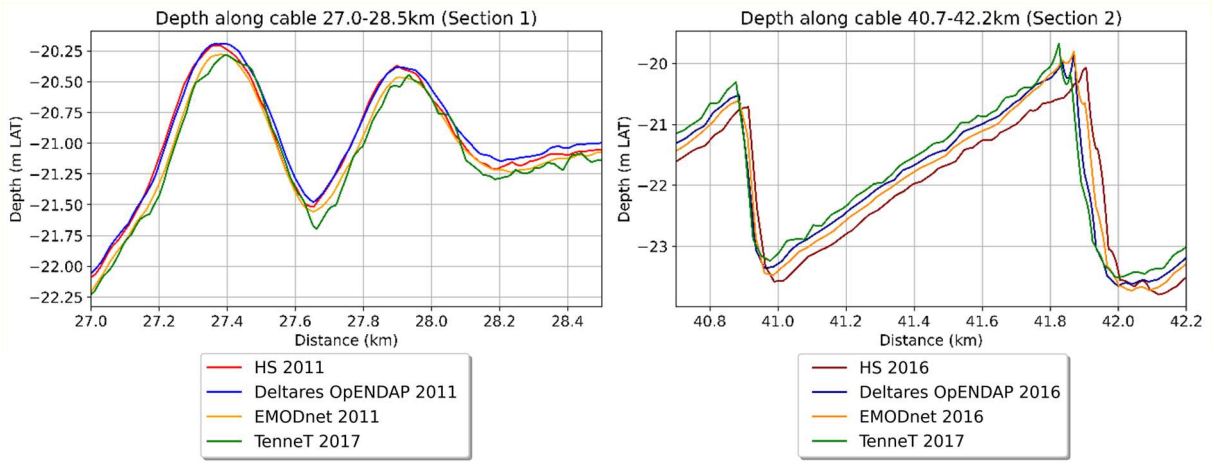

Figure 7: Depth along cable route from different repositories, EMODnet, NLHO and TenneT are down sampled to 25m resolution, see Figure 6 for location Section 1 and Section 2.

Due to variations in reference levels across the different repositories, a correction is required. The 2011 and 2016 surveys from the OPeNDAP repository are assumed to have the correct reference level. These surveys were chosen since they collectively provide the most extensive coverage and thus

overlap most of the other surveys. Besides, they are both the latest survey available on the two cable sections (2011 for Cable Section 1 and 2016 for Cable Section 2).

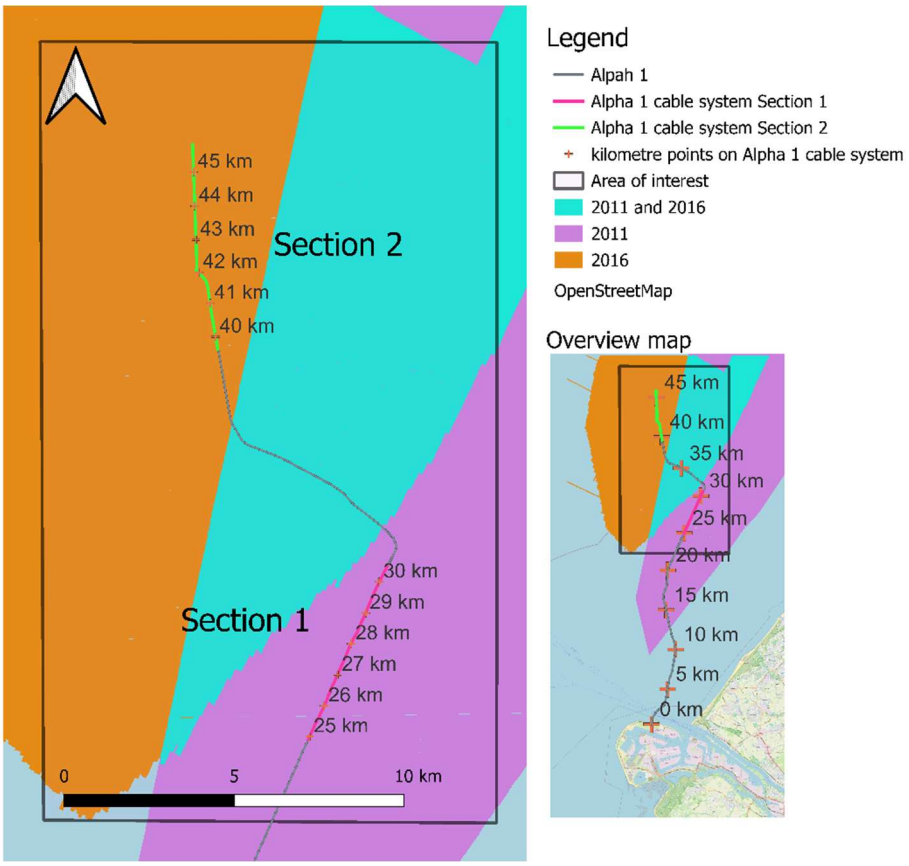

Figure 8: Coverage of 2011 and 2016 survey from Detlares OPeNDAP repository

Additionally, the surveys from 2011 and 2016 are present in all repositories. Assuming a closed sediment balance of the area is zero over time, the other surveys were corrected by calculating the mean depth in the overlapping areas with the 2011 or 2016 surveys and adjusting the entire survey by subtracting the difference in mean depth (see Appendix F for detailed methodology and results).

3.2. PROBABILISTIC METHOD FOR ESTABLISHING NON-MOBILE REFERENCE LEVEL

The NMRL is a data-driven probabilistic lowest seabed level during the cable's lifespan. The standard method utilised by WaterProof uses the MRSL for every 25x25 metres grid cell from the selected available bathymetric surveys. This MRSL, also called the Original Seabed Level (OSL), covers the entire area of interest. To obtain sand waves from the OSL, the local mean value is subtracted from the OSL. Using an ellipse-shaped kernel of 1500 by 500 metres with the long axis oriented to the mean propagation direction of sand waves in the Dutch North Sea (20 degrees of the North axis), the local mean is created by applying a two-dimensional convolution operation (Laan et al., 2023). The OSL subtracted by the local mean is called the Dynamic Seabed Level (DSL). From the DSL, cross-sections in the local migration direction of the tidal sand waves of 5,500 metres (note that this is different than the length of the cable within the sections; orange line in Figure 9) are taken at an interval of 100 metres (white dots in Figure 9) along a line perpendicular on a 20 degree off north line (as this is perpendicular on the mean propagation direction of sand waves; red line in Figure 9) crossing a point on the power cable as illustrated in Figure 9. The cross-sections are in the local migration direction, determined by calculating the arithmetic mean of the directions of the maximum slope of present sand

waves determined by the hill-shading method of Horn (1981) within a radius of 1500 m around the centre of the cross-section (the white dots in Figure 9).

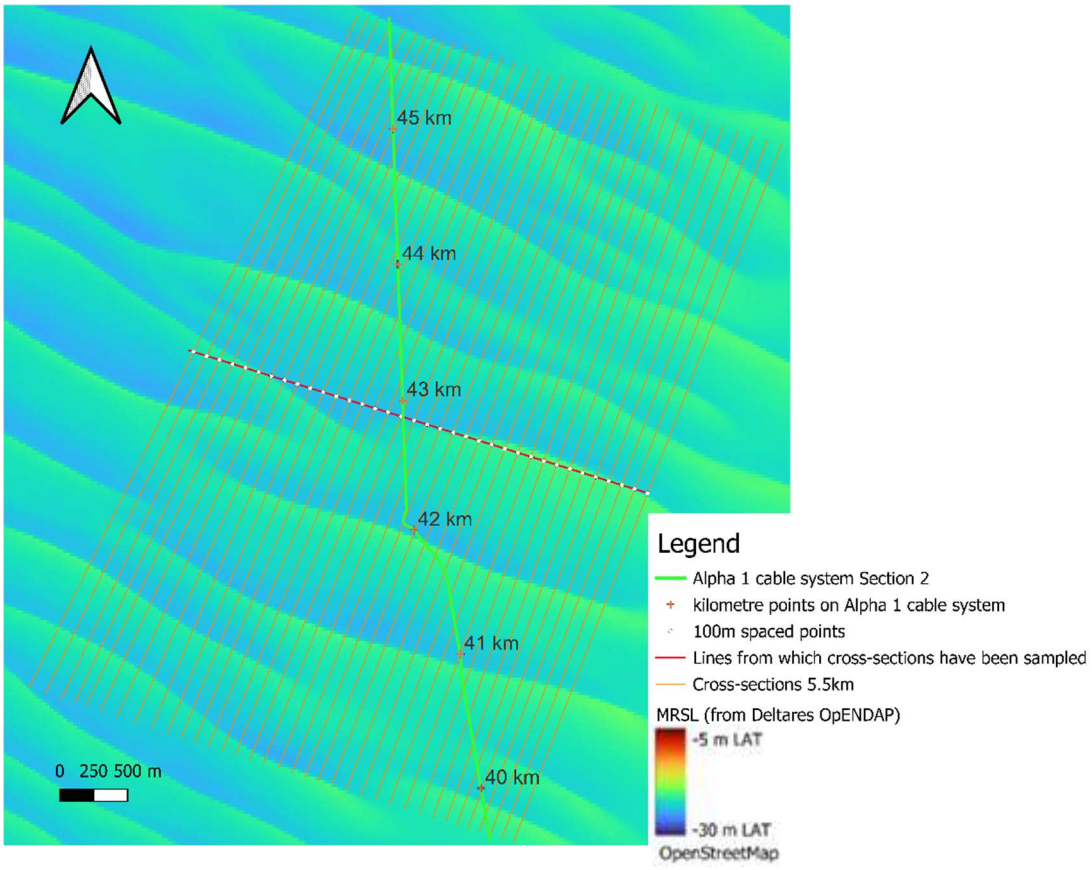

Figure 9: Cross-sections in local sand wave migration direction sampled from a line which is perpendicular to the 20 degrees off the North direction.

The DSL is also created for the oldest available seabed level per grid cell, and cross-sections at the same locations are taken. The individual migration and growth rate for each sand wave are then determined between these two sets of cross-sections. A peak is identified when there is at least 75 meter between the previous peak and has a prominence of at least 0.4, the throughs are found with the same approach but the z-axis is reversed for computational purposes. The migration rate is then determined by calculating the lag for which the maximum cross-correlation is found between two trough-crest-trough sequence on one cross-section. This method to find the migration rate via the spatial cross-correlation is used by, among others, Duffy & Hughes-Clarke (2005), Buijsman & Ridderinkhof (2008) and more recently by van der Meijden et al. (2023). This method is suitable for calculating migration rates which are not necessarily perpendicular to the crest (Buijsman & Ridderinkhof, 2008). The vertical displacement of the sequence determines the growth rate. Herein, a distinction was made between the crests and troughs. One crest results in both one migration rate (dx/dt) and one growth rate ($dz/dt\ peak$). One trough only results in a growth rate of the through ($dz/dt\ trough$). An individual crest or through, within one cross-section, is seen as a unique observation. The variability in individual sand wave migration and growth rates per cross-section can then converted to probability density functions (PDFs) based on at least 100 observations. These three PDFs represent the migration rate and growth rates of crests and troughs. With a cross-section length of 5.5 km and sand waves with wavelengths of 0.1-1km, less than 100 observations can be found per cross-section. Therefore, the cross-sections within a radius of 500 m are included. If there are still less than 100 observations, the radius is enlarged until there are 100 observations or the radius is equal to 1 km.

Using a Monte Carlo simulation (with 10,000 runs), rates out of the three PDFs are taken to translate the DSL to the year 2078 and all in between years. With this, it is assumed that all sand waves on one cross-section during one run migrate and grow with the same rates. A limitation is put on the growth and decay such that unrealistic outcomes are discarded (such as, in extreme cases, an inversion of the crests and troughs). The shallowest depth over the cross-section over time per experiment was taken, resulting in an assemble per cross-section. From the 10,000 simulated assembles (grey band in Figure 10), the 25th percentile is chosen as the probabilistic-based representative for this cross-section in consultation with TenneT (de Swart & van der Laan, 2024). Note that since the MRSL is included in this calculation, the representative per cross-section cannot exceed the MRSL, since this may be the shallowest depth over time. Finally, the local mean (which was subtracted from the OSL) is added to the NMRL per cross-section to obtain the representative on the original reference level (metres LAT) on a single cross-section.

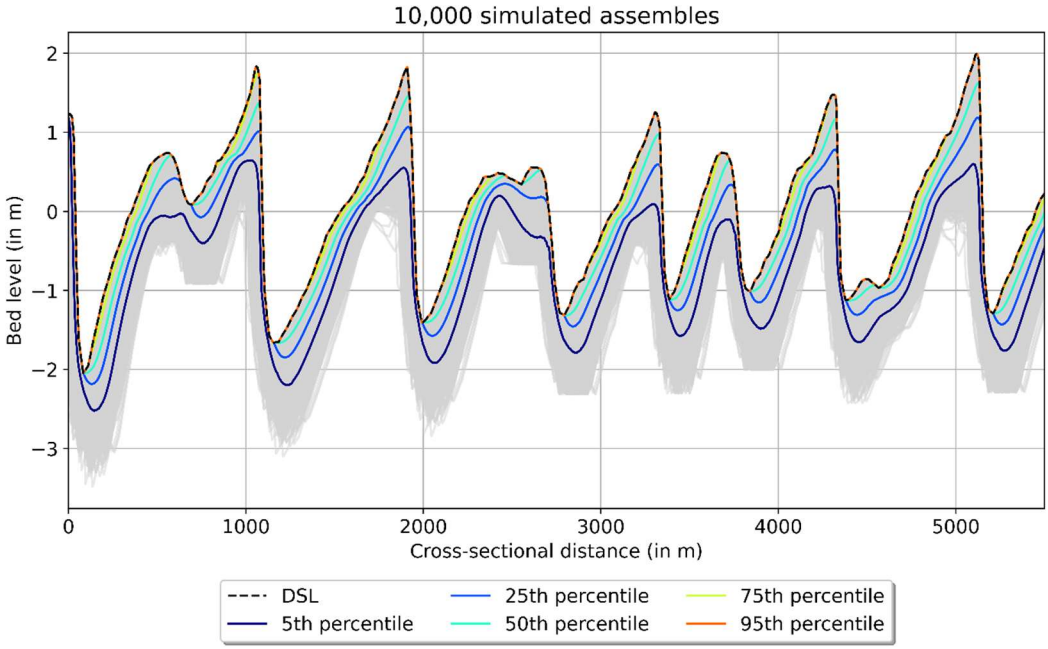

Figure 10: Distribution of assembles, in grey, and different percentile NMRL assembles at the 18th cross-section within Cable Section 2 for one of the simulations.

From the representative per cross-section, via interpolation, a 3D representative level on 25x25m resolution is created. To include uncertainties in bathymetric surveys, tectonic subsidence and the height of (mega) ripples, this 3D level is lowered with an additional 25 cm resulting in the 3D NMRL (de Swart & van der Laan, 2024). The NMRL is reprojected on the cable system (z_{NMRL}), from which the DoC will be measured, by bilinear interpolation per meter cable system. These reprojections are in metres relative to LAT with positive z-direction pointing upwards (as was defined in Section 3.1.1).

3.3. COMPARISON METHOD

To answer the two research questions, a comparison method was established to assess the difference between the NMRL without changing settings/input data in WaterProof's method, the Reference Case and the NMRL where settings/input data is changed, the Experiment Case. The Reference Case projected on the cable is referred as $z_{NMRL\,Ref}$. The NMRL projected on the cable of the different Experiment Cases, as will be discussed in Section 3.5 and 3.6, are referred as $z_{NMRL\,Exp}$. The MRSL projected on the cable is referred as z_{MRSL}. In Figure 11a, an illustration is provided of these three projections on the cable.

For cable installation purposes, the vertical distance is between the NMRL and the MRSL is important since this influences de burial depth of the cable (see Section 1.2.2). For the NMRL of the Reference Case ($z_{NMRL\ Ref}$) and the NMRL of the different Experiment Cases ($z_{NMRL\ Exp}$), the depth relative to the MRSL (z_{MRSL}) is determined with the following equations:

$$\delta z^{Ref} = z_{NMRL\ Ref} - z_{MRSL} \quad [1]$$

$$\delta z^{Exp} = z_{NMRL\ Exp} - z_{MRSL} \quad [2]$$

The δz^{Ref} and δz^{Exp} are the $z_{NMRL\ Ref}$ and $z_{NMRL\ Exp}$ respectively relative to the MRSL in metres (as illustrated in Figure 11b). A negative value for δz^{Ref} or δz^{Exp} implies that the NMRL is located below the MRSL, which is always the case for the first research question but not necessarily for the second research question.

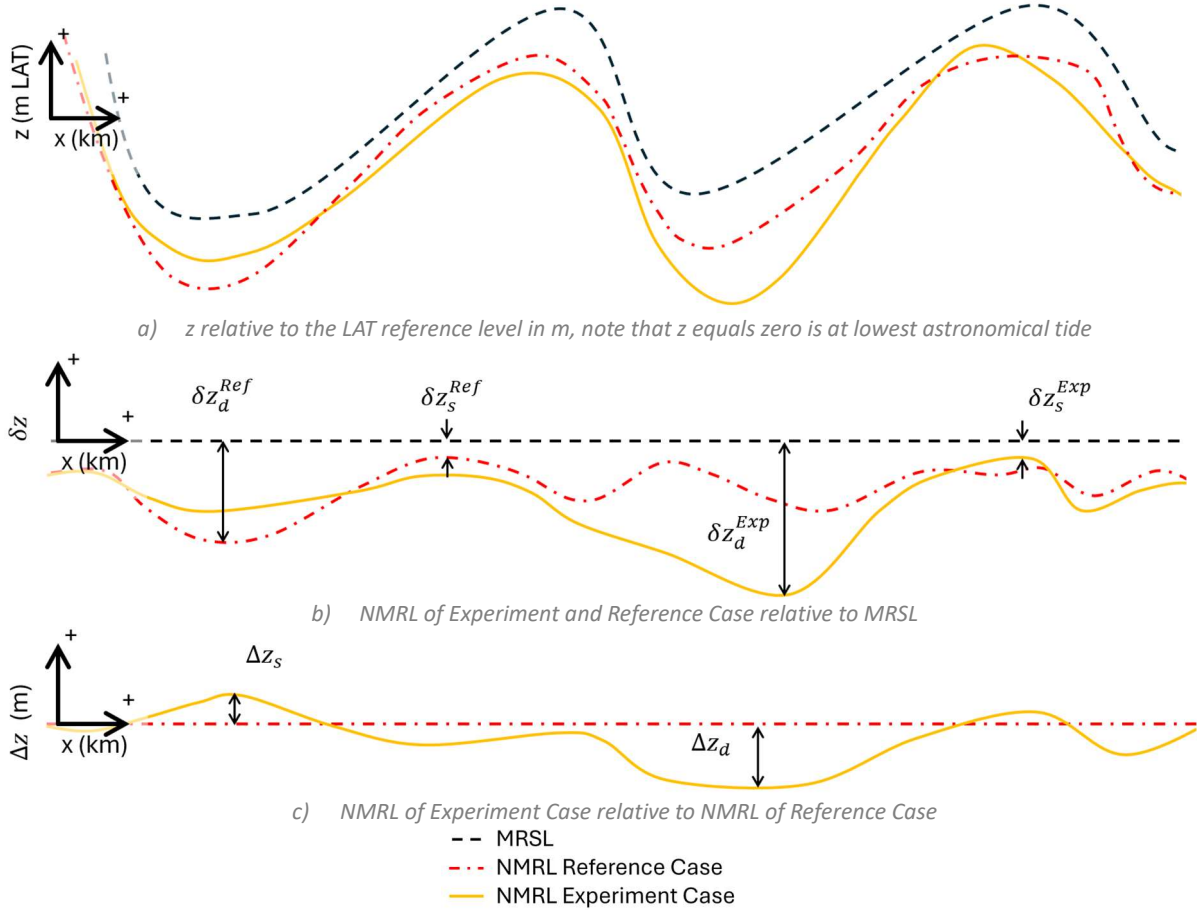

Figure 11: Illustration of the NMRL of an Experimental case compared to a Reference Case projected on the cable, not on scale.

The $z_{NMRL\ Case}$ can also be compared relative to the $z_{NMRL\ Ref}$, with the following equation:

$$\Delta z = z_{NMRL\ Exp} - z_{NMRL\ Ref} = \delta z^{Exp} - \delta z^{Ref} \quad [3]$$

Note that Equations 3 and 4 have the same outcome. The Δz is the $z_{NMRL\ Ref}$ relative to the $z_{NMRL\ Exp}$ in metres (as illustrated in Figure 11b). A negative value for Δz implies that the NMRL of the Experimental Case is below the NMRL of the Reference Case.

To compare the different Experimental Cases with each other and with the Reference Case, several Key Performance Indicators were used. The Nash-Sutcliff model efficiency coefficient (NSE) was used.

The NSE is sensitive to outliers (Motovilov et al., 1999; Zhong, X. & Dutta, U., 2015). Therefore, another KPI is also used, the Root Mean Square Error (RMSE). The RMSE is a measure of absolute error between the Reference Case and the Experimental Case (Kouzehgar & Eslamian, 2023).

The NSE and RMSE value are calculated via the following equations:

$$NSE = 1 - \frac{\sum_{x=xmin}^{xmin+L} \left(\delta z^{Ref}\big|_x - \delta z^{Exp}|_x\right)^2}{\sum_{x=xmin}^{xmin+L} \left(\delta z^{Ref}|_x - \overline{\delta z^{Ref}|_{xmin \le x \le L}}\right)^2}, \qquad NSE \le 1 \qquad [4]$$

$$RMSE = \frac{\sqrt{\sum_{x=xmin}^{xmin+L} \left(\delta z^{Ref}|_x - \delta z^{Exp}|_x\right)^2}}{L}, \qquad RMSE \ge 0 \qquad [5]$$

With:
NSE being the Nash-Sutcliff efficiency coefficient value
$RMSE$ being the Root-Mean Square Error (in m)
$\delta z^{Ref}\big|_x$ equals the NMRL relative to the MRSL (in m) of the Reference Case at location x
$\delta z^{Exp}|_x$ equals the NMRL relative to the MRSL (in m) of the Experiment Case at location x
L is the length of the cable within the sections, set on 5000 m for both Cable Section 1 and 2[2]
$xmin$ the start distance of the cable within a section, 25km and 40km for Sections 1 and 2 respectively

A NSE value of 1 means that there is no difference between the NMRL of the Reference Case and the Experimental Case, the optimum value. The NSE value can become negative, implying that the Experimental Case is not representing the NMRL of the Reference Case (Motovilov et al., 1999; Zhong, X. & Dutta, U., 2015).

The RMSE is equal or larger than 0, where 0 means that there is no difference between the NMRL of the Reference Case and the Experimental Case, the optimum value (Heddam et al., 2022; Kouzehgar & Eslamian, 2023).

The DoC is determined per 5 or 25m cable length for cable monitoring. Since minor differences were observed between the 5m and 25m moving average (the difference in the median is below 1%; see Appendix G.1), the moving average (MA) per 25m cable length was used in this study.

$$\delta z_{MA}^{Ref}\big|_x = \frac{1}{25}\sum_{i=x-24}^{x} \delta z^{Ref}\big|_i \qquad [6]$$

$$\delta z_{MA}^{Exp}\big|_x = \frac{1}{25}\sum_{i=x-24}^{x} \delta z^{Exp}|_i \qquad [7]$$

With x and i being a location on the cable in metres. The δz_{MA}^{Ref} and δz_{MA}^{Exp} still have a value per meter cable.

[2] This value differed for some cases where the sections were not completely covered by the minimum of two temporal different surveys or for the cases where the cross-sections were smaller than 5.5km (see Section 3.5.2).

For cable installation, it is of interest what the depth of the deepest and shallowest location of the $NMRL_{MA}$ on a cable section with length L (5km) relative to MRSL ($\delta z_d^{Exp}$and δz_s^{Exp} respectively as illustrated in Figure 11b). This can be calculated with the following equations:

$$\delta z_d^{Exp} = \delta z_{deepest}^{Exp} = \min_{xmin \le x \le xmin+L} \left(\delta z_{MA}^{Exp}\right) \quad [8]$$

$$\delta z_s^{Exp} = \delta z_{shallowest}^{Exp} = \max_{xmin \le x \le xmin+L} \left(\delta z_{MA}^{Exp}\right) \quad [9]$$

To obtain the deepest depth relative to the MRSL, the minimum of δz_{MA}^{Exp} over the before mentioned Cable Section should be taken. The shallowest depth relative to the MRSL is obtained by taking the maximum. In principle the $z_{NMRL\ Exp}$ is below -0.25m since the NMRL cannot exceed the MRSL and is lowered by 25cm. This holds for the Experimental Cases of RQ1. With this approach, the δz_s^{Ref} and δz_d^{Ref} were also determined, since the MRSL and Reference Case are always on the same datasets, the δz_s^{Ref} will, by definition, not exceed a value higher than -0.25m.

Similarly, for comparing the extreme differences between the Experimental and Reference Case, the deepest and shallowest values of the Δz_{MA} can be calculated via the following two equations:

$$\Delta z_{MA}|_x = \frac{1}{25} \sum_{i=x-24}^{x} \Delta z|_i \quad [10]$$

$$\Delta z_d = \Delta z_{deepest} = \min_{xmin \le x \le xmin+L} (\Delta z_{MA}) \quad [11]$$

$$\Delta z_s = \Delta z_{shallowest} = \max_{xmin \le x \le xmin+L} (\Delta z_{MA}) \quad [12]$$

A negative $\Delta z|_s$ in metres implies that the complete $NMRL_{MA}$ of the Experimental Case is located below the $NMRL_{MA}$ of the Reference Case.

3.4. OVERVIEW DATA USED PER EXPERIMENT

The surveys used for each experiment are displayed in Table 1. For all experiments related to RQ1 and from the data inclusion part of RQ2, only surveys from the OPeNDAP repository were used since this repository is openly available and information could be found about the applied smoothing method. The experiment cases were compared relative to the NMRL established on the same surveys.

Table 1: Overview of surveys used per Experiment Case and the Reference Case with which it is compared to. The letter indicates which repository has been used. The O, E, and H stand for the OPeNDAP, the NLHO and the EMODnet repository, respectively. The letter in bold indicates which repository has been used for compiling the Reference Case and from which the MRSL has been drafted.

			Years					
		Experiment group	1999	2001	2007	2011	2012	2016
RQ1	1	Percentile	**O**	**O**	**O**	**O**	**O**	**O**
	2	Length cross-sections	**O**	**O**	**O**	**O**	**O**	**O**
	3	Distance between cross-sections	**O**	**O**	**O**	**O**	**O**	**O**
	4	Period between surveys	**O**	**O**	**O**	**O**	**O**	**O**
RQ2	1	Repositories			**O**EH	**O**EH	**O**EH	**O**EH
	2	Grid resolution			**H**	**H**	**H**	**H**
	3	Grid origin			**H**	**H**	**H**	**H**
	4	Including intermediate surveys	**O**		**O**	**O**	**O**	**O**

All the Reference Cases are based on 25m resolution data sets on the same grid as the OPeNDAP surveys. Since the Reference Case is different for the three experiment groups, the letters, as shown in Table 1 will be used in the KPI's to clarify which surveys were used. Besides, the years will be included as well. $t1$ means that the surveys from the years 1999, 2001, 2007, 2011, 2012 and 2016 are used (RQ1). $t2$ means that the surveys from the years 2007, 2011, 2012, and 2016 are used (RQ2.1-3). In RQ2.4, as will be explained in Section 3.6.4, the surveys used differed per run; thus, no abbreviation was made. For example, the NMRL of an Experiment Case for RQ1.2 projected on the cable system is shortened to $z_{NMRL\,Exp\,(O,t1)}$. For RQ2.2, the NMRL of the Reference Case projected on the cable system is shortened to $z_{NMRL\,Ref\,(H,t2)}$.

3.5. RQ1. SENSITIVITY TO PARAMETER SETTINGS

Four parameter settings within the WaterProof's method were tested. Parameter settings refer to the adjustable configurations within the software for establishing the NRML.

3.5.1. Percentile

As WaterProof's method employs a Monte Carlo simulation, 10,000 assemblies are generated (see Section 3.2). Based on assessments of results of earlier modelling by WaterProof and others and based on conversations with WaterProof, the 25th percentile is selected by TenneT as being the representative for the installation of the 'Net op zee' cables, as this was considered at that moment in time to best match with the objective of the lowest lifecycle impact to society for the installation and maintenance of the Net op zee cables (de Swart & van der Laan, 2024). By choosing different percentiles, the NMRL changes directly. The NMRLs based on the 5th, 10th, 15th, 20th, 30th, 35th and 40th percentile were determined for this experiment group. The seven established $z_{NMRL\,Exp(O,t1)}$ were compared relative to the $z_{NMRL\,Ref(O,t1)}$ ($\Delta z_{(O,t1)}$) and relative to the $z_{MRSL,O}$ ($\delta z^{Exp}_{(O,t1)}$).

3.5.2. Length cross-sections

The method of WaterProof to establish the NMRL uses cross-sections with a length of 5.5 kilometres. The PDFs for sand wave migration and growth rate are determined from these cross-sections. When increasing/decreasing the length, more/less sand waves are captured in the cross-section, thus increasing/decreasing the observed migration and growth of sand waves. The cross-section length parameter varied from 1 km, 2km, 3km, 4km, 7km, 8km, 9km, and 10km. Figure 12 shows the cross-sections of the Reference Case (5.5km) and the longest Experiment Case (10km).

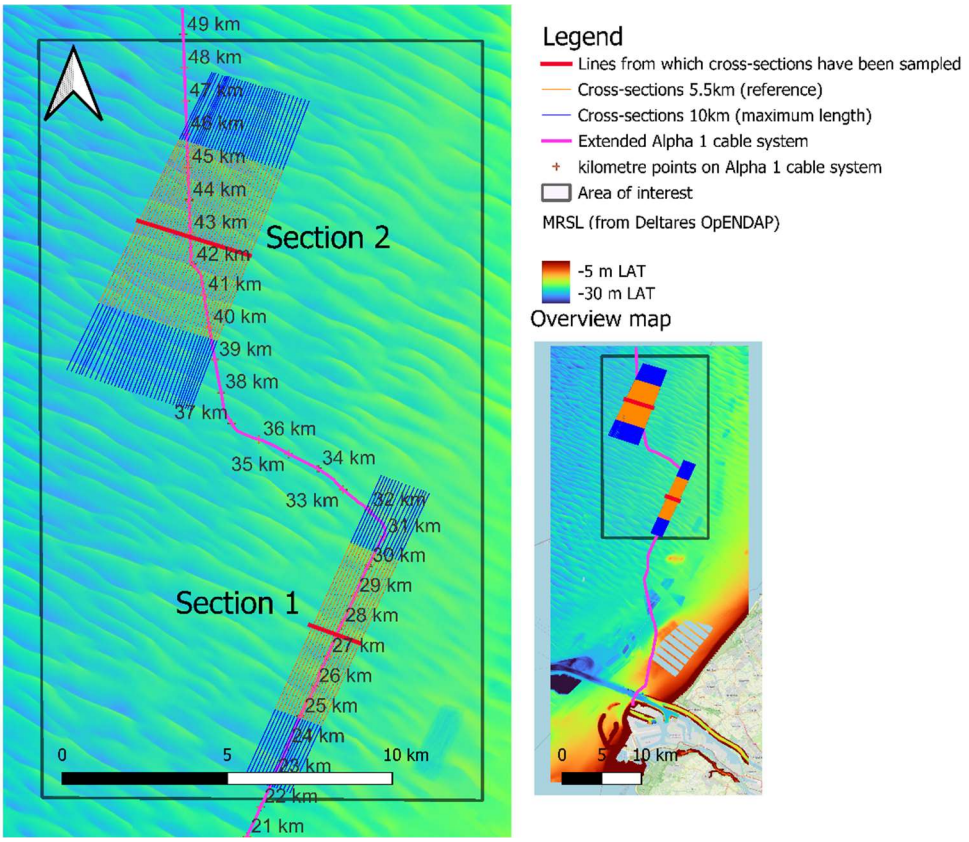

Figure 12: Cross-sections Reference Case (5.5 km) and the maximum length (10 km) on Cable Sections 1 and 2 on the Alpha 1 cable system. The background is the MRSL from the Deltares OPeNDAP repository.

In Cable Section 2, the cross-sections diverge at the Southern side of Section 2 and converge in the North. This is due to the direction of the cross-section following the local perpendicular crest/trough orientation of the tidal sand waves (see Section 3.2). The 10km long cross-sections do not intersect with each other (the minimal distance between cross-sections is 35m; the maximum distance equals 173m). Varying the length of the cross-sections resulted in 8 different $z_{NMRL\ Exp(O,t1)}$. The different $z_{NMRL\ Exp(O,t1)}$ were compared relative to the $z_{NMRL\ Ref(O,t1)}$ with the cross-section of 5.5km ($\Delta z_{(O,t1)}$), and relative to the $z_{MRSL,O}$ ($\delta z^{Exp}_{(O,t1)}$).

3.5.3. Distance between cross-sections

The cross-sections are, in the default settings, 100 m spaced from each other. The cross-sections can be spaced at a higher/lower frequency to include more/less observed migration and growth rates in the probability density functions, which would reduce/increase the need to include cross-sections further away to meet the minimal number of observations (which is 100, see Section 3.2). The cross-sections have been spaced 25m, 50m, 200m, and 400 m apart, as well as the default spacing of 100 m but with an offset of 50m. The impact of the change in distance on the $z_{NMRL\ Exp(O,t1)}$ has been compared relative to the $z_{NMRL\ Ref(O,t1)}$ ($\Delta z_{(O,t1)}$).

3.5.4. Period between surveys

WaterProof's method includes the period between surveys as a parameter but with an accuracy limited to years, as the exact survey dates were unknown for the available datasets. To assess the impact of this period uncertainty, the parameter will be increased and decreased, assuming that the surveys were not held in the same month. The most extreme case was tested, assuming that the first survey was conducted on January 1st and the last survey was held on the 31st of December, the period increases by one year. The other extreme case, assuming that the first survey was carried out on the

31st of December and the last survey on the 1st of January, decreases the period by one year. Besides, the impact on the NMRL will be assessed by assuming that the first survey is executed on the first day of the month and the last survey is executed on the last day of the month and vice versa, extending or decreasing the period by one month. The established $z_{NMRL\ Exp(O,t1)}$ were compared relative to the $z_{NMRL\ Ref(O,t1)}$ ($\Delta z_{(O,t1)}$) and relative to the $z_{MRSL,O}$ ($\delta z^{Exp}_{(O,t1)}$).

3.6. RQ2. SENSITIVITY TO INPUT DATA

3.6.1. Repositories

Despite the difference in data published in the repository of Deltares OPeNDAP and EMODnet, the location of the troughs and crests seems similar. In contrast, the shape of the sand waves in EMODnet seems steeper than in Deltares OPeNDAP (L. Perk et al., personal communication, 27 February 2024). Thus, the datasets from EMODnet could potentially be used to obtain comparable migration rates for the tidal sand waves. Since surveys from the NLHO repository had been obtained, a comparison between the three could be made. This was done by creating an NMRL based on the 2007, 2011, 2012 and 2016 surveys ($z_{NMRL\ Exp(OEH,t2)}$), as these years surveys are available in the OPeNDAP, EMODnet and NLHO repositories. During data pre-processing, all surveys were converted to the same coordinate system and grid resolution (see Section 3.1). After adjusting for the mean difference, see Figure 13, it was observed that there is a constant difference in the 2016 peak/through location between the surveys (lag).

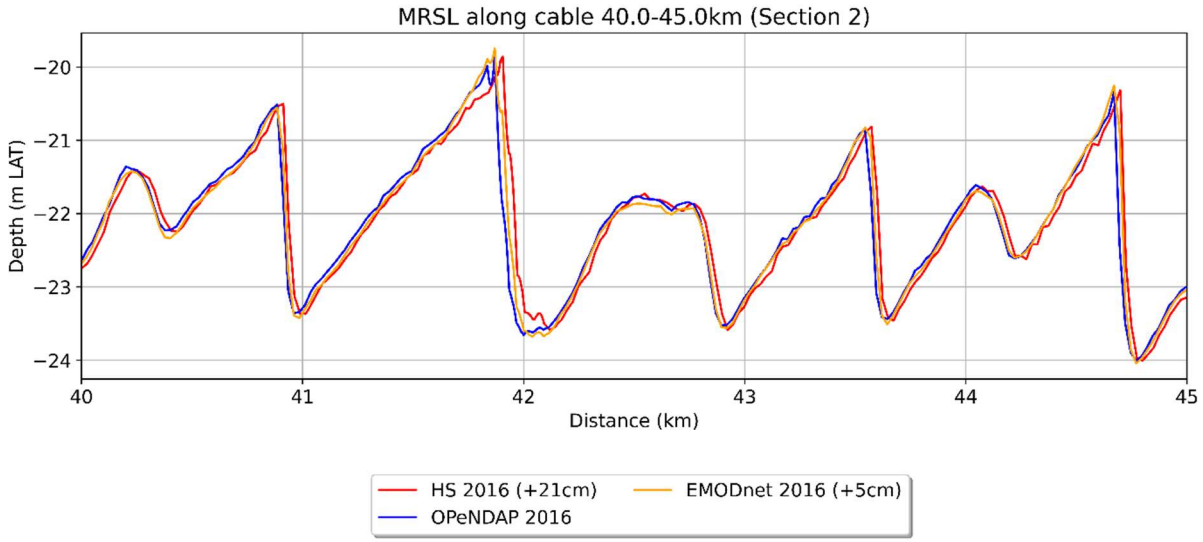

Figure 13: Depth of MRSL (2016) different repositories, after correcting by mean difference

To study the effect of including lag correction, the decision was made to create an NMRL for the different repositories for where the observed lag is corrected for and a case where there has not be corrected for the observed lag.

The surveys available in all repositories differ from those used for the Reference Case, which also includes the year 1999; thus, the comparison between the NMRL will be between the repositories themselves on Cable Section 2 only. Using different repositories also results in a different MRSL. For comparing the NMRL relative to the MRSL ($\delta z^{Exp}_{(O,t2)}$) the MRSL of the OPeNDAP repository ($z_{MRSL(O,t2)}$) was used.

3.6.2. Grid resolution

WaterProof's method for establishing the NMRL currently employs bathymetric data with a grid resolution of 25x25m. This resolution aligns with the resolution mostly available in the bathymetric data in OPeNDAP (see Section 3.1.1). To assess the impact of a different grid resolution on the NMRL established using WaterProof's method, the NLHO datasets were downsampled by averaging to resolutions on a 5m, 10m, and 50 m grid. Due to computational limitations in this research, a resolution smaller than 5x5m was not possible. WaterProof's method was slightly adapted to utilise bathymetric data with a different resolution. This change in resolution could only be done on the datasets out of the NLHO repository from 2007 onwards ($t2$) since these were MBES-obtained bathymetric surveys of a higher resolution (2-4.2m resolution). This implies that the Reference Case used for RQ 1 cannot be used. NLHO Reference Case has been created for this reason ($z_{NMRL,Ref\ (H,t2)}$), this NLHO Reference has the same grid origin and resolution as the surveys in the OPeNDAP repository. The NMRL determined on the different resolutions ($z_{NMRL,Exp\ (H,t2)}$) will be compared relative to the $z_{NMRL,Ref\ (H,t2)}$ ($\Delta z_{(H,t2)}$). Besides, the $z_{NMRL,Exp\ (H,t2)}$ will be compared relative to the 25m resolution MRSL from the NLHO repository ($\delta z^{Exp}_{(H,t2)}$).

According to the method of WaterProof, all representative per cross-section (2D) are interpolated to obtain the 3D NMRL. Since the cross-sections were spaced 100 m from each other, over this distance interpolation was done to obtain a 3D NMRL with the corresponding begin resolution (5m, 10 m and 50m). From there, interpolation was applied again to obtain the NMRL projected on the cable system with metre spacing. The effect of this double interpolation is discussed in Section 5.3.2.

3.6.3. Grid origin

WaterProof's method, utilised to establish the NMRL, uses bathymetric data with a resolution of 25x25m (see Section 3.1.1). The method sets the exact locations for the troughs and crests of sand waves. However, due to the grid resolution and origin, these locations do not necessarily align with the actual crest and trough locations. This difference may affect the calculated migration rate PDF. In addition, the sand wave's height may differ, changing the growth/decay rate. To assess the impact of grid origin location, the bathymetric datasets of NLHO will be downsampled to the 25x25m resolution with a different origin.

The origin found in Deltares OPeNDAP, will be shifted 12.5m (half the grid-cell size) in the mean sand wave migration direction found on Cable Section 2, which is 21.9 degrees. This resampling process is explained in detail in Appendix A.3. An illustration of this shift can be seen in Figure 14, where the blue grid is the grid used Deltares OPeNDAP and orange illustrate the grid used for the Experiment Case.

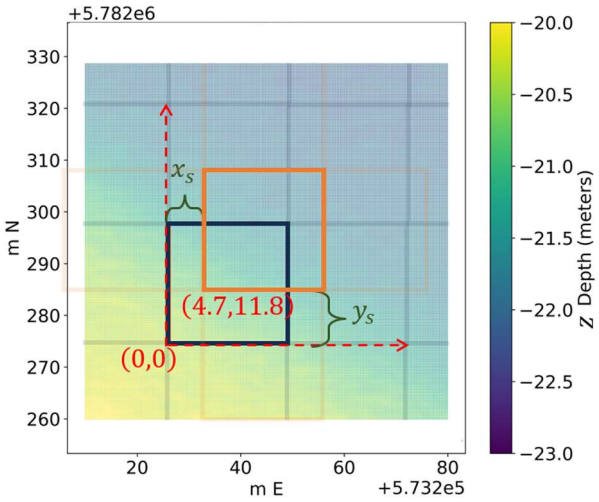

Figure 14: Illustration of relocating the grid origin 12.5m in mean sandwave migration direction, background of TenneT 2017 survey. Blue grid is the grid used in Deltares OPeNDAP and orange indicates the grid used for the Experiment Case.

The created NMRL ($z_{NMRL\ Exp(H,t2)}$) will be compared relative to the NLHO Reference Case ($\Delta z_{(H,t2)}$), the $z_{NMRL\ Ref(H,t2)}$ is described in Section 3.6.2. And to the 25m resolution MRSL from the NLHO repository, which has the same origin as the OPeNDAP repository ($\delta z^{Exp}_{(H,t2)}$).

3.6.4. Including intermediate data sets

On Cable Section 2, five datasets in Deltares OPeNDAP are available (see Appendix B). The NMRL created via WaterProof's method is determined based on the oldest and newest bathymetric survey available; in the case of Cable Section 2 this corresponds to 1999 and 2016. respectively. Between these datasets, the migration (dx) and growth (dz) are determined (see Figure 15a for illustration), which are then divided by the period (eleven years) to get the corresponding migration and growth rates ($dxdt$ and $dzdt$). This means intermediate surveys are not used (except for some missing data in the other surveys). The use of intermediate surveys to observe sand wave growth and migration is investigated here. This results in more observed growth and rates (see Figure 15b for illustration). Note that this can result in growth observed in locations with only decay and vice versa.

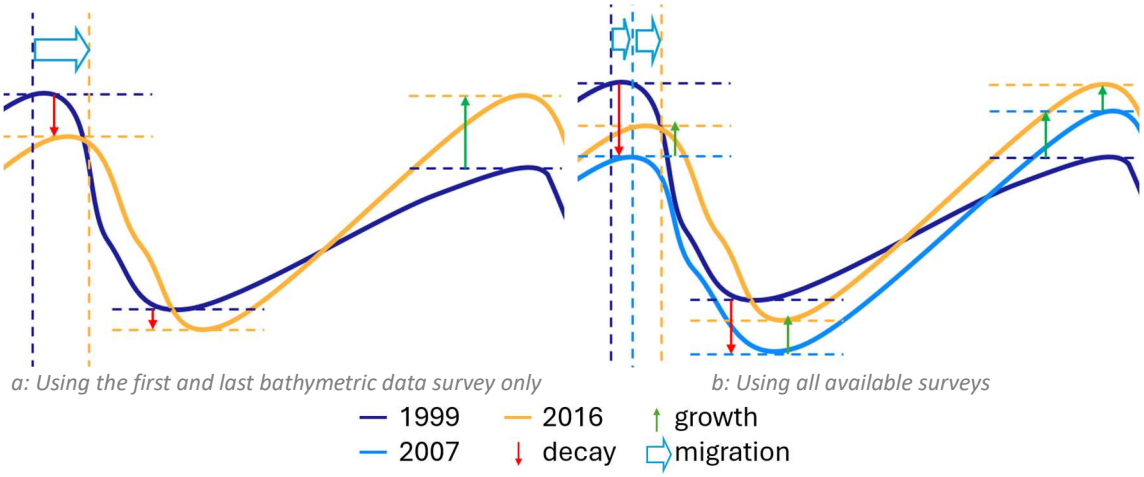

Figure 15: Illustration of the migration and growth/decay rates between surveys of a crest/through/crest sequence along one cross-section, not on scale.

Adding one intermediate survey results in twice the number of observed growth/decay and migration rates. This growth is linear and follows the following equation:

$$n_{obs} = N \times (n_{survey} - 1) \quad [13]$$

Where n_{obs} is the total number of observations on one cross-section, N is the number of observations per cross-section and the $n_{surveys}$ is the number of surveys used.

Besides including intermediate surveys, it is also possible to exclude surveys. With this, the effect of changing the first and last survey was investigated. By doing this, it was tested what NMRL would be estimated when surveys (for example the 2016 survey) would not be available. For Cable Section 2, all possible combinations are shown in Table 2, note that 2011 and 2012 are seen as one survey since together they cover the whole area of interest (see Appendix C) and are carried out only four months after each other (see Appendix A.1).

Table 2: Possible combinations with four different surveys for Cable Section 2

	Years included			
Name case	1999	2007	2011/2012	2016
Reference*	**x**			**x**
Temp0	**x**			**x**
Temp1	**x**	**x**		
Temp2	**x**		**x**	
Temp3		**x**	**x**	
Temp4		**x**		**x**
Temp5			**x**	**x**
Temp6	**x**	**x**		**x**
Temp7	**x**		**x**	**x**
Temp8	**x**	**x**	**x**	
Temp9		**x**	**x**	**x**
Temp10	**x**	**x**	**x**	**x**

**The Reference Case utilises only the oldest and newest available survey. The 1999 survey contains voids in the coverage, so some cross-sections were filled with survey data from 2007, 2011, or 2012. Thus, the Reference Case is slightly different from the Temp 0 case.*

All Experiment Cases determined the NMRL for 2078. Temp0 up to Temp5 were used to study the effect of changing the first and the last survey and Temp6 up to Temp10 were used to assess the effect of including intermediate surveys on the NMRL.

4. RESULTS

4.1. RQ1. SENSITIVITY TO PARAMETER SETTINGS

4.1.1. Percentile

Changing the percentile parameter in WaterProof's method directly results in a different $z_{NMRL\ Exp(O,t1)}$. Increasing the percentile results in a deeper-located NMRL. To quantify the change of the NMRL, the depth relative to the Reference Case was determined. The probability of occurrence is plotted against the depth relative to the Reference Case in Figure 16. For this, the $NMRL_{MA}$ was determined. For example, in Cable Section 1, for the 5th percentile, 20% of the $NMRL_{MA}$ is more than 38cm deeper than the $z^{\times}_{NMRL\ Ref}$. For the 20th percentile, 50% of the $NMRL_{MA}$ is 3 cm lower in Section 1 and 5 cm lower in Section 2 compared to the 25th percentile of the Reference Case. At the 30th percentile, 50% is 2 cm higher in Section 1 and 4 cm higher in Section 2 than the 25th percentile. The 10th, 15th, 35th and 50th percentiles were also tested and can be seen in Appendix G.1.

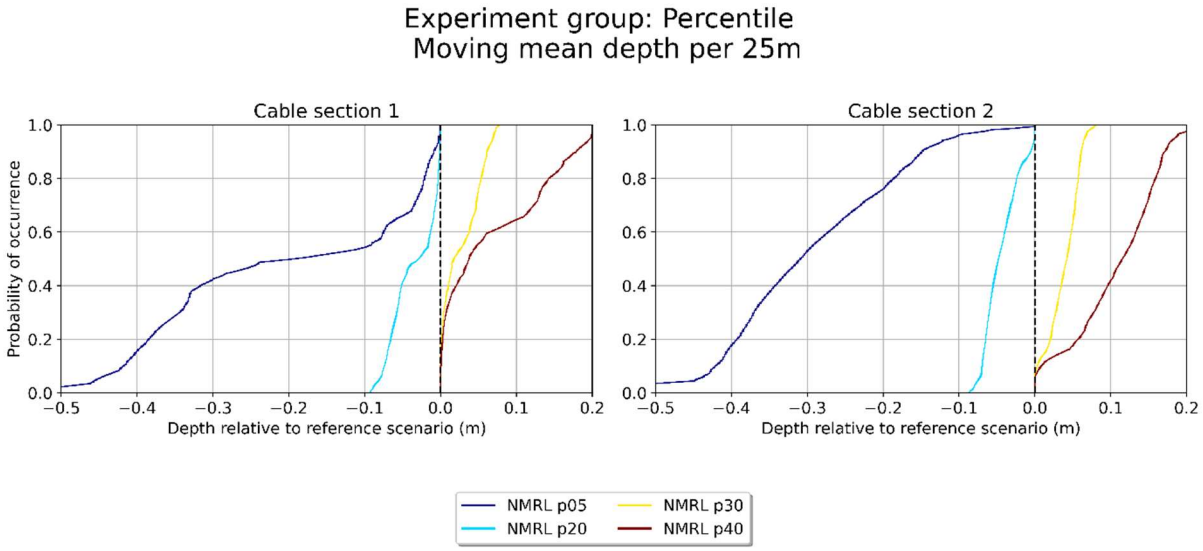

Figure 16: Moving mean depth of the NMRL for a 25m cable length relative to the Reference Case for the full sections. The NMRL is shown for various cases with different percentiles.

In Figure 16, the $NMRL_{MA}$ per 25m cable relative to the Reference Case is shown. This was also done for the moving average per 5m cable (see Appendix G.1), minor differences were seen between the moving average NMRL per 25m and the moving average NMRL per 5m cable (the median difference is below 0.3% for all cases; see Appendix G.1). Locally, the absolute difference between the 5 and 25m moving average is more prominent, up to 5 cm for the p05 cm, whereas this is around 3 cm for the Reference Case.

The effects of changing the percentile regarding the position in the seabed of the NMRL are summarised in Table 3. The p20 and p30 cases have the highest NSE and lowest RMSE values, indicating that these NMRLs are the closest to the $z_{NMRL\ Ref(O,t1)}$. Deviating the percentile more from the 25th percentile (Reference Case) results in a lowering of the NSE value and an increase in the RMSE value. Increasing the percentile results in a deeper $\delta z^{Exp}_{(O,t1),d}$.

Table 3: KPIs for case group Percentile

Case	NSE (-)	RMSE (in cm)	$\delta z^{Exp}_{(O,t1),d}$ (in cm)	$\Delta z_{(O,t1),d}$ (in cm)	$\Delta z_{(O,t1),s}$ (in cm)
Reference (p25)	-	-	-123	-	-
p05	-0.54	29.63	-201	-54	0
p10	0.46	17.57	-156	-33	0
p15	0.81	10.31	-141	-20	0
p20	0.96	4.73	-131	-9	0
p30	0.97	4.07	-117	0	8
p35	0.90	7.71	-111	0	15
p40	0.78	11.11	-107	0	22
p50	0.47	17.41	-97	0	36

4.1.2. Length cross-sections

To study the effects of the cross-section length in WaterProof's method on the NMRL, the cross-section length was varied between 1,000 m and 10,000 m (see Section 3.5.2). In doing so, fewer or more migration rates (dx/dt), peak growth rates ($dz/dt,p$) and through growth rates ($dz/dt,t$) observations were captured per cross-section. The resulting number of observations is lowest for the shortest cross-sections (1 km), with an average of 37 observations per cross-section. In total, 73 crests and 63 throughs were observed resulting in 73 dx/dt and $dz/dt,p$, and 63 $dzdt,t$ on the cross-sections with a length of 1 km (for comparison, 894 crests or troughs were observed for the reference length of 5.5 km; resulting in 456 dx/dt and $dz/dt,p$, and 438 $dz/dt,t$). The number of observations increases when lengthening the cross-sections up to 148 crests/throughs on average for the cross-sections with a length of 10 km (with 860 $dxdt$ and $dz/dt,p$, and 839 $dz/dt,t$).

In Figure 17, the boxplots show the distribution of the number of observations per cross-section created for Cable Section 1. In the boxplot, the Inter Quartile Range (IQR) is shown, running from the 1st quadrant (25th percentile) to the 3rd quadrant (75th percentile). The median is displayed as orange line and outliers (smaller than the 1st quadrant minus 1.5 times the IQR or larger than the 3rd quadrant plus 1.5 times the IQR) are marked as circles. The average number of observations for the three rates for the 10,000 m case for Cable Section 1 equals 98 observations; for Cable Section 2, the average number of observations is 171 (see Figure 18). In Figure 17and Figure 18, it is seen that lengthening the cross-sections results in more observations used per cross-section.

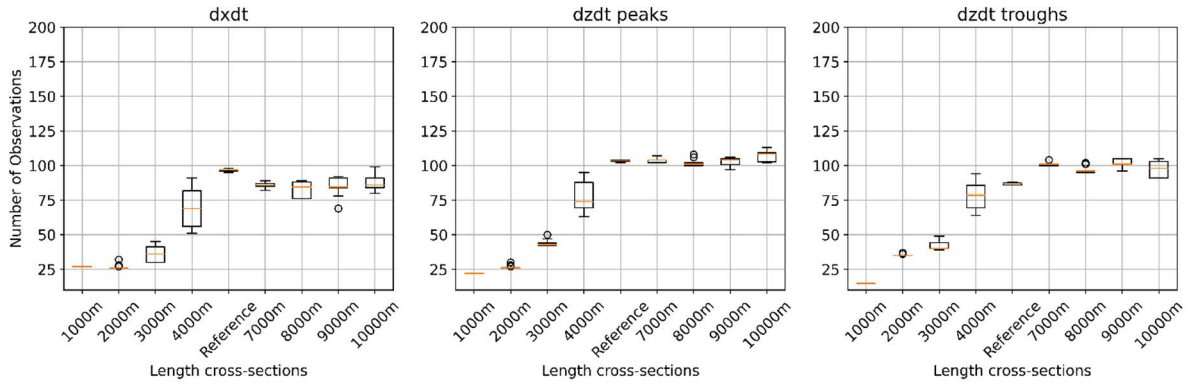

Figure 17: Boxplot showing the number of observations per cross-section created for Cable Section 1 for different cross-section lengths.

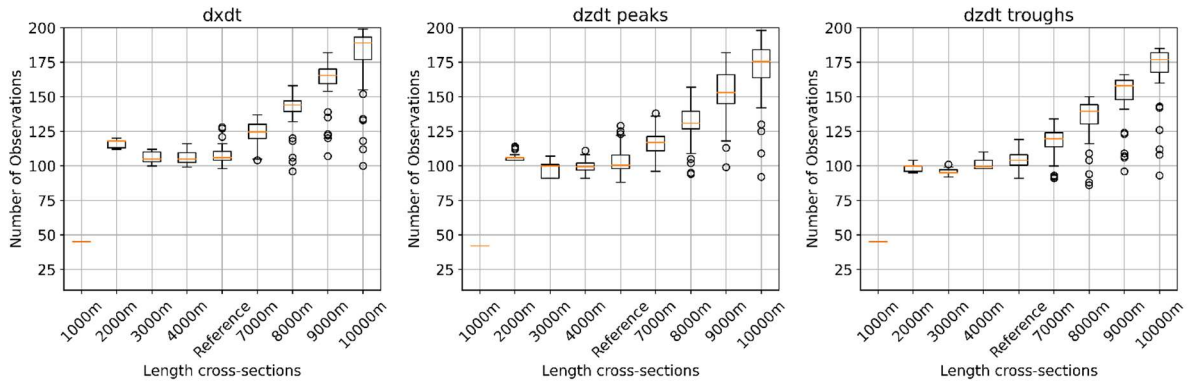

Figure 18: Boxplot showing the number of observations per cross-section in Cable Section 2 for different cross-section lengths.

The observations were used to establish a PDF for the migration and growth rates per cross-section. Figure 19 shows the effect of the cross-section length on the average PDF estimations of the 1,000 m, 5,500 m (reference) and 10,000 m cross-sections. The average PDF was estimated by using all the individual observations for all individual cross-sections within a case for a given Cable Section. This figure shows that despite shortening or lengthening the cross-section, it does not lead to a large change in the average PDFs for Cable Section 2. For Cable Section 1, the PDF of the migration rate for the 1,000 m case is wider (mainly affecting the right tail of the distribution) and thus, on average, higher migration rates will be sampled compared to the Reference and 10,000 m case.

A large difference in the median of the migration rate PDF estimation between Cable Section 1 and 2 is seen. The median migration rate on Cable Section 2 is for the Reference Case 1.0 m/year whereas on Cable Section 1 this is 0.26 m/year (as shown in Figure 19).

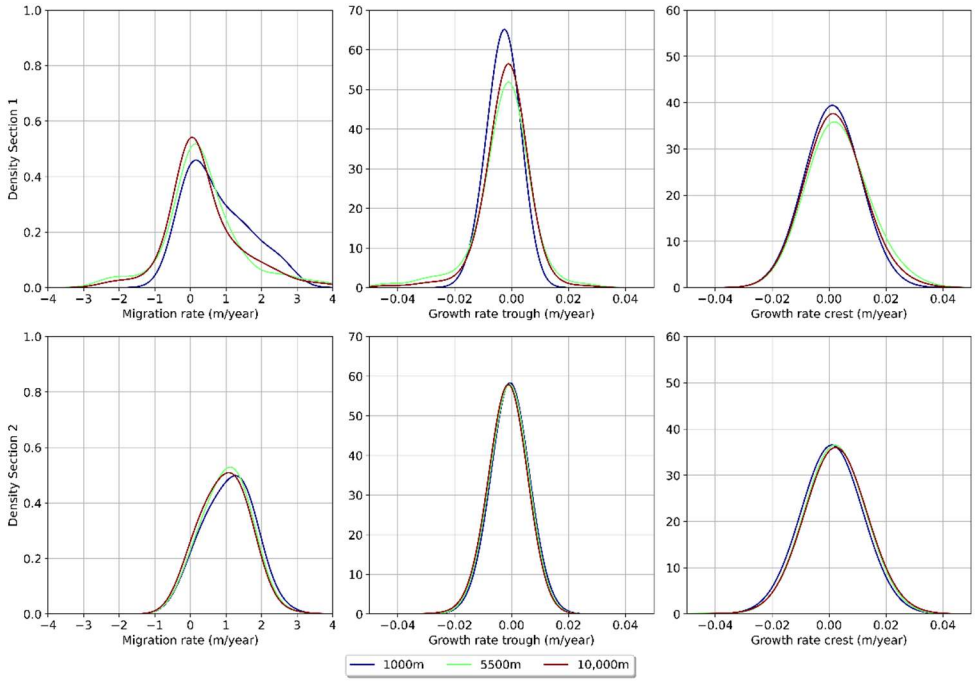

Figure 19: PDF estimations for varying cross-section length for migration and growth rates.

Looking more closely at the migration rate per cross-section, it can be observed that there is no variation between the different PDFs per cross-section for the 1,000 m length in Section 2. Besides, lengthening the cross-section increases the interquartile range of PDFs.

Figure 20 shows the NMRL for each case for the varying cross-section lengths along two Cable Sections[3]. The MRSL is displayed alongside the NMRLs; for Section 1, the MRSL dates from 2011, while for Section 2, it is from 2016.

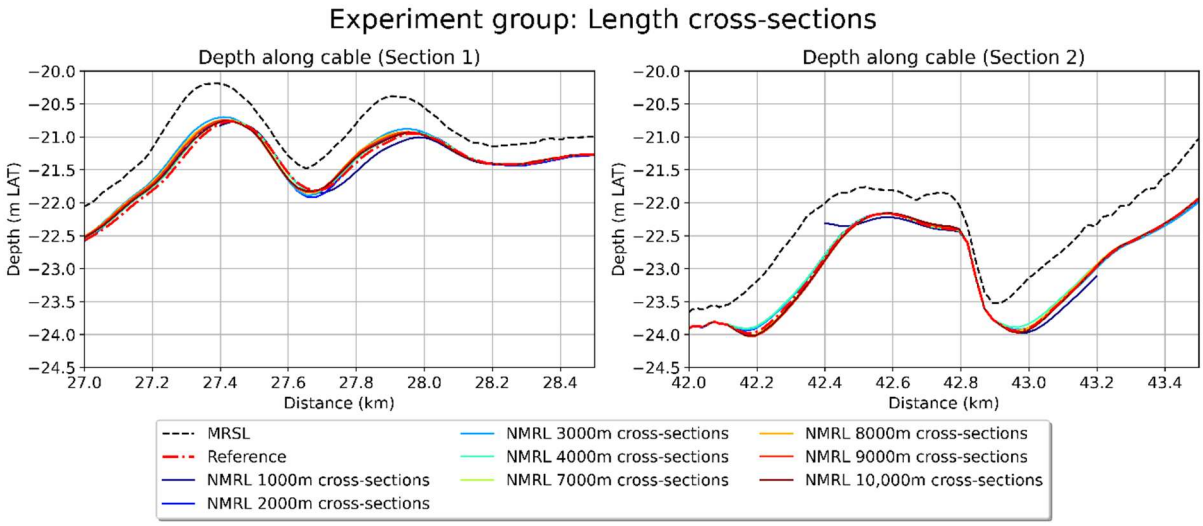

Figure 20: NMRL on extended Alpha 1 cable system computed with different cross-section lengths.

To compare the differences in the NMRL, the MRSL was subtracted from the NMRL, resulting in a depth relative to the MRSL, $\delta z_{(0,t1)}^{Exp}$ (see Figure 21). The method of WaterProof prevents the NMRL from exceeding the MRSL, after which it includes an additional uncertainty margin of 25cm (see Section 3.2). Therefore, the NMRLs displayed in Figure 21 do not exceed 25cm below the MRSL. The 1,000 m long cross-sections do not cover the complete section of the cable and, therefore, show some boundary effects.

Lengthening the cross-section results in a lower NMRL at the onset of the stoss side of the sand wave on Cable Section 2. This stays in the order of centimetres. Also, a difference is seen between the different sections; in Cable Section 2, the NMRLs are located up to 0.55 m deeper (8000 m case) relative to the MRSL than Cable Section 1. This may be due that the height of the sand waves present in Cable Section 2 is slightly higher compared to the sand waves present in Cable Section 1.

[3] Note that firstly, the NMRL was interpolated on these Cable Sections and secondly, the shown sections do not represent the entire investigated area, but a smaller section of it (Section 1: 27.00-28.50 km; Section 2: 42.00-43.50 km). These smaller parts were chosen so that at least one peak and two troughs could be seen.

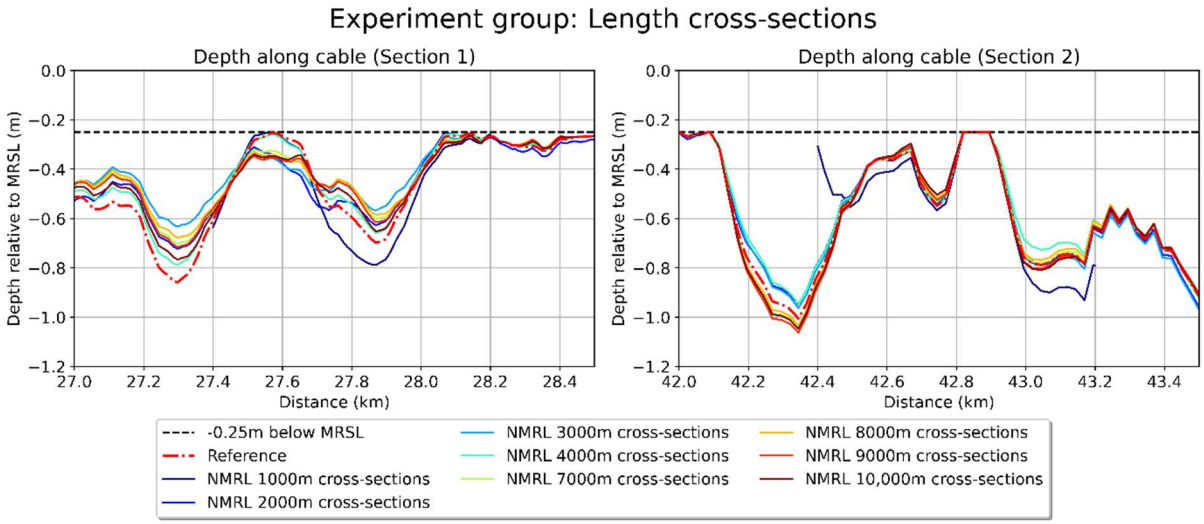

Figure 21: NMRL on extended Alpha 1 cable system relative to the MRSL computed with different cross-section lengths

The effects of the cross-section length on the NMRL are summarised in Table 3. Here, the NSE, RMSE, the $\delta z^{Exp}_{(O,t1),d}$, $\Delta z_{(O,t1),d}$ and $\Delta z_{(O,t1),s}$ are presented for Section 1 and Section 2 combined. Note that negative numbers correspond with a deeper $z_{NMRL\,Exp(O,t1)}$ relative to the $z_{MRSL\,(O,t1)}$ or $z_{NMRL\,Ref\,(O,t1)}$. The 1,000 m long cross-section case has the lowest NSE and the highest RMSE, implying that this case differs the most from the Reference Case. Lengthening the cross-sections from the Reference Case to 10,000 m, does not increase/decrease the maximum depth relative to the MRSL ($\delta z^{Exp}_{(O,t1),d}$).

Table 4: KPIs for case group Length cross-sections

Case	NSE (-)	RMSE (in cm)	$\delta z^{Exp}_{(O,t1),d}$ (in cm)	$\Delta z_{(O,t1),d}$ (in cm)	$\Delta z_{(O,t1),s}$ (in cm)
Reference (5500m)	-	-	-123	-	-
Length cross-section 1000m*	0.74	9.08	-91	-1.7	13.7
Length cross-section 2000m*	0.94	5.23	-99	-6.7	7.0
Length cross-section 3000m*	0.90	7.04	-132	-6.5	10.1
Length cross-section 4000m*	0.98	3.50	-125	-8.9	3.5
Length cross-section 7000m	0.94	5.85	-123	-8.1	5.5
Length cross-section 8000m	0.93	6.13	-123	-6.8	3.6
Length cross-section 9000m	0.94	5.73	-123	-6.1	6.9
Length cross-section 10,000m	0.96	4.87	-123	-6.1	5.2

**This cross-section is shorter than the Cable Section, and therefore, the NSE and RMSE have been determined on a shorter Cable Section than the 5km Cable Section, as explained in Section 3.3.*

4.1.3. Distance between cross-sections

To examine the effects of spacing the cross-sections in WaterProof's method on the NMRL, the distance between the cross-sections was varied between 25m and 400m. At a 25m distance, 64 cross-sections were generated for Cable Section 1 and 142 for Cable Section 2. This resulted in 3,533 unique observations, with an average of almost 290 observed migration and growth rates used per cross-section. In contrast, at a 400 m interval, only five cross-sections were created on Cable Section 1 and eight on Cable Section 2, yielding 218 unique observations and an average of 71 migration and growth rates used per cross-section.

In Figure 22, the boxplots show the distribution of the number of observations used per cross-section. Decreasing the length between cross-sections increases the number of observations used per cross-section. The median of the Reference Case (103 observations) and the case with a 50 m offset (102) barely differ. The interquartile range of the 25m distance between cross-sections case (345) is larger compared to the Reference Case (5). This difference is caused by the difference in the median number of observations used per cross-section between Section 1 (148) and Cable Section 2 (370) (see Appendix G.2).

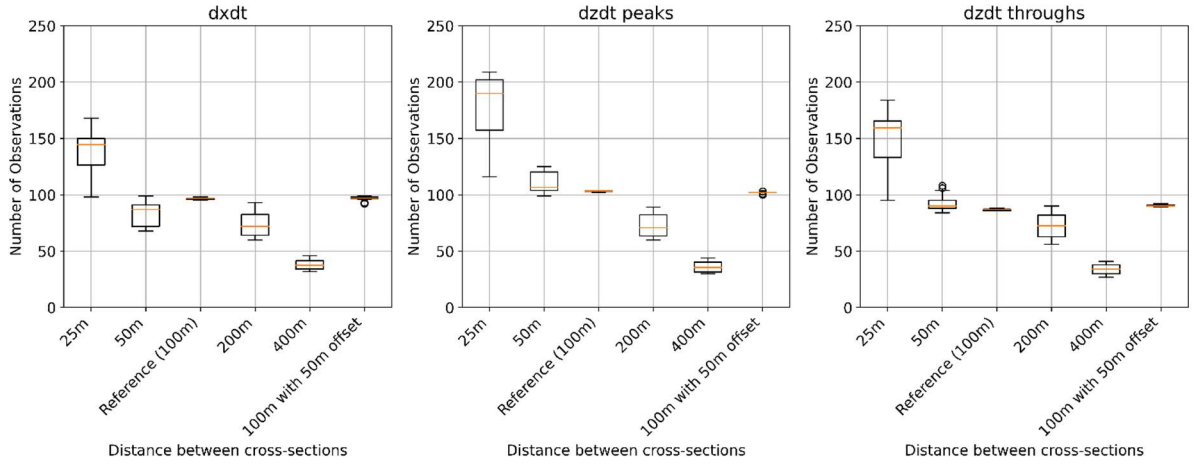

Figure 22: Boxplot showing the number of observations per cross-section in Cable Section 1 for different spacing of cross-sections.

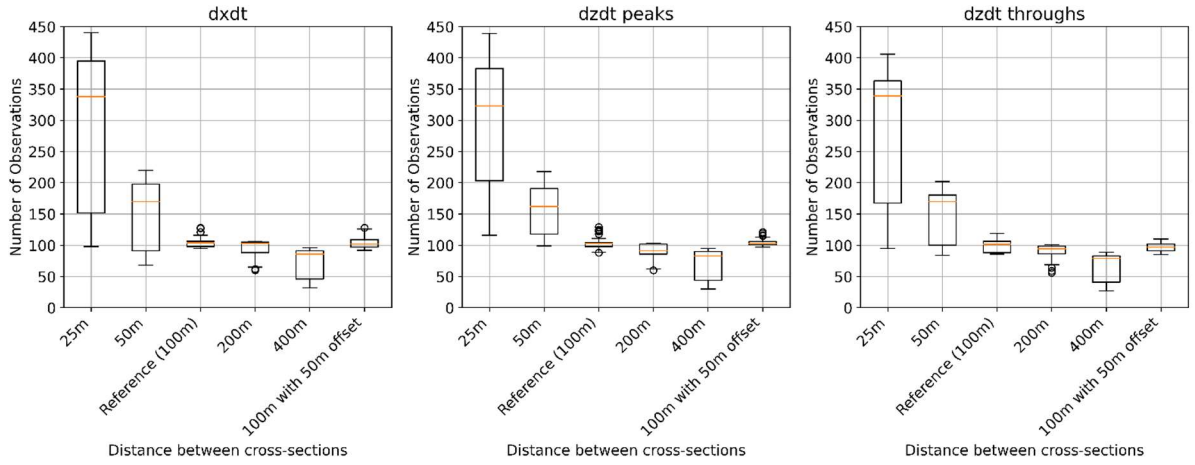

Figure 23: Boxplot showing the number of observations per cross-section in Cable Section 1 for different spacing of cross-sections.

The observations were used to establish a PDF for the migration and growth rates per cross-section. In Figure 24, the different PDFs for the migration rate per cross-section of Section 2 are displayed for three cases. The 50 m case displays 103 PDFs, 51 more than the Reference and the 100 m distance with a 50 m offset case.

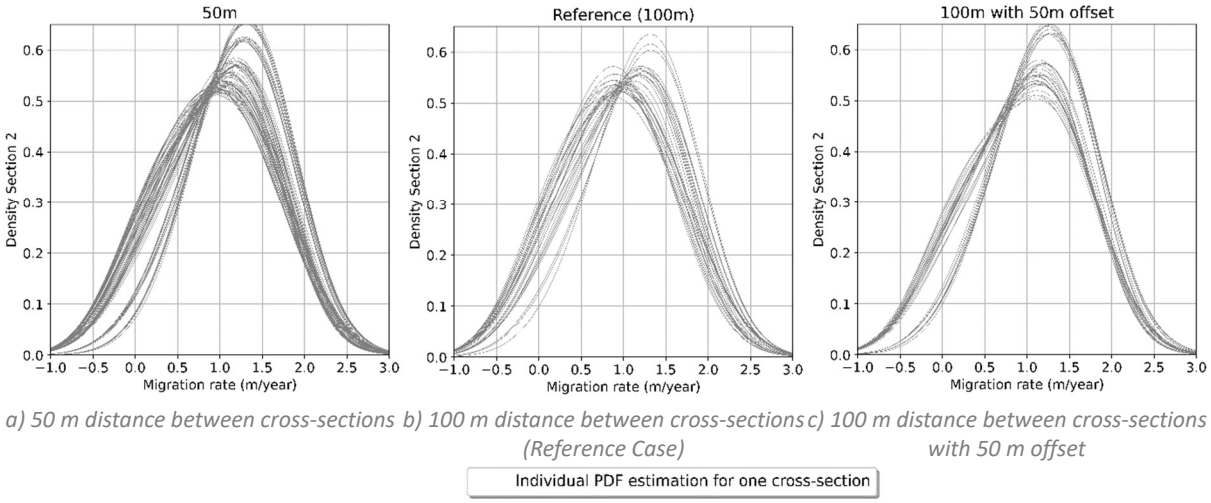

a) 50 m distance between cross-sections *b) 100 m distance between cross-sections (Reference Case)* *c) 100 m distance between cross-sections with 50 m offset*

Figure 24: Individual migration PDF estimation per cross-section within Cable Section 2 for different spaced cross-sections (50m, 100 m (Reference) and 100 m with 50 m offset).

Figure 25 shows the effect of the distance between cross-sections on the NMRL relative to the MRSL[4] ($\delta z^{Exp}_{(O,t1)}$). Increasing the distance between cross-sections results in a shallower stoss side, a higher crest, and a deeper trough in the NMRL compared to the Reference Case for Cable Section 1. For Cable Section 2, a larger distance between cross-sections results in a, on average, deeper NMRL (on average, 8cm deeper for a 400 m distance between cross-sections).

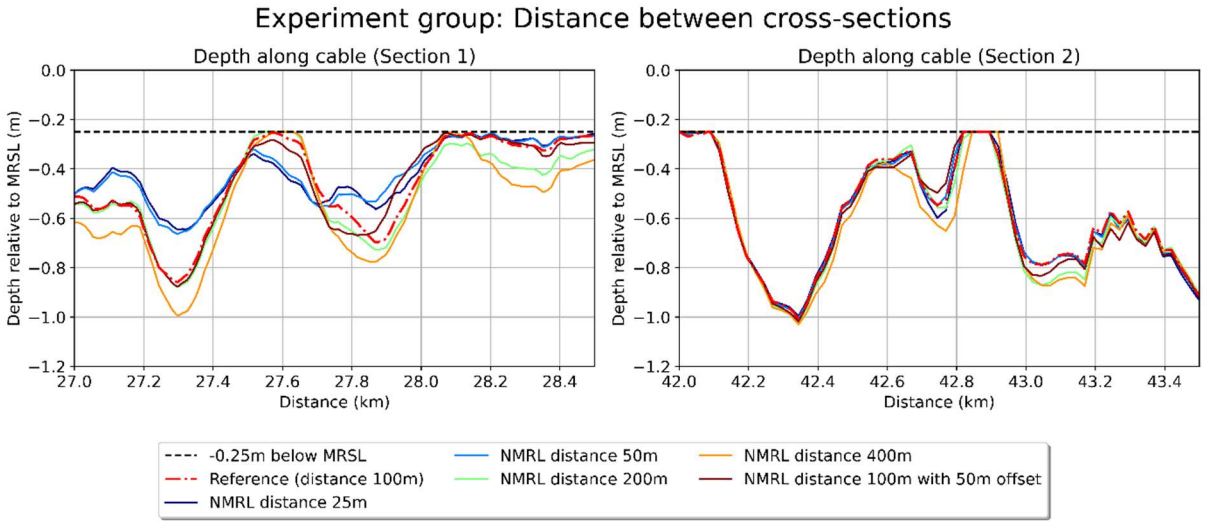

Figure 25: NMRL on extended Alpha 1 cable system relative to the MRSL computed with different distances between the cross-sections.

The effects of changing the distance between the cross-sections or introducing an offset are summarised in Table 5. The 50 m offset has the highest NSE value and lowest RMSE, indicating that the NMRL of this case is the closest to the NMRL of the Reference Case. However, the NMRL depth in

[4] Note that 1) the NMRL was projected by interpolation on these Cable Sections and 2) the shown sections do not represent the entire investigated area, but a smaller section of it (Section 1: 27.00-28.50 km; Section 2: 42.00-43.50 km)

this case is locally almost 10cm deeper than the Reference Case, which is larger than for the 25 and 50 m cases. The 400 m distance has the lowest NSE and highest RMSE, and has the deepest $\delta z^{Exp}_{(O,t1),d}$.

Table 5: KPIs for case group Distance between cross-sections.

Case	NSE (-)	RMSE (in cm)	$\delta z^{Exp}_{(O,t1),d}$ (in cm)	$\Delta z_{(O,t1),d}$ (in cm)	$\Delta z_{(O,t1),s}$ (in cm)
Reference (100 m distance)	-	-	-123	-	-
25m distance	0.92	6.68	-127	-5	8
50 m distance	0.94	6.03	-126	-5	8
200 m distance	0.96	4.70	-126	-14	7
400 m distance	0.86	8.87	-151	-29	9
50 m offset and 100 m distance	0.97	4.28	-132	-10	11

4.1.4. Period between surveys

The sensitivity of using survey data with monthly accuracy instead of yearly accuracy in WaterProof's method on the NMRL was examined by varying the period between surveys between minus one and plus one year (see Section 3.5.4). Increasing the period between surveys divides the observed migration and growth by a larger period, thereby decreasing the rate and narrowing the PDF (by extending the period by one year (6-8% increase[5]), the IQR reduces by approximately 5%; see Appendix G.4). Decreasing the period on the other hand results in larger rates and an increase of the width of the PDF (by decreasing the period by one year, the IQR increases by approximately 4%; see Appendix G.4).

The effects of changing the period between the surveys are summarised in Table 6. Varying the period by extending it to the maximum, minimum, and one-month difference caused a few centimetres deviation compared to the Reference Case. Decreasing the period by one year, the minimal period between surveys results in the largest deviation in $\delta z^{Exp}_{(O,t1),d}$ of -121cm.

Table 6: KPIs for case group Period between surveys.

Case	NSE (-)	RMSE (in cm)	$\delta z^{Exp}_{(O,t1),d}$ (in cm)	$\Delta z_{(O,t1),d}$ (in cm)	$\Delta z_{(O,t1),s}$ (in cm)
Reference	-	-	-123	-	-
Maximal period	1.00	1.49	-124	-4	2
Plus one month period	1.00	0.59	-123	-2	2
Minus one month period	1.00	0.46	-122	-1	1
Minimal period	1.00	1.92	-121	-3	5

In this study, the exact execution dates were obtained via data requests, which were obtained later than the experiments were executed. The possible impact of implementing the actual dates is discussed in Section 5.2.4.

[5] Depending on the Cable Section, a different period is between the first and last survey.

4.2. RQ2. SENSITIVITY TO INPUT DATA

4.2.1. Repositories

To study the effect of different data sources on the NMRL determined via WaterProof's method, three different repositories were investigated and used to establish different NMRLs (see Section 3.6.1). The repositories, NLHO, EMODnet and the used repository of RQ1, OPeNDAP. Some pre-processing had to be carried out before the different repositories could be used to establish the NMRLs (see Section 3.1). The surveys in the NLHO and EMODnet repositories had to be reprojected and resampled first to be on the same grid and resolution as the OPeNDAP repository (see Appendix A.2 and D.1 for NLHO and EMODnet, respectively). Only the via MBES obtained datasets of 2007, 2011, 2012, and 2016 ($t2$) could be used, and therefore only an NMRL comparison could be obtained on Cable Section 2 (see Section 3.6.1).

From all three repositories, the observations were obtained via the same method as for previously discussed cases (see Section 3.2). The average PDF estimations (where all observations per experiment case are included) for the growth rate of the trough and crest in Figure 26 show an almost perfectly symmetrical shape for all repositories. This implies that the variability in sampled growth rates is evenly distributed around the median. The crest's growth rate observed in OPeNDAP tends to be the largest (median at 0.4 cm/year). The median growth rate of the trough is negative for all repositories; the largest deepening is present in the EMODnet repository, with a median trough growth rate of -0.5 cm/year. Note that differences between the PDF estimations of OPeNDAP in Figure 26, and previously shown PDF estimations of the Reference Case (RQ1) are present due to the difference in surveys used (1999 is excluded in RQ2). The migration rate is less symmetrical compared to the growth rates. This broader distribution implies that migration rates will be sampled with more variability.

Despite looking at the same survey years, the migration and growth PDFs created on observations of the surveys from the NLHO have the lowest peak, around zero, compared to the other repositories. This implies that fewer migration rates are concentrated around zero, resulting in more extensively (positive and negative) sampled migration and growth rates.

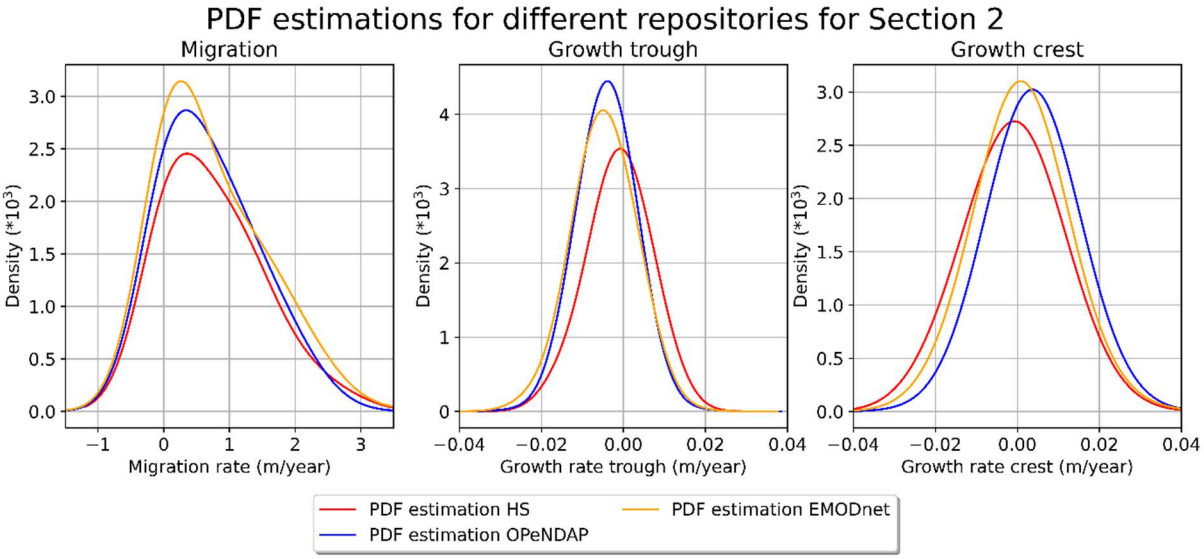

Figure 26: Estimated PDFs for the migration and growth rates of the crest and trough for every repository.

Some further pre-processing had to be carried out before the different repositories could be used to establish the NMRLs (see Section 3.1). The difference in reference level had to be corrected and optionally, the observed lag (-29 m between NLHO and OPeNDAP and -13 m between EMODnet and

OPeNDAP; see Appendix F) between surveys had to be corrected. These steps from pre-processing can be seen in Figure 27 on the 2016 survey (MRSL present on Cable Section 2): the reprojected and resampled depth profile (left), the corrected by mean difference over an area of 20.1 km^2 (middle), and the corrected by mean and by lag (right).

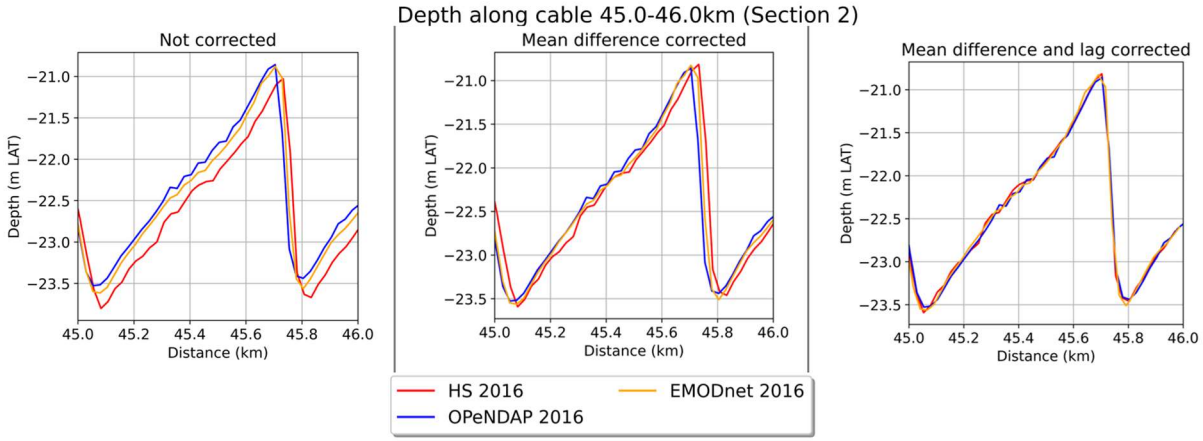

Figure 27: MRSLs illustrating the data pre-processing on Cable Section 2.

After reprojecting and resampling, the datasets of the NLHO and EMODnet repositories have the same 25m resolution as the OPeNDAP repository. After correcting the repositories by mean difference, the NMRL per repository relative to the $z_{MRSL\ (O,t2)}$ was determined. As displayed in Figure 28a, it is seen that the $z_{NMRL\ Exp(H,t2)}$ (NLHO) and $z_{NMRL\ Exp(E,t2)}$ are exceeding the $z_{MRSL\ (O,t2)}$ (for the NLHO and EMODnet repositories up to 77 and 68 cm, respectively). This is because the NMRLs established on the NLHO and EMODnet repositories are bounded by the MRSL from the corresponding repository when creating the NMRL and thus may exceed the MRSL of the OPeNDAP repository when compared.

The $\delta z^{Exp}_{(OEH,t2)}$ for the different repositories were also determined after executing the last pre-processing step, correcting for the observed lag difference as can be seen in Figure 28b. The $z_{NMRL\ Exp(H,t2)}$ (NLHO) does not exceed the $z_{MRSL\ (O,t2)}$ (16 cm as minimal depth between the MRSL and the NMRL). The $z_{NMRL\ Exp\ (E,t2)}$ (EMODnet) exceeds the $z_{MRSL\ (O,t2)}$ by 4 cm.

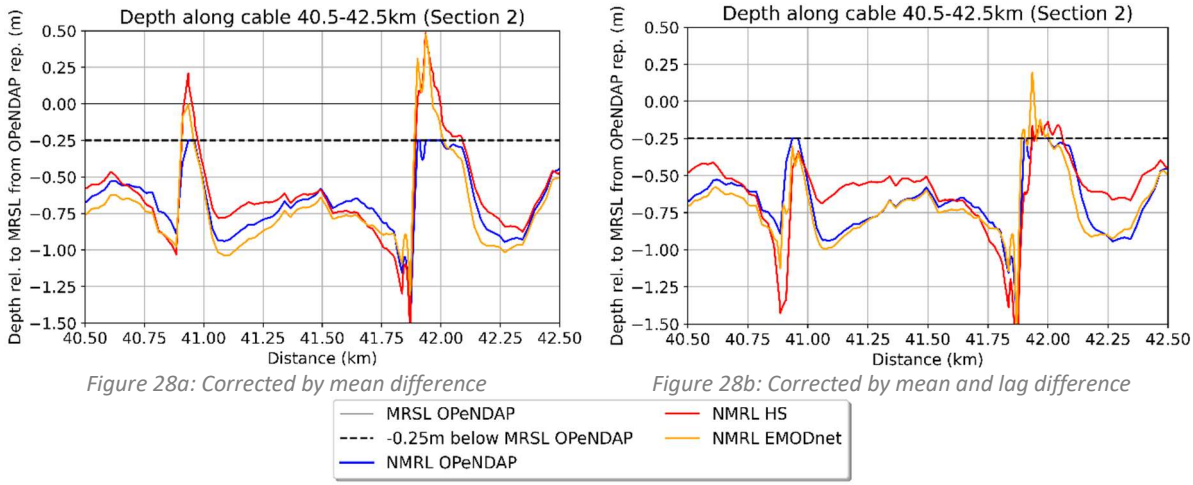

Figure 28a: Corrected by mean difference

Figure 28b: Corrected by mean and lag difference

Figure 28: NMRL on extended Alpha 1 cable system Section 2, relative to the OPeNDAP MRSL, computed with different repositories.

Table 7 summarises the impact of using different repositories on establishing the NMRLs. Here, the NSE, RMSE, the $\delta z^{Exp}_{(O,t2),d}$, $\delta z^{Exp}_{(O,t2),s}$ $\Delta z_{(O,t2),d}$ and $\Delta z_{(O,t2),s}$ are shown. The EMODnet, corrected by mean and with or without lag correction, demonstrates higher NSE and lower RMSE values than the

NLHO cases. This indicates that the NMRL derived from the EMODnet repository aligns more closely with the NMRL generated from the OPeNDAP repository than the NLHO repository. The NLHO corrected by both mean and lag shows the lowest NSE and highest RMSE value, implying this case is the most overall different to the OPeNDAP created NMRL. However, this case also has the smallest $\Delta z_{(O,t2),d}$ and $\Delta z_{(O,t2),s}$.

Table 7: KPIs for case group Repositories

Case	NSE (-)	RMSE (in cm)	$\delta z^{Exp}_{(O,t2),d}$ (in cm)	$\delta z^{Exp}_{(O,t2),s}$ (in cm)	$\Delta z_{(O,t2),d}$ (in cm)	$\Delta z_{(O,t2),s}$ (in cm)
OPeNDAP	-	-	-130	-25	-	-
NLHO only mean difference correction	0.39	17.22	-128	77	-19	102
EMODnet only mean difference correction	0.61	13.75	-107	68	-19	98
NLHO mean and lag difference correction	0.29	18.47	-163	-16	-25	34
EMODnet mean and lag difference correction	0.81	9.70	-120	4	-33	36

4.2.2. Grid resolution

To study the effects of the grid resolution of the survey data on the NMRL established via WaterProof's method, the grid resolution of the NLHO repository was varied from 5 m up to 50 m. The NLHO repository was used since it had the highest resolution available with sufficient coverage (see Appendix A.1 for these resolutions). The following figure shows the MRSL (from 2016) of one peak and trough with resolutions varying from 2 m to 50 m.

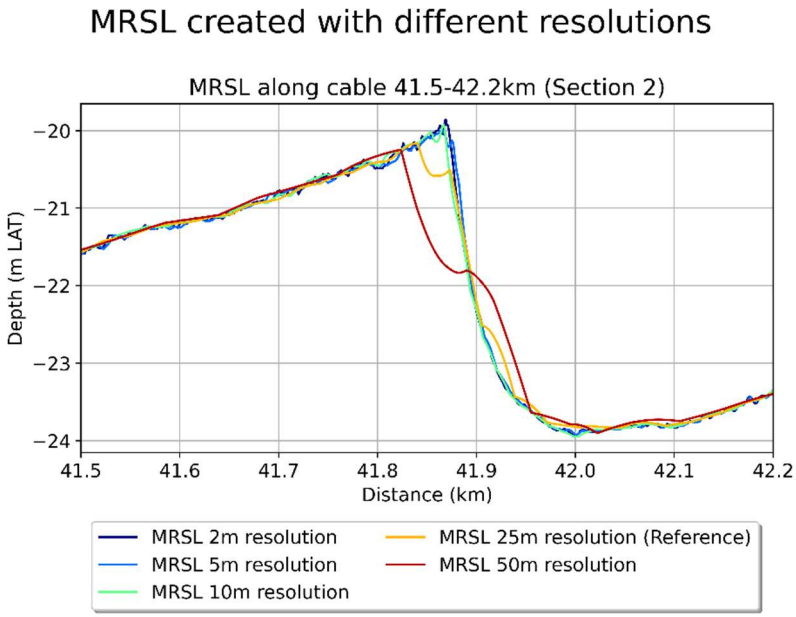

Figure 29: MRSL obtained from NLHO on different resolutions.

Note that due to bilinear interpolation on the cable route, a depth is determined per meter. This causes a sharp drop in height followed by a bump in the MRSL on the 25m and 50 m (between 41.8 and 41.9 km). Due to this, the height of the peaks decreases when the resolution increases. The maximum difference in MRSL between the 50 m and 2m resolutions is 1.89 metres and is observed in the peak shown in the Figure 29. The depth of the throughs reduces when resolution increases. However, this difference is less significant than in the peaks.

Figure 30 displays the average PDFs (where all observations per experiment case are included) for the migration and growth rate for the different resolutions by using all observations within Cable Section 2. A slight deviation (less than 4%) in IQR is seen for the growth rates. The 50 m resolution significantly lowers the migration rate. The median migration rate is 0.10 m/year, whereas this is for the Reference Case, 0.7 m/year. The migration rate PDF estimation is for the 10 m resolution the highest, with a median of 1.0 m/year.

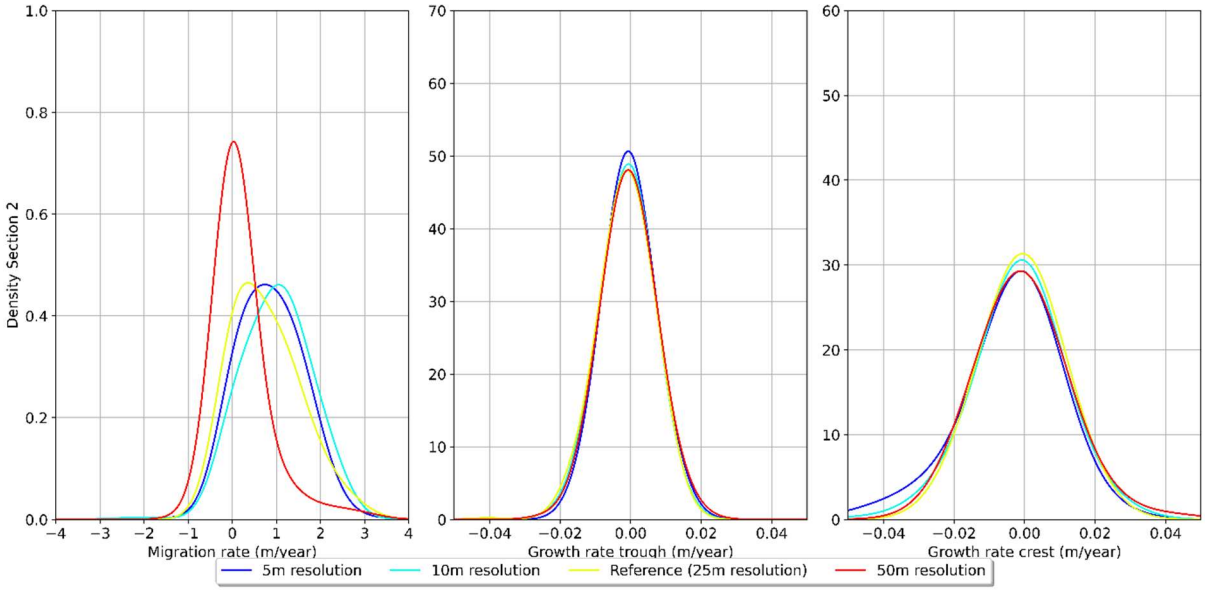

Figure 30: PDF estimations for migration and growth rates for various resolutions.

In Figure 31 the $z_{NMRL\ Exp(H,t2)}$ established on the 5, 10, 25 and 50-metre resolutions are displayed. The $z_{NMRL\ Exp(H,t2)}$, determined on the 50-meter resolution, has a lower depth on the stoss side of the sand waves; the $z_{NMRL\ Exp(H,t2)}$ is up to 25cm higher than the $z_{NMRL\ Exp(H,t2)}s$ determined on other resolutions. In the throughs, the depths of the different $z_{NMRL\ Exp(H,t2)}s$ are similar.

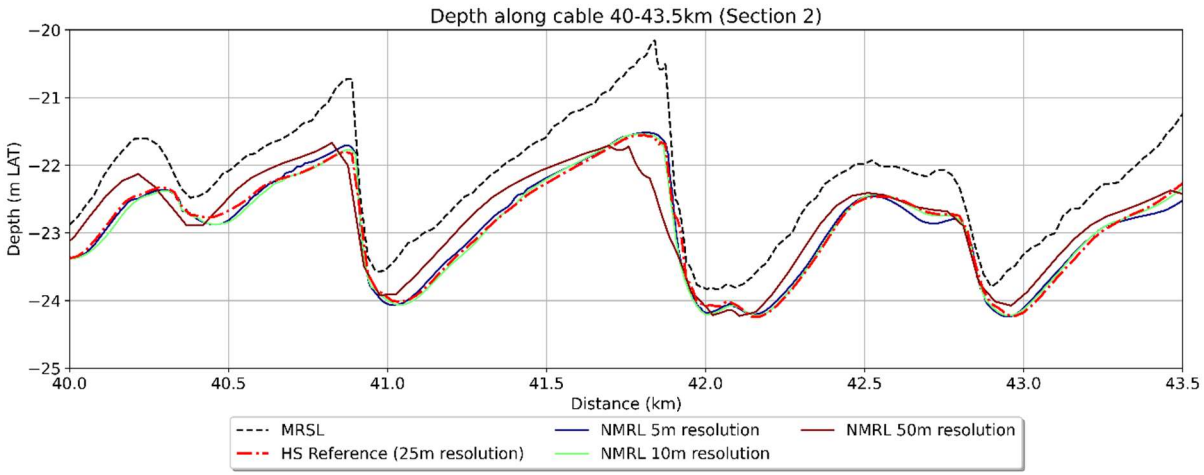

Figure 31: NMRL on extended Alpha 1 cable system computed with datasets of the NLHO with different grid resolutions.

The 50 m resolution $z_{NMRL\ Exp(H,t2)}$ a bump in the peak (around 41.5-42km). This is caused by a similar bump in the peak of the MRSL, as shown in Figure 29.

The $z_{NMRL\ Exp(H,t2)}s$ relative to the 25m resolution MRSL of the NLHO repository ($z_{MRSL\ (H,t2)}$) are displayed in Figure 32. The $\delta z^{Exp}_{(H,t2)}$ established on the 5m and 50 m resolution grid are sometimes

above the 25cm below MRSL level. This is due to the usage of different MRSLs for the cases; for every resolution, an MRSL was created on the down-sampled NLHO survey data but is displayed in Figure 32 relative to the 25m resolution MRSL.

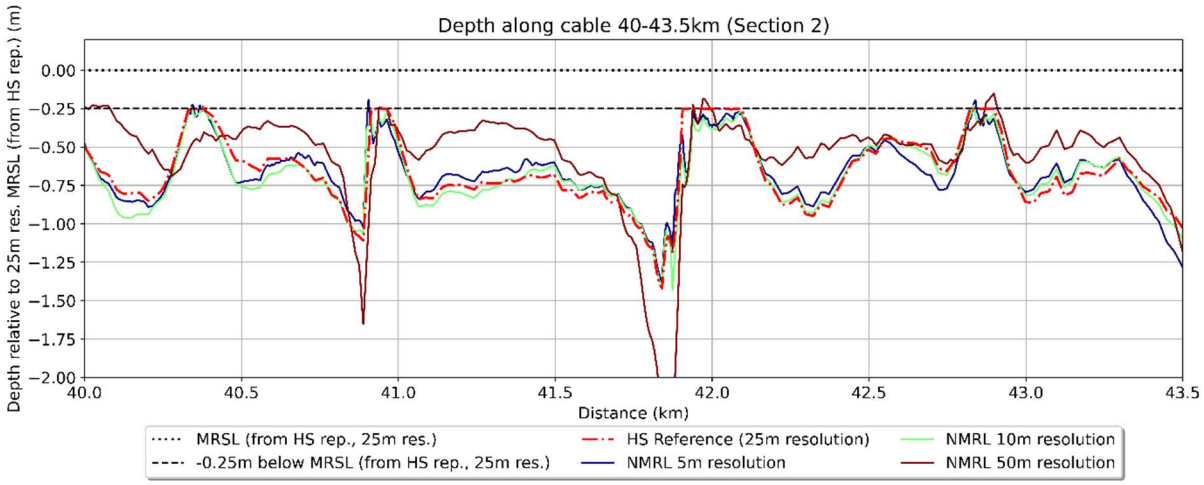

Figure 32: NMRL on extended Alpha 1 cable system Section 2, relative to the NLHO 25m resolution MRSL, computed on different resolutions.

Table 8 summarises the effects of using different resolutions on the NMRL. The $z_{NMRL\ Exp(H,t2)}$ based on the 10 m resolution corresponds the closest to the $z_{NMRL\ Ref(H,t2)}$ as the NSE value is the highest and RMSE is the lowest. The 5m resolution $z_{NMRL\ Exp(H,t2)}$ shows the same $\delta z^{Exp}_{(H,t2),s}$ as the NLHO Reference Case but is locally 35 cm deeper than the Reference Case ($\Delta z_{(H,t2),d}$).

Table 8: KPIs for case group Grid resolution

Case	NSE (-)	RMSE (in cm)	$\delta z^{Exp}_{(H,t2),d}$ (in cm)	$\delta z^{Exp}_{(H,t2),s}$ (in cm)	$\Delta z_{(H,t2),d}$ (in cm)	$\Delta z_{(H,t2),s}$ (in cm)
NLHO reference (25m resolution)	-	-	-136	-25	-	-
5m resolution	0.84	9.56	-142	-25	-35	24
10 m resolution	0.90	7.77	-134	-24	-42	18
50 m resolution	0.40	28.47	-221	-14	-109	54

4.2.3. Grid origin

The impact of grid origin choice on the NMLR established by WaterProof's method is tested by changing the grid's origin in the NLHO repository with one resampling strategy as was explained in Section 3.6.3. This resulted in a $z_{NMRL\ Exp(H,t2)}$ which is shown in Figure 33. The $z_{NMRL\ Exp(H,t2)}$ 21.9 degrees case is comparable to the $z_{NMRL\ Ref(H,t2)}$ over Cable Section 2. Nevertheless, there is a large difference in the lee side with a 63 cm deeper located NMRL (at 41.94 km).

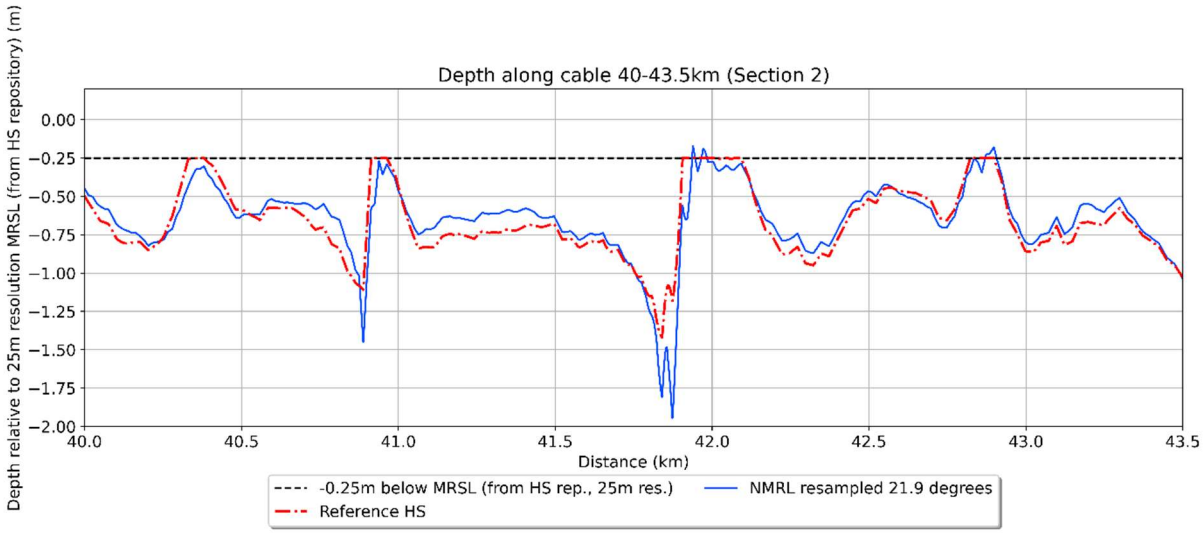

Figure 33: NMRL on extended Alpha 1 cable system Section 2, relative to the NLHO 25m resolution MRSL, computed on resampled survey data of the NLHO repository.

Besides a difference in NMRL, the MRSL is also different. Due to the sampling, especially the peaks can be higher (up to 15cm) and at a slightly other location; an example is provided in Figure 34.

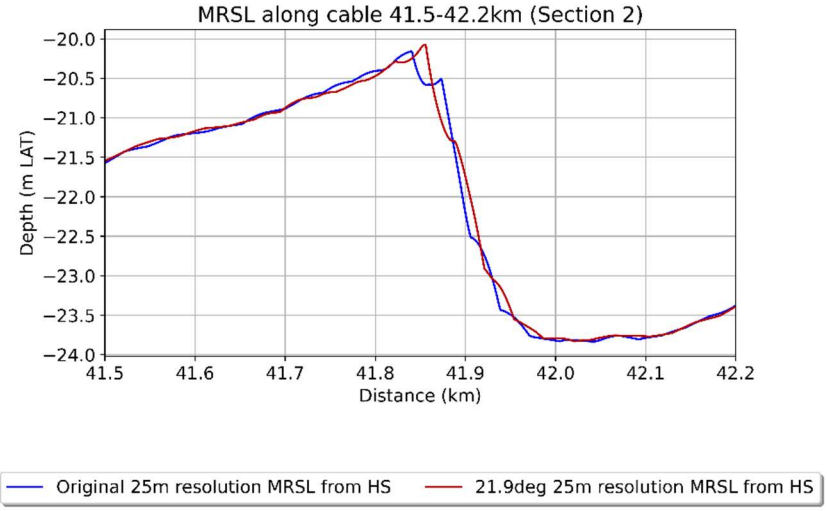

Figure 34: MRSL from NLHO repository on 25m resolution with different sampling grids. Note that this is interpolated bilinearly to the Alpha 1 Cable route.

Looking at the KPIs, the $z_{NMRL\ Exp(H,t2)}$ is different to the $z_{NMRL\ Ref(H,t2)}$ the NSE value is 0.79. Locally, the $\delta z^{Exp}_{(H,t2),s}$ is with -17 cm, 8 cm closer to the MRSL than the NLHO Reference Case. Also, the distance between the $z_{NMRL\ Ref(H,t2)}$ and the $z_{NMRL\ Exp(H,t2)}$ shows deeper levels (maximum of -63 cm).

Table 9: KPIs for case group Grid origin

Case	NSE (-)	RMSE (in cm)	$\delta z^{Exp}_{(H,t2),d}$ (in cm)	$\delta z^{Exp}_{(H,t2),s}$ (in cm)	$\Delta z_{(H,t2),d}$ (in cm)	$\Delta z_{(H,t2),s}$ (in cm)
NLHO reference (no resampling)	-	-	-136	-25	-	-
21.9 deg	0.79	10.91	-174	-17	-63	20

4.2.4. Including intermediate data sets

To observe the sensitivity of changing the first and last survey used for establishing the NMLR. Temp 0 up to Temp 5 were created, including only two surveys, excluding the others available in the OPeNDAP repository on Cable Section 2. In Figure 35 the average PDF estimation (where all observations per experiment case are included) for Temp 0-5 are displayed. Varying the first and last survey does impact the average PDF estimation. The median of the migration rate of Temp 0 (1999 and 2016) is the largest with 1.0 m/year, followed by Temp 2 (1999 and 2011/12) with 0.9 m/year. The lowest median migration rate is observed for Temp 5 (2011/12 and 2016) with 0.3 m/year. Temp 5 also displays the lowest peak and most negative median in the growth rate of the through implying that the through will decay more relative to the other cases.

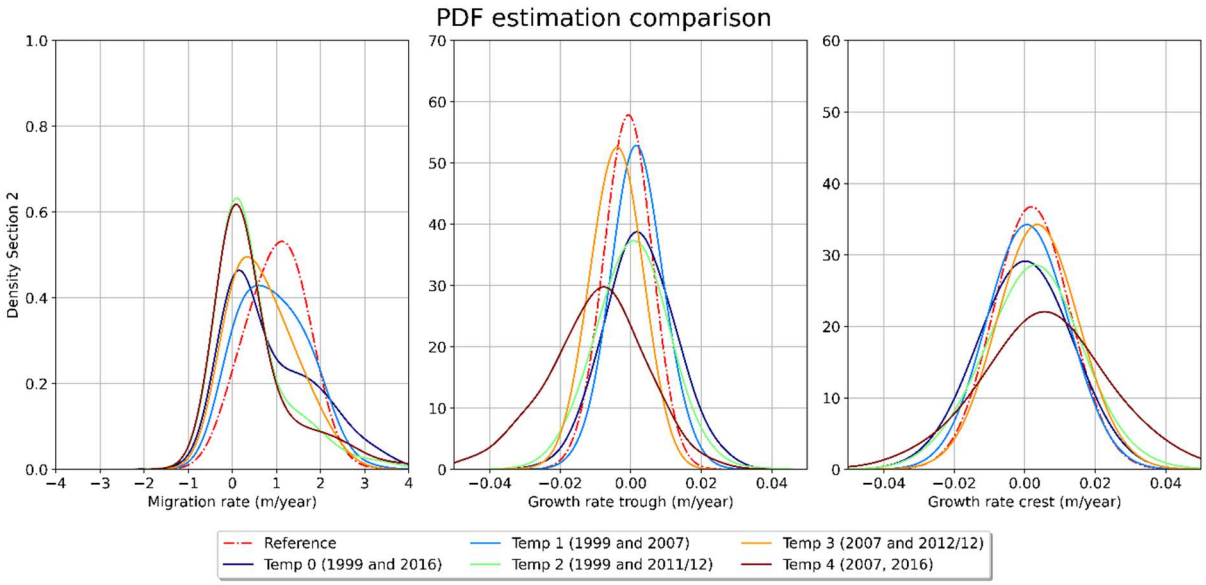

Figure 35: PDF estimations for migration and growth rates for various combinations of the first and last surveys.

The $z_{NMRL\ Exp\ (O)}$ values of these cases are displayed in Figure 36 relative to the $z_{MRSL\ (O,t1)}$ ($\delta z^{Exp}_{(O,t1)}$). It shows that the NMRLs with the shortest intermediate period (4 years), Temp 3 and Temp 5, have deep troughs relative to the MRSL ($\delta z^{Exp}_{(O,t1),d}$), namely 201 and 190 cm and show the most difference compared to the $z_{NMRL\ Ref\ (O,t1)}$ (with a RMSE above 25 cm). The oldest possible survey combination Temp 1, with 1999 and 2007, is with a $\delta z^{Exp}_{(O,t1),d}$ of 199 cm, also much deeper compared to the deepest depth (123 cm) of the $z_{NMRL\ Ref\ (O,t1)}$ relative to the MRSL. The experiments which did not use the 2016 survey (Temp 1, 2 and 3) are exceeding the 25cm below the MRSL ($z_{MRSL\ (O,t1)}$) by up to 14 cm.

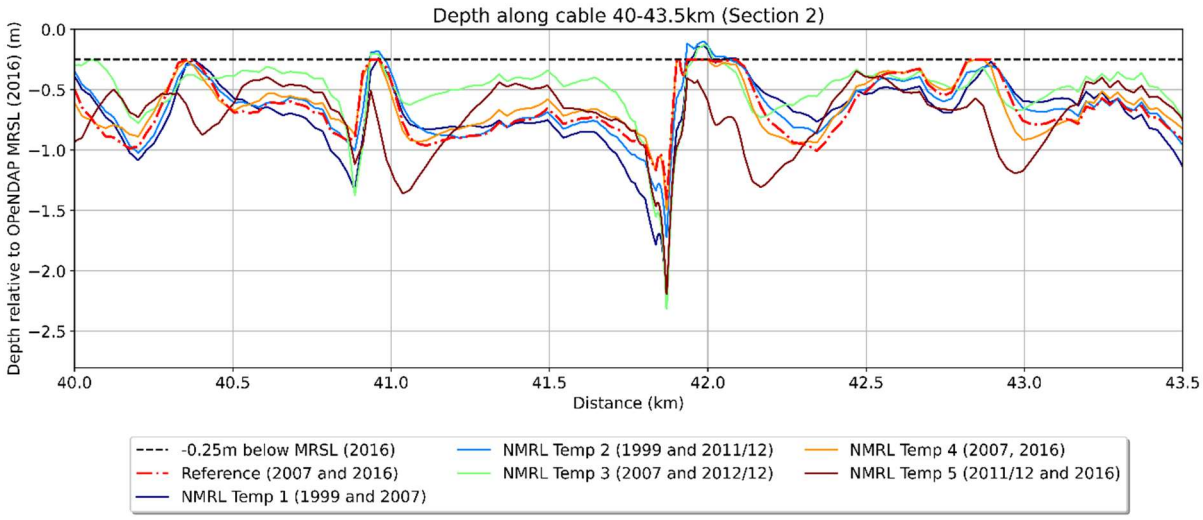

Figure 36: NMRL on extended Alpha 1 cable system Section 2, relative to the NLHO 25m resolution MRSL, using only two surveys per NMRL.

The differences caused by including intermediate surveys in determining the migration and growth rates ($dxdt$ and $dzdt$) of observed sand waves was tested by Temp 6-10. Figure 37 shows the average PDF estimations for the migration and growth rates. Including intermediate surveys, the differences between Temp 6-10 are smaller compared to the observed differences in Temp 0-5. With 0.8 m/year the median migration of Temp 6 (1999, 2007 and 2016) is slightly larger than Temp 7 (1999, 2011/12 and 2016). Temp 9 (2007, 2011/12 and 2016) has the lowest median migration rate of 0.4 m/year. The IQR of the Reference Case for the growth rate of the crest is the smallest (0.05 m/year), implying that the variation in the sampled crest growth rates for the Experiment Cases is larger.

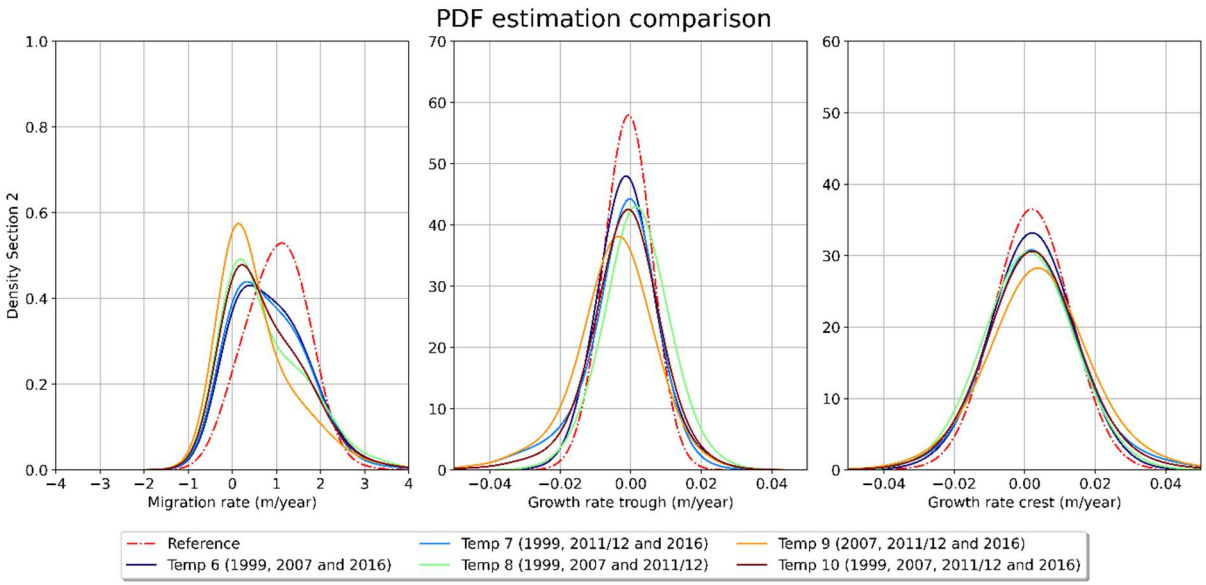

Figure 37: PDF estimations for migration and growth rates for various combinations for including intermediate surveys.

In Figure 38, the NMRLs which include the surveys 1999 and 2007 (Temp 6 and 8), have a longer deepening on the stoss side compared to the other surveys. The deepest NMRL relative to the current present MRSL and was created on this MRSL is the Temp 9 case (not including 1999) with $\delta z_{(O,t1)}^{Exp}$ equal to -160cm.

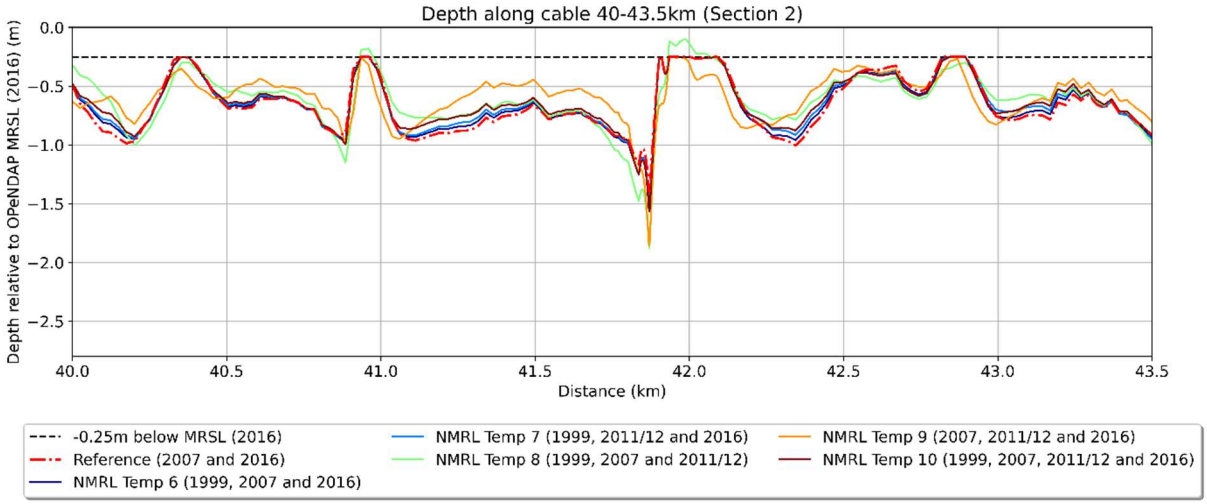

Figure 38: NMRL on extended Alpha 1 cable system Section 2, relative to the NLHO 25m resolution MRSL, using three or four surveys per NMRL and intermediate migration and growth observations.

Table 11 summarises the KPIs determined for Temp 0-10 and shows that the NMRL with intermediate periods of 4 years, Temp 3 and Temp 5, result in a negative NSE value and the highest RMSE value.

The differences between the surveys which use 1999 and 2016 (Temp 0, 6, 7 and 10) show the highest NSE and lowest RMSE values and show to be the closest to the Reference Case. None of the experiment cases does exceed the MRSL of 2016, which was seen in Section 4.2.2 and Section 4.2.3 when the MRSL was not included in the Experiment Case

Table 10: KPIs for case group Data Inclusion

Case	NSE (-)	RMSE (in cm)	$\delta z^{Exp}_{(O,t2),d}$ (in cm)	$\delta z^{Exp}_{(O,t2),s}$ (in cm)	$\Delta z_{(O,t2),d}$ (in cm)	$\Delta z_{(O,t2),s}$ (in cm)
Reference	-	-	-123	-25	-	-
Temp0 (1999 and 2016)	1.00	0.63	-122	-25	-1	3
Temp1 (1999 and 2007)	0.38	18.38	-199	-11	-77	26
Temp2 (1999 and 2011/12)	0.81	10.09	-152	-11	-30	21
Temp3 (2007 and 2011/12)	-0.31	26.58	-201	-14	-79	55
Temp4 (2007 and 2016)	0.88	7.96	-129	-25	-21	13
Temp5 (2011/12 and 2016)	-0.66	29.97	-190	-25	-77	34
Temp6 (1999, 2007 and 2016)	0.99	2.79	-132	-25	-9	7
Temp7 (1999, 2011/12 and 2016)	0.96	4.45	-133	-25	-11	10
Temp8 (1999, 2007 and 2011/12)	0.65	13.68	-164	-11	-42	32
Temp9 (2007, 2011/12 and 2016)	0.55	15.68	-160	-25	-38	31
Temp10 (all surveys)	0.92	6.48	-136	-25	-14	16

5. DISCUSSION

The discussion is split into several parts. Firstly, the topics applicable to all experiments will be discussed; the used bathymetric data and the, in this thesis, applied methodology of WaterProof for establishing the NMRL. After this, the sensitivity to the different tested parameter settings (RQ1) is discussed, followed by the sensitivity to the input data (RQ2).

5.1. GENERAL METHODOLOGY FOR ESTABLISHING THE NON-MOBILE REFERENCE LEVEL

The two cable sections studied within the study area had been carefully selected based on data availability and differences between Cable Sections 1 and 2. Therefore, results and conclusions drafted within this study should be considered in the light of the scope as defined in Section 1.6. A discussion point is the choice to use only two locations to obtain the results presented in this thesis. Due to limited data availability, the study was constrained to these specific sites, which introduces a limitation regarding the generalizability of the quantitative outcomes. It is likely that conducting this research in other locations could yield different quantitative results, reflecting the site-specific sand waves.

However, the experiments addressing RQ1 reveal variations in migration and growth rates between Cable Section 1 and Cable Section 2. These observed differences enhance the study's findings by providing comparative insights that strengthen the qualitative conclusions. By incorporating data two sites, even within this limited scope, the thesis offers an understanding of the patterns and mechanisms under investigation. Therefore, while additional sites would likely provide even richer insights, the current study design still significantly supports the qualitative conclusions by offering comparative results across the two chosen cable sections.

In this thesis, the NMRL for the year timeframe between 2011 and 2078 (for Cable Section 1) and 2016 and 2078 (for Cable Section 2) was projected. This was partly done since earlier studies were also projecting the NMRL for this year (see Section 2.2 for complete reasoning). This projection implies that all sampled migration and growth rates out of the created PDFs in this study are multiplied by the duration of the extrapolation period of approximately 50-70 years[6] to establish the NMRL. The created NMRL and thus the depth of the δz_d are in relation to the extrapolation period. Increasing/decreasing the extrapolation period results in an overall deeper/shallower NMRL and thus may lead to a deeper/shallower δz_d. Therefore, all results should be considered in light of this extrapolation period. When this research would be carried out with another projection year, the results of this thesis are likely to scale with this. This is likely due to that the MRSL is extrapolated towards this projection year, increasing/decreasing the projection year would thus only affect the extrapolation.

The $z_{NMRL\ Exp}$s from all experiment groups have been compared relative to the matching (one of the three) $z_{NMRL\ Ref}$. The comparison with a reference case was carried out since the NMRL cannot be compared with an observed NMRL due to data scarcity; there are no surveys available with high enough resolution and/or accuracy over a period of 50-70 years[6]. While the Δz^{Exp} provides a view on the impact of changing parameters and input data on the NMRL, less can be said since there is no 'true' $z_{NMRL\ Ref}$. A small to zero Δz^{Exp} does not imply that the $z_{NMRL\ Exp}$ will turn out to be the lowest observed seabed over the lifespan of the cable.

[6] Depending on the surveys used, this could differ. In general, for Cable Section 1, the period is 67 years and for Cable Section 2 this period is 52.

5.2. RQ1. SENSITIVITY TO PARAMETER SETTINGS

In this study, four different parameter settings within WaterProof's method for projecting an NMRL have been tested. For every approach, the results and possible explanations are discussed.

5.2.1. Percentile

Changing the percentile chosen as NMRL directly changes the position of the NMRL in the seabed. The NMRL of the 20th percentile and 30th percentile were comparably with the Reference Case (25th percentile). Deviating more from the Reference Case percentile (25), resulted in large deviations in the maximum depth relative to the MRSL.

5.2.2. Length cross-sections

The length of a cross-section influences the number of troughs and crests that are included in the observations and, therefore, influences the migration and growth rates. At the moment, WaterProof's method tries to include at least 100 observations by increasing the search radius from 500 m up to 1 km, as illustrated in Figure 39. For the cross-sections with a length of 1 km, the used observations for all cross-sections were, on average, 37, implying that even with the maximum search radius, not enough observations could be found. Lengthening the cross-sections leads to more observations per cross-section, resulting in fewer cross-sections needed to obtain 100 observations, thus reducing the search radius. This resulted in that when the cross-sections were long enough that, with the maximum search radius, the minimum number of 100 observations was found. The length of the cross-section could increase while the number of observations used per cross-section stayed around 100. Increasing the cross-section length does not necessarily increase the number of observations used for the PDF estimation.

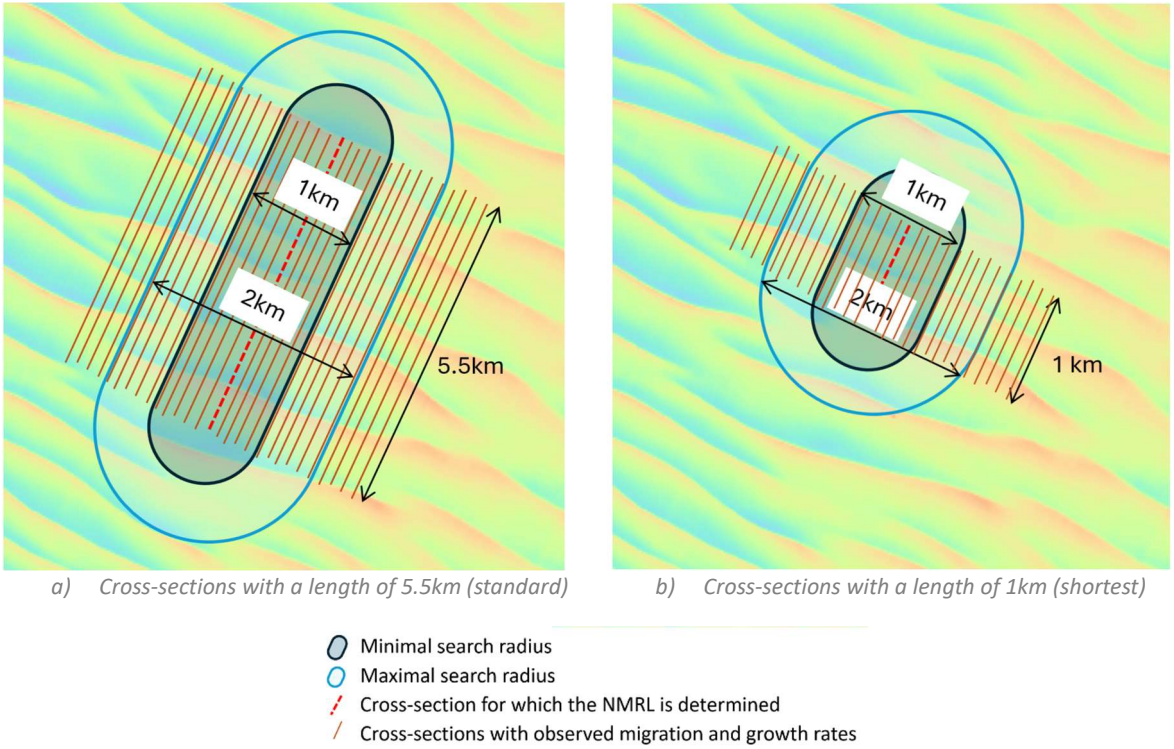

a) Cross-sections with a length of 5.5km (standard) *b) Cross-sections with a length of 1km (shortest)*

Figure 39: Illustration of search radius to achieve 100 observations on scale.

Lengthening the cross-sections barely changes the PDF estimations, and thus the $z_{NMRL\ Exp(O,t1)}$. An explanation for this could be that the sand waves present in the areas surrounding Cable Sections 1 and 2 have similar migration and growth rates, and thus, increasing the number of observations does

not change the PDF estimations. This would imply that, within the Cable Sections investigated, there is not a lot of variability within the migration rate and growth rates of the sand wave.

Decreasing the cross-sections length led to larger differences between the $z_{NMRL\ Exp(O,t1)}$ and $z_{NMRL\ Ref(O,t1)}$ compared to increasing the cross-sections. A reason could be that with decreasing the cross-sections, the comparison between the Reference Case and the Experiment Case was carried out on a smaller stretch of cable. This could allow boundary effects to have a larger impact on the KPIs. Besides, decreasing the length of the cross-sections lead to that less unique sand waves are observed (since the cross-section are almost parallel to each other, they capture the same sand-wave but at a slight other location). With that the non-uniformity of different sand waves is less captured which might resulted in larger differences between the $z_{NMRL\ Exp(O,t1)}$ and $z_{NMRL\ Ref(O,t1)}$.

5.2.3. Distance between cross-sections

Like the length in cross-sections, the distance between cross-sections parameter affects the number of observed migration and growth rates. When decreasing the distance between cross-sections, the search range decreases (see also previous section). Due to the decreasing search radius, the number of used observations remained for the 50 m distance around 100, which is similar to the Reference Case. For the case with 25 m between the cross-sections, the number of observations used is almost 300, implying that the search radius was reduced to 500 m.

Comparing the individual PDFs of the Reference Case and the Experiment Case, where an offset of 50 m had been applied, differences were seen; while having the same distance between the cross-sections, different migrations rates were found to estimate the PDFs. Despite that, the offset experiment had the largest correspondence with the Reference Case compared with the other Experiment Cases; looking at the NSE and RMSE values, the local difference could be up to 11 cm. This could be caused by the method of interpolation: The NMRL was generated from the representative of each individual cross-section (with a 1 m accuracy in the direction of the cross-section) and subsequently was interpolated to a 25m resolution 3D NMRL. The NMRL was then projected to the cable per metre of cable length. Increasing the number of cross-sections reduces the interpolation distance between cross-sections for creating the 3D NMRL, potentially influencing the eventual interpolation of the NMRL on the Cable Section.

Increasing the distance between the cross-sections does not significantly change the average PDF estimations but does impact the NMRL compared to the MRSL and the Reference Case. This may also be due to the increase in interpolation distance from the representative per cross-section to 3D NMRL.

The results from increasing or decreasing the distance between cross-sections are expected to be less impacted by the natural variability in sand wave migration and growth rates compared with lengthening the cross-sections. This since changing the distance between the cross-sections does not lead to capturing other sand waves, but do observe the same sand wave at another location.

5.2.4. Period between surveys

The execution dates of the surveys used in this thesis were found in the metadata retrieved via NLHO (see Appendix A.1), with this it could be seen that the surveys are not carried out in the same period of the year. The 1999 survey, for example, was executed from October up to and including December 1999 whereas the 2016 survey was executed in March and April. When including the survey month, the period between the surveys is not 17 years but rather 16 years and 4 months. This is not as large as the investigated maximum decrease in period (one year) between surveys but is also larger than the decrease of one month.

5.3. RQ2. SENSITIVITY TO INPUT DATA

In this study, four different approaches to handling and selecting input data within WaterProof's method for projecting an NMRL were tested. For every approach, firstly, the results and possible explanations are discussed.

5.3.1. Repositories

To study the effect of different data sources on the NMLR determined via WaterProof's method, three different repositories were used. Due to a difference in reference level, a correction method was applied in a certain order, firstly reprojecting and resampling, secondly correcting for mean depth difference and thirdly (if applied) correcting for the lag difference (see Section 3.6.1). It is possible to correct for the lag difference before applying a mean difference correction. This may result in a slight difference in MRSL and, thus, the NMRL. This difference is expected to be small due to that the largest deviation in mean is caused on the stoss side of the sand waves which is barely impacted by correcting the MRSL by lag first.

The lag (in spatial direction) was determined from the 1D cross-sections using a method for 1D-spatial cross-correlation (see Appendix A.3). An alternative approach, as proposed by Duffy & Hughes-Clarke (2005), involves correcting for lag obtained using 2D-spatial cross-correlation. This was not implemented in this study, as the lag predominantly affects the MRSL in the *x*-direction of cross-sections due to the shape of sand waves and the way the cross-sections intersect with them.

The lag difference could be caused due to the, for the author unknown, applied transformation between coordinate system and the origin of the used grid. A value within a raster is most often assigned to the coordinate in the middle of a cell but can also be assigned to the coordinate in the left lower corner (A. Wolowicz-Trouwborst, personal communication, 12 March 2024). This could be an explanation for the EMODnet repository, where the lag is around this value (-13 m for the EMODnet repository 2016 survey). However, this lag could also be coincidentally matching the distance between the lower left corner and the middle of a grid cell since this was not provided in the NLHO metadata, nor is it known for the OPeNDAP and EMODnet repository. More likely, the lag difference is caused by the method of smoothing carried out on the NLHO data by Deltares and the unknown smoothing method of EMODnet.

The NSE and RMSE were calculated based on the NMRL of the NLHO and EMODnet repository relative to the MRSL and NMRL established from the OPeNDAP repository. WaterProof's method uses the MRSL as limitation for the NMRL. However, since a different MRSL had been used for each repository, the outcome is directly influenced by the location differences where the $z_{NMRL\,Exp}$ is limited by the MRSL.

It was expected that despite the lag and mean difference between the repositories, the migration and growth rates would be almost identical to each other. The results show that there is a difference between the different growth rates. The NLHO repository shows the largest migration and absolute growth rates compared to the other repositories. This is interestingly since the surveys obtained from the EMODnet and OPeNDAP repositories are using the NLHO surveys as input, supporting research from de Swart & van der Laan (2024) that there are differences present between the repositories which is most likely due to the method of smoothing.

5.3.2. Grid resolution

In this study, the grid resolution was varied between 5 m to 50 m with surveys from the NLHO repository. Having a resolution of 5 m led to a 6 cm deeper depth relative to the MRSL compared to the Reference Case. This small difference could be possible due to the method developed by

WaterProof itself. Increasing the resolution does not lead to a change in the distance between cross-sections. The cross-sections are 100 m spaced apart from each other, and thus, to establish the 3D NMRL, the representative from the cross-sections were interpolated over a distance of 100 m, after which it is projected to the cable. It is likely that this 100 m interpolation causes to limit the effect of having a higher resolution on the NMRL. Due to this, it is expected that despite the differences between the NLHO repository and the OPeNDAP repository, the effect on the NMRL by having the data sets from the OPeNDAP repository available in a higher resolution, is comparable.

The 50 m resolution NMRL projected on the cable has a lower depth on the stoss side of the sand waves than the other cases (up to 25 cm). This is most likely due to the low migration rate seen in the PDF estimation of the 50 m resolution case (0.10 m/year as median). Hence, the predicted migration of sand waves is not as high as in the other cases.

5.3.3. Grid origin

Relocating the origin before downsampling to 25m resolution can be carried out in various ways; in this study, one approach was used. Using the direction of sand wave migration, the resampling is expected to have the most impact due to the location of the crests and throughs of sand waves are most likely to appear on a different location than the Reference Case, possibly impacting the NMRL. Other origins could also have been selected for this study. This was not done due to time limitations.

The large local differences between the MRSL and the NMRL of the Experiment Case and the Reference Case could be caused due to the same phenomenon as discussed earlier, the NMRL of the 21.9 degrees case was compared relative to the not resampled MRSL. However, comparing the $z_{NMRL\ Exp\ (H,t2)}$ with the $z_{NMRL\ Ref\ (H,t2)}$ results in differences locally up to 63 cm.

5.3.4. Including intermediate surveys

Changing the first or last survey has a large impact on the PDF estimation for the migration rate and growth rates. A possible explanation could be that between some surveys the intermediate period is 4 years. When not including the monthly accuracy, the effect as discussed in RQ1.4 (Section 6.2.4) becomes relatively larger. Including intermediate surveys has less impact on the PDF estimations. This is mainly due to that more observations are included, limiting the effect of having shorter periods between surveys.

The NMRL Experiment Cases established with use of the MRSL show the closest coherence with the NMRL Experiment Case. This is understandable with the comparison method deployed since the comparison is made with the MRSL of the latest survey. Therefore, for comparing the sensitivity caused by varying the first or last survey, conclusions can only be drafted when comparing the Experiment Case with the Reference Case.

6. CONCLUSION

During this research much effort was put into obtaining and understanding the obtained survey data. From this several conclusions could be drafted.

6.1. BATHYMETRIC DATA

Despite using high standards for surveying (see Section 3.1.1), there are uncertainties in the survey horizontal and vertical accuracies. This study did not test directly whether these uncertainties impact the NMRL. However, the surveys provided by NLHO display patterns that can only be explained by insufficiently compensated effects of rolling of the survey vessels due to likely waves. These repetitive patterns in the vessel's sailing direction are, due to down-sampling towards a 25 m resolution, smoothed and are hardly visible in the utilised surveys. Since these shapes are not visible in the other repositories, small differences due to singular errors in surveying are not expected to impact the NMRL; they are smoothed out in the dataset before the surveys are utilised.

Besides singular errors, the whole data set can be shifted due to incorrect calibration with a reference level. In this thesis this was also shown, between the surveys obtained from the NLHO repository and the OPeNDAP and EMODnet repositories (see Appendix F). Mean differences between surveys from the same repository do not impact WaterProof's method. This is because the method uses the DSL from which the local present mean had been subtracted, and thus, mean differences in calibration with reference levels within the repository are removed. The difference in mean becomes important when the MRSL is extrapolated towards the NMRL.

While varying the parameters or changing the input data, there appeared to be almost no difference in the moving average depth per 5 m or 25 m cable relative to the MRSL. Very small differences (less than 1%) have been seen on the overall sections and in the order of 4 cm for the maximum local difference of the Reference Case relative to the MRSL. Hence, this would imply that there is no need to obtain the moving average depth of 5 m but rather use the moving average per 25 m.

6.2. RQ1. SENSITIVITY TO PARAMETER SETTINGS

In this study, four different parameter settings within WaterProof's method for projecting an NMRL have been tested. For every parameter a conclusion about the effect of this parameter setting is presented, answering the first research question.

6.2.1. Percentile

No conclusion can be drafted on which percentile is better, but this study showed that the percentile has a large impact on the position of the NMRL in the seabed. The effects of a different percentile on the dredging required for the installation of the cable and on the maintenance required to the cover on the cable during its lifetime have not been assessed in this study. Those would have to be studied in conjunction with the effects on the position in the seabed in order to be able to assess the lifecycle impact on society of changing the percentile.

6.2.2. Length cross-sections

Increasing the cross-section length does not lead to a different PDF and NMRL. Decreasing the cross-section shorter than 4,000 m seemed to cause boundary effects, which in this study are not compensated for.

6.2.3. Distance between cross-sections

Increasing or decreasing the distance between the cross-sections did not lead to notable differences in estimated average PDF per growth rate and migration rate. Decreasing the distance between the cross-sections resulted in a difference in NMRL due to the applied interpolation method since the PDF

estimations seem unaffected by decreasing the distance. The interpolation method could also explain why there is an absolute difference between the with and without offset creased NMRL.

6.2.4. Period between surveys

Increasing the temporal accuracy from yearly to monthly did not significantly affect the NMRL. The period influenced observed migration and growth rates; extending the period by 6-8% reduced the IQR of the PDF by approximately 5%. Changing the period between surveys by one month resulted in less than 1.2% variation in the IQR, yielding an absolute difference in NMRL of less than 3cm. However, since the metadata had been retrieved via NLHO, the execution dates of the surveys are available and thus can straightforwardly be included in WaterProof's method, which will not increase computational complexity.

6.3. RQ2. SENSITIVITY TO INPUT DATA

In this study, four different approaches to handling and selecting input data within WaterProof's method for projecting an NMRL were tested. For every handling and selection of input data approach, a conclusion is presented, answering the second research question.

6.3.1. Repositories

he NMRL created on the NLHO and EMODnet repository exceeds the MRSL of the OPeNDAP repository since the NMRL it is not limited by the same MRSL. The NMRLs of the different repositories are, due to the method of comparison, having a lower NSE and higher RMSE value. Due to the large differences between surveys of the repositories, it is not possible to combine the different repositories for obtaining migration rates and growth rates of sand waves.

6.3.2. Grid resolution

Decreasing the resolution has a large effect on the NMRL. Increasing the resolution has less effect on the NMRL in general due to the method of interpolation from 2D cross-sections to the 3D NMRL, but can locally cause differences up to -42cm.

6.3.3. Grid origin

Changing the grid origin does affect the NMRL compared with the Reference Case locally up to -63 cm. Since there is almost no change in the PDF estimations, the large differences are caused by the method of comparison.

6.3.4. Including intermediate surveys

Changing the first or last survey has a large impact on the PDF estimation for the migration rate and growth rates. This works through to the NMRLs and thus shows that the NMRL is affected by introducing new data. Including intermediate surveys has less impact on the PDF estimations but seems to be affected by using smaller intermediate periods between the surveys and the uncertainties involved with this.

6.4. REFLECTION ON RESEARCH AIM

This study aimed to evaluate the uncertainties in the NMRL determined by the method developed by WaterProof in the offshore seabed of the Dutch North Sea, by testing various settings of the method and using various bathymetric input. Below the two research questions have been answered satisfying the aim of this research.

RQ1: What is the sensitivity of the parameter settings in WaterProof's method on the Non-Mobile Reference level?

Overall, considering the results and the discussion as presented in this study, the NMRL established with WaterProof's method showed to be sensitive by changes in parameter settings. The most sensitive parameter in WaterProof's method is the percentile setting, selecting the representative per cross-section. WaterProof's method has shown to be sensitive to the parameters of the length of and the distance between cross-sections. The period between surveys does slightly have an impact on the NMRL.

WaterProof's method compensates for possible changes within the parameter settings by for example changing the search radius limiting the effect of having a different number of cross-sections.

RQ2: To what extent is the Non-Mobile Reference Level, as determined by WaterProof's method, sensitive to handling and selection of input data?

Using different methods of pre-processing input data from various bathymetric inputs show that there are differences between the repositories which do impact the NMRL. Comparing the different computed cases and quantitively describe these differences is hard as it can only be compared relative to other established NMRLs or the MRSL which both influenced by the data handling itself.

Despite this, the conclusion can be made that the NMRL as determined by WaterProof's method is sensitive to handling and selection of input data. Increasing the resolution may influence the NMRL but this is not shown due to that the method of WaterProof is interpolating from 100 m spaced 2D cross-sections towards a 3D NMRL. Including intermediate surveys show potential to be useful in obtaining more observations of the same sand waves but attention should be given to the decrease in period between used the surveys.

7. RECOMMENDATIONS

During this thesis, several recommendations were found for improving the method for creating an NMRL for cable installation. Also, recommendations were formulated for further research.

7.1. METHOD FOR ESTABLISHING NMRL

Some considerations have been made to reduce uncertainties within WaterProof's method for establishing the NMRL. All these considerations have also a downside which is also stated.

1. Include the execution date of the survey campaign. At the moment, the method proposed by WaterProof uses the difference between years as a period for determining the migration and growth rate. Including the month could potentially reduce the uncertainty of the maximum distance between the NMRL and MRSL up to 3cm. While decreasing this uncertainty, a new uncertainty is introduced. Survey campaigns are executed during a period, not at one moment specific in time.
2. Decrease the distance between the cross-sections. Having the same number of cross-sections but with an offset increased the NMRL depth locally up to 10 cm relative to the MRSL. Doubling the number of cross-sections would decrease this difference but almost double the computational time needed to establish the NMRL.
3. It is not recommended to combine different repositories to estimate the growth rates and migration rate. Due to the application of, for the EMODnet repository unknown, smoothing of survey data, the different repositories differ too much from each other. A lag between the surveys was observed, but it remains unclear how this lag was introduced in the source data. Estimating the migration rate between surveys from, for example the EMODnet and OPeNDAP is therefore unwanted.
4. However, the growth rates observed in the areas do appear to be similar. Thus, it could be an option to use the growth rates of the observed sand waves from the OPeNDAP repository to extrapolate the MRSL of for example a survey found in EMODnet. However, this was not investigated in this research.
5. In this study it was found that there is almost no difference in the moving average depth per 5 m or 25 m cable relative to the MRSL and the NMRL. This implies that there is no need to obtain the moving average depth of 5 m; instead, the moving average per 25 m is recommended to be used as this reduces the impact of small mobile seabed features such as mega ripples.

7.2. FURTHER RESEARCH

During this thesis project, some suggestions for further research were found.

6. At the moment, the 25^{th} percentile is chosen as an acceptable probability of exceedance. Changing this parameter below the 20^{th} or above the 30^{th} percentile has the most effect on the depth of the NMRL compared to all other investigated parameters. Therefore, it is recommended that more research is carried out on this parameter in further research such that this parameter is understand better.
7. In this study, the effect of varying the resolution in the input data on the NMRL was tested. As discussed in Section 6.3.2, an increase in resolution does lead to a significant change in the NMRL. However, this might be due to the effect of interpolation between the cross-sections to form a 2D NMRL. Therefore, to test the impact of an increase in resolution on the NMRL, it is also recommended to decrease the distance between cross-sections. In this way, the impact of increasing the resolution is expected not to be limited by interpolation.
8. Implementing a non-linear cross-section that aligns with the migration direction of each sand wave was suggested during this thesis in one of the conversations with WaterProof. This

approach could enhance the accuracy of the estimation of sand wave migration rate. However, it is not expected to reduce uncertainties in growth rate measurements, as the orientation of the cross-section does not affect the observed height of the sand waves. Therefore, this suggestion may improve the method proposed by WaterProof, but probably only to a moderate extent.

9. TenneT executes its own survey campaigns; this thesis did not investigate how these surveys can be used to create the NMRL as the coverage is too little. However, there is a potential for using this survey data to assess the created NMRL during the cable's lifespan. This should not be done with the NMRL located on the cable route since, due to installation, a trench is formed at this location. Using the depth located in the trench would give an unrealistic change to the seabed and thus would not reflect the sand wave migration/growth over time. It cannot reflect the development of the seabed and thus cannot be used for assessment. Despite this, the author thinks there is a potential for using the survey campaigns executed by TenneT. An extra NMRL should be determined at least 25 metres from the cable route, as the trench of the cable is can still be visible at this distance (see Appendix E). It is likely that this imaginary cable route is limited and impacted by the cable installation. Therefore, new survey data would show the migration and growth of present sand waves and thus could be used to assess the correctness of the NMRL locally. However, this potential should be exploited in further research.
10. The method, as WaterProof proposed, uses 25x25m resolution data and eventually returns a NMRL projected on the cable route per meter. Increasing the data resolution, as tested with data from the NLHO repository, slightly changed the NMRL. However, as was discussed in Section 6.3.2, the effect may be limited due to the spacing of the cross-sections. Thus, combining the increase in the number in cross-sections and increase in data resolution may turn into a positive combined effect in reducing uncertainties with the NMRL relative to the MRSL in the areas between the cross-sections. However, this approach would significantly increase the computational effort. Despite this, the author thinks that further research in this could lead to a decrease in uncertainties in the NMRL.

8. REFERENCES

ACRB. (2022). *IJmuiden Ver + Nederwiek Risk Based Burial Depth export cables* (Q320R1-RBBD-IJV+NW_r1 13apr2022.docx).

Anthony, E. J., & Aagaard, T. (2020). The lower shoreface: Morphodynamics and sediment connectivity with the upper shoreface and beach. *Earth-Science Reviews*, *210*, 103334. https://doi.org/10.1016/j.earscirev.2020.103334

Boone, W., & Sonderen, C. (2015). *Copper in Comparison with Aluminium as common Material in Conductors of LV and MV cables*. http://cired.net/publications/cired2015/papers/CIRED2015_0026_final.pdf

BritNed. (2019). *BritNed | Access the UK and NL Electricity Markets*. BritNed. https://www.britned.com/

Buijsman, M. C., & Ridderinkhof, H. (2008). Long-term evolution of sand waves in the Marsdiep inlet. I: High-resolution observations. *Continental Shelf Research*, *28*(9), 1190–1201. https://doi.org/10.1016/j.csr.2007.10.011

Campmans, G. H. P., Roos, P. C., Van der Sleen, N. R., & Hulscher, S. J. M. H. (2021). Modeling tidal sand wave recovery after dredging: Effect of different types of dredging strategies. *Coastal Engineering*, *165*, 103862. https://doi.org/10.1016/j.coastaleng.2021.103862

CBS. (2023, October 12). *Hernieuwbare energie in Nederland 2022* [Webpagina]. Centraal Bureau voor de Statistiek. https://www.cbs.nl/nl-nl/longread/rapportages/2023/hernieuwbare-energie-in-nederland-2022

CBS. (2024, June 7). *Energy from renewable sources rises to 17 percent* [Webpagina]. Statistics Netherlands. https://www.cbs.nl/en-gb/news/2024/23/energy-from-renewable-sources-rises-to-17-percent

Cheng, C. (2021). *Biogeomorphological aspects within tidal sand wave fields* [Ghent University]. https://www.researchgate.net/publication/354237656_Biogeomorphological_aspects_within_tidal_sand_wave_fields

CIGRE. (2022). *Installation of Submarine Power Cables* (B1, 883, ISBN: 978-2-85873-588–4). CIGRE.

COGEA. (2014). *EMODnet Product Catalogue—EMODnet* (Power cables; Shapefiles EMODnet_HA_Cables_Power_20230628). EMODnet; Human activities. https://emodnet.ec.europa.eu/geonetwork/emodnet/eng/catalog.search#/metadata/41b339f8-b29c-4550-b787-3d68f08fdbcc

Damen, J. M., van Dijk, T. a. G. P., & Hulscher, S. J. M. H. (2018). Spatially Varying Environmental Properties Controlling Observed Sand Wave Morphology. *Journal of Geophysical Research: Earth Surface*, *123*(2), 262–280. https://doi.org/10.1002/2017JF004322

de Swart, R. L., & van der Laan, K. J. (2024). *Extended and adjusted NMRL for the IJmuiden Ver/Nederwiek cables* (WP1306-3_R1r1). WaterProof Marine Consultancy & Services BV.

Deltares. (2020). *Server Information*. https://opendap.deltares.nl/thredds/info/serverInfo.html

Dienst der Hydrografie. (2022). *Bathymetrische datasets van 1969 tot en met 2022 voor aangevraagd stuk Noordzee, ref.nr: 2024007087* (Dataset 15541, 15514, 15534, 15538, 8149, 2418, 2420, 4709/4823, 4819, 10149, 7221, 10315–2, 11323, 12221, 18454, 18633, HKZRVO, 20757/20758 and 22323B_C) [ASCII xyz and GeoTIFF]. Dienst der Hydrografie. https://www.defensie.nl/onderwerpen/hydrografie/downloads/formulieren/2022/08/08/aanvraagformulier-hydrografische-data

Dodd, N., Blondeaux, P., Calvete, D., Swart, H. E. D., Falqués, A., Hulscher, S. J. M. H., Różyński, G., & Vittori, G. (2003). Understanding Coastal Morphodynamics Using Stability Methods. *Journal of Coastal Research*, *19*(4), 849–865. https://www.jstor.org/stable/4299224

Duffy, G. P., & Hughes-Clarke, J. E. (2005). Application of spatial cross correlation to detection of migration of submarine sand dunes. *Journal of Geophysical Research: Earth Surface*, *110*(F4). https://doi.org/10.1029/2004JF000192

E-Connection. (2001). *Milieueffect rapport Offshore windpark Q7-WP*. https://www.commissiemer.nl/docs/mer/p11/p1104/1104-080mer_004.pdf

Elia Group. (2022). *TritonLink*. Elia, onze projecten. https://www.elia.be/nl/infrastructuur-en-projecten/infrastructuurprojecten/tritonlink

European Commission. (2023, October 24). *Communication from the Commission to the European Parliament, the Council, the European Economic and Social Committee and the Committee and the Committee and of the regions. Delivering on the EU offshore renewable energy ambitions*. https://eur-lex.europa.eu/legal-content/EN/TXT/?uri=CELEX%3A52023DC0668&qid=1702455230867

Heddam, S., Kim, S., Elbeltagi, A., & Kisi, O. (2022). Chapter 15—Random vector functional link network based on variational mode decomposition for predicting river water turbidity. In M. Zakwan, A. Wahid, M. Niazkar, & U. Chatterjee (Eds.), *Current Directions in Water Scarcity Research* (Vol. 7, pp. 245–264). Elsevier. https://doi.org/10.1016/B978-0-323-91910-4.00015-7

Hellenic Cables. (2022). *Hollandse Kust (zuid) brochure*. https://www.hellenic-cables.com/wp-content/uploads/PR16608_Hollandse-Kust-Zuid-AB-Brochure-4p_BB-v2.pdf

Horn, B. (1981). Hill shading and the reflectance map. *Proceedings of the IEEE*, *69*, 14–47. https://doi.org/10.1109/PROC.1981.11918

Hulscher, S. J. M. H. (1996). Tidal-induced large-scale regular bed form patterns in a three-dimensional shallow water model. *Journal of Geophysical Research: Oceans*, *101*(C9), 20727–20744. https://doi.org/10.1029/96JC01662

ICPC. (2009). *Loss prevention bulletin* (p. 4). ICPC, International Cable Protection Committee. https://www.iscpc.org/documents/?id=139

Jan De Nul. (2021, October 21). *Sunfish successfully reburies export cable at Eneco's Luchterduinen Wind Farm*. Jan De Nul. https://www.jandenul.com/news/sunfish-successfully-reburies-export-cable-enecos-luchterduinen-wind-farm

Jetten, R. A. A. (2022, September 16). *Kamerbrief windenergie op zee 2030-2050* [Brief]. Ministerie van Algemene Zaken. https://open.overheid.nl/documenten/ronl-b34f5ea2f405a4b9dbdfe676288ace0736599264/pdf

Knaapen, M. A. F. (2005). Sandwave migration predictor based on shape information. *Journal of Geophysical Research: Earth Surface*, *110*(F4), 2004JF000195. https://doi.org/10.1029/2004JF000195

Kouzehgar, K., & Eslamian, S. (2023). Chapter 2—Application of experimental data and soft computing techniques in determining the outflow and breach characteristics in embankments and landslide dams. In S. Eslamian & F. Eslamian (Eds.), *Handbook of Hydroinformatics* (pp. 11–31). Elsevier. https://doi.org/10.1016/B978-0-12-821962-1.00002-7

Krabbendam, J. M., Roche, M., Van Lancker, V. R. M., Nnafie, A., Terseleer, N., Degrendele, K., & De Swart, H. E. (2022). Do tidal sand waves always regenerate after dredging? *Marine Geology*, *451*, 106866. https://doi.org/10.1016/j.margeo.2022.106866

Laan, K. vd, Geleynse, N., Perk, L., & Snip, D. W. (2023, June). *Modelling Seabed Mobilit for Offshore Grid Security*. 11th International Conference on Insulated Power Cables, Lyon, France.

Leenders, S., Damveld, J. H., Schouten, J., Hoekstra, R., Roetert, T. J., & Borsje, B. W. (2021). Numerical modelling of the migration direction of tidal sand waves over sand banks. *Coastal Engineering*, *163*, 103790. https://doi.org/10.1016/j.coastaleng.2020.103790

Ministerie van Defensie. (2018, April 6). *Area of expertise of the Hydrographic Service—Royal Netherlands Navy* [Webpagina]. Royal Netherlands Navy; Ministerie van Defensie. https://english.defensie.nl/organisation/navy/navy-units/hydrographic-service/area-of-expertise

Ministerie van Defensie. (2020, June 12). *NLLAT2018—Application—Defensie.nl* [Applicatie]. Ministerie van Defensie. https://english.defensie.nl/downloads/applications/2020/06/12/nllat2018

Ministerie van Defensie. (2023, July 27). *Online availability of data from the Hydrographic Service—Publication—Defensie.nl* [Publicatie]. Ministerie van Defensie. https://english.defensie.nl/downloads/publications/2023/07/27/online-availability-of-data-from-the-hydrographic-service

Morelissen, R., Hulscher, S. J. M. H., Knaapen, M. A. F., Németh, A. A., & Bijker, R. (2003). Mathematical modelling of sand wave migration and the interaction with pipelines. *Coastal Engineering*, *48*(3), 197–209. https://doi.org/10.1016/S0378-3839(03)00028-0

Motovilov, Y. G., Gottschalk, L., Engeland, K., & Rodhe, A. (1999). Validation of a distributed hydrological model against spatial observations. *Agricultural and Forest Meteorology*, *98–99*, 257–277. https://doi.org/10.1016/S0168-1923(99)00102-1

NeuConnect. (2023, November 3). *NeuConnect completes first phase of UK construction*. NeuConnect Interconnector. https://neuconnect-interconnector.com/neuconnect-completes-first-phase-of-uk-construction-keeping-first-uk-german-energy-link-on-track/

Noordzeeloket. (2023a). *Cables and pipelines*. Noordzeeloket. https://www.noordzeeloket.nl/en/functions-and-use/kabels-leidingen/

Noordzeeloket. (2023b, April). *Net op Zee*. Noordzeeloket. https://www.noordzeeloket.nl/publish/pages/187394/woz_variant_windenergie-op-zee-met-netten-op-zee_v4_nl.pdf

Olijve, N. (2019, August). *T10 Dynamic DC cable rating*. https://offshore-documents.tennet.eu/fileadmin/offshore_document_uploads/Consultation_documents/11._Dynamic_DC_cable_rating/ONL_TTB-05419_T10_Dynamic_DC_cable_rating_V2.0.pdf

Paulsen, B. T., Roetert, T., Raaijmakers, T., Forzoni, A., Hoekstra, R., & van Steijn, P. (2016). *Hollandse Kust (zuid) Wind Farm Zone, Certification Report Morphodynamics* (CR-SC-DNVGL-SE-0190-02453-2_Morphodynamics). Deltares. https://offshorewind.rvo.nl/file/download/bd489750-e879-4da5-beb3-51ac88ead3f6/1483456263hkz_20161222_deltares_morphologystudy_del_v03_f_compleet.pdf

Perk, L., de Swart, R., van der Laan, K., Bentvelsen, B., Snip, D. W., Geleynse, N., & Pieter, R. (2024, February 27). *Betrokkenheid WaterProof bij afstuderen Maarten Verbom* [Physical].

Pondera, & Arcadis. (2023). *Net op zee Nederwiek 1, aanvraag ontheffing wet natuurbescherming. Bijlage 1.*

Prysmian Group. (2019). *Linking the Sustainable future, Sustainability Report*. https://www.prysmian.com/sites/default/files/Prysmian_DNF_2019_ENG_April_3_0.pdf

Rijksoverheid. (2024). Regeerprogramma—Energietransitie, leveringszekerheid en klimaatadaptatie. In *Regeerprogramma* (Vol. 5, pp. 55–65). https://open.overheid.nl/documenten/ronl-f525d4046079b0beabc6f897f79045ccf2246e08/pdf

Rijkswaterstaat Zee en Delta. (2018, February). *Beschikking Waterwet net op zee Hollandse Kust*. https://www.rvo.nl/sites/default/files/2018/02/beschikking%20Waterwet%20net%20op%20zee%20Hollandse%20Kust_0.pdf

Rijkswaterstaat Zee en Delta. (2021a). *Ontwerp watervergunning offshore Net op zee IJmuiden Ver Alpha*. Rijkswaterstaat. https://www.rvo.nl/sites/default/files/2021/12/Ontwerp-watervergunning-offshore-Net-op-zee-IJmuiden-Ver-Alpha.pdf

Rijkswaterstaat Zee en Delta. (2021b). *Ontwerp watervergunning offshore Net op zee IJmuiden Ver Beta*. Rijkswaterstaat. https://www.rvo.nl/sites/default/files/2021/12/Ontwerp-watervergunning-Net-op-zee-IJmuiden-Ver-Beta.pdf

Rijkswaterstaat Zee en Delta. (2022, September 22). *RWSZ2022-00013716 Watervergunning voor het installeren, gebruiken en verwijderen van Net op zee IJmuiden Ver (Gamma) van TenneT TSO B.V.* https://www.rvo.nl/sites/default/files/2022-12/OB03-Ontwerp-Watervergunning-Net-op-zee-IJmuiden-Ver-Gamma.pdf

RVO. (2017). *Factsheet Driving Down Offshore wind costs the Dutch way*. Netherlands Enterprise Agency (RVO). https://english.rvo.nl/sites/default/files/2017/05/Factsheet%20Driving%20down%20offshore%20wind%20costs%20the%20Dutch%20way.pdf

Snip, D. W. (2024, October 18). *Discussie over belang kabels* [Personal communication].

Snip, D. W., & Liefferink, D. (2023, December 21). *Interview Wino Snip and Daniel Liefferink about the current framework for installing and maintaining high voltage subsea power cables in the (Dutch) North Sea* [Personal communication].

Stal, C., De Sloover, L., Verbeurgt, J., & De Wulf, A. (2022). On Finding a Projected Coordinate Reference System. *Geographies*, *2*(2), Article 2. https://doi.org/10.3390/geographies2020017

Stive, M., Meerendonk, van E., Rijn, van L., Weck, vd A., Walstra, D.-J., & Roelvink, D. (1998). *Expert judgement morfologische ontwikkeling grootschalige zandwinning* (Z2566).

TenneT. (2008). *NorNed*. TenneT. https://www.tennet.eu/nl/projecten/norned

TenneT. (2019a). *COBRAcable*. TenneT. https://www.tennet.eu/nl/projecten/cobracable

TenneT. (2019b). *T16—Cable laying configurations* (Technical ONL TTB-05579; Position Paper, p. 12). https://offshore-documents.tennet.eu/fileadmin/offshore_document_uploads/Consultation_documents/17._Cable_laying_configurations_and_availability/ONL_TTB-05579_T16_Cable_laying_configurations_and_availability_V3.0.pdf

TenneT. (2023a). *LionLink*. TenneT. https://www.tennet.eu/lionlink

TenneT. (2023b). *Transport Market Update 2022* (Transport Market Update 2022; Electricity Market Insights). https://tennet-drupal.s3.eu-central-1.amazonaws.com/default/2023-09/Transport%20Market%20Update%202022.pdf

TenneT. (2023c, March 29). *TenneT selecteert NKT en Prysmian voor 's werelds grootste offshore kabelverbindingen om groeiende Nederlandse offshore windvolumes aan te sluiten*. TenneT.

https://www.tennet.eu/nl/nieuws/tennet-selecteert-nkt-en-prysmian-voor-s-werelds-grootste-offshore-kabelverbindingen-om

TenneT. (2023d, December 31). *Offshore wind energy*. https://www.tennet.eu/nl/projecten/provincies/offshore#overview

TenneT. (2024, January 2). *TenneT Legal Structure*. TenneT. https://tennet-drupal.s3.eu-central-1.amazonaws.com/default/2024-01/TenneT_LegalStructure_NL%20231215.pdf

The Open University. (1999). Chapter 4—Principles and Processes of Sediment Transport. In The Open University (Ed.), *Waves, Tides and Shallow-Water Processes* (pp. 96–124). Butterworth-Heinemann. https://doi.org/10.1016/B978-008036372-1/50005-2

Usbeck, R., Dillon, M., Kaul, N., Lohrberg, A., Nehring, F., & Ploetz, A. C. (2023). High variability and exceptionally low thermal conductivities in nearshore sediments: A case study from the Eckernförde Bay. *Marine Geophysical Research*, *44*(4), 24. https://doi.org/10.1007/s11001-023-09531-2

van der Meijden, R., Damveld, J. H., Ecclestone, D. W., van der Werf, J. J., & Roos, P. C. (2023). Shelf-wide analyses of sand wave migration using GIS: A case study on the Netherlands Continental Shelf. *Geomorphology*, *424*, 108559. https://doi.org/10.1016/j.geomorph.2022.108559

van der Spek, A., van der Werf, J., Oost, A., Vermaas, T., Grasmeijer, B., & Schrijvershof, R. (2022). The lower shoreface of the Dutch coast – An overview. *Ocean and Coastal Management*, *230*. Scopus. https://doi.org/10.1016/j.ocecoaman.2022.106367

van Dijk, T. A. G. P., & Kleinhans, M. G. (2005). Processes controlling the dynamics of compound sand waves in the North Sea, Netherlands. *Journal of Geophysical Research: Earth Surface*, *110*(F4). https://doi.org/10.1029/2004JF000173

van Dijk, T. A. G. P., van der Tak, C., de Boer, W. P., Kleuskens, M. H. P., Doornenbal, P. J., Noorlandt, R. P., & Marges, V. C. (2011, January 1). *The scientific validation of the hydrographic survey policy of the Netherlands Hydrographic Office, Royal Netherlands Navy | Deltares*. Deltares. https://www.deltares.nl/en/expertise/publicaties/the-scientific-validation-of-the-hydrographic-survey-policy-of-the-netherlands-hydrographic-office-royal-netherlands-navy

Van Oord. (2020, December). *Trencher with jetting & chain cutting tool, Trencher Deep DIG-IT*. https://www.vanoord.com/drupal/media/data/default/2020-12/Printed%20matters%20-%20Equipment%20leaflet%20-%20Trencher%20with%20jetting%20%26%20chain%20cutting%20tool%20-%20Deep%20Dig-It%20-%20LR%20-%20Clean.PDF?

Vermaas, T. (2017, May 9). *OPeNDAP Dataset Query Form* [OPeNDAP Deltares]. Hydrografie Surveys. https://opendap.deltares.nl/thredds/dodsC/opendap/hydrografie/surveys/x575000y5815000.nc.html

Vermaas, T. (2024, July 5). *Publicatie van bathymetrische data Hydrografische Dienst in Deltares OPeNDAP* [Personal communication].

Voet, P. C. W., & Moes, C. J. B. (2005). *EIS, SEA and Habitat assessment for BritNed* (9M3538.B1/R031/PCWV/Nijm; p. 27). https://www.eib.org/attachments/pipeline/20070229_nts_en.pdf

Windopzee. (2023, November 30). *Waar staan en komen de windparken op zee?* [Overzichtspagina]. Wind op zee. https://windopzee.nl/onderwerpen/wind-zee/waar/

Wolowicz-Trouwborst, A. (2024, March 12). *Consultation about uncertainties in bathymetric surveys* [Personal communication].

Zhang, Y., Chen, X., Zhang, H., Liu, J., Zhang, C., & Jiao, J. (2020). Analysis on the Temperature Field and the Ampacity of XLPE Submarine HV Cable Based on Electro-Thermal-Flow Multiphysics Coupling Simulation. *Polymers*, *12*(4), Article 4. https://doi.org/10.3390/polym12040952

Zhong, X. & Dutta, U. (2015). Engaging Nash-Sutcliffe Efficiency and Model Efficiency Factor Indicators in Selecting and Validating Effective Light Rail System Operation and Maintenance Cost Models. *Journal of Traffic and Transportation Engineering*, *3*(5). https://doi.org/10.17265/2328-2142/2015.05.001

APPENDIX

A. DATA FROM HYDROGRAPHIC SERVICE

A.1. Received data

The following surveys had been received via data requests from the Hydrographic Service (NLHO).

Table A.1: Obtained surveys with their type of surveying (points or raster), the survey campaign start and end date and the resolution (Dienst der Hydrografie, 2022)

Year	ID	Type	Start survey	End survey	Resolution*	Comment
1969	15541	Points – SBES	1969-04-01	1969-05-31	Track distance 400m	Least depth filter
1984	15514	Points – SBES	1984-09-10	1984-10-15	Track distance 250m	Least depth filter
1984	15534	Points – SBES	1984-07-15	1984-08-19	Track distance 250m	Least depth filter
1984	15538	Points – SBES	1976-08-10	1976-08-25	Track distance 250m	Least depth filter
1995	8149	Points – SBES	1995-03-01	1995-03-15	Track distance 100m	Least depth filter
1996	2418	Points – SBES	1996-02-01	1996-02-28	Track distance 125m	Least depth filter
1996	2420	Points – SBES	1996-02-01	1996-03-31	Track distance 125m	Least depth filter
1999	4709/4823	Points – SBES	1999-10-01	1999-12-31	Track distance 125m	Two vessels used, least depth filter
2000	4819	Points – SBES	2000-04-01	2000-04-30	Track distance 125m	Least depth filter
2002	10149	Points – SBES	2002-08-01	2002-11-30	Track distance 200m	Least depth filter
2007	07221	Raster – MBES	2007-06-26	2007-09-06	4x4m, S-44 order 2 (order 1A)	
2010	10315-2	Raster – MBES	2009-12-20	2010-11-10	4x4m, S-44 order 2 (order 1A)	
2011	11323	Raster – MBES	2011-04-29	2011-10-14	4x4m, S-44 order 2 (order 1A)	
2012	12221	Raster – MBES	2012-02-24	2012-03-21	4x4m, S-44 order 2 (order 1A)	
2015	18454	Points - SBES	2015-02-23	2015-02-27	Track distance 5m	Least depth filter
2015	18633	Points – SBES	2015-02-27	2015-05-01	Track distance 5m	Least depth filter
2016	HKZRVO	Raster – Unkn	2016-03-07	2016-04-18	2x2m, S-44 order undefined	
2018	20757/20758	Points – SBES	2018-02-28	2018-03-29	Track distance 5m	Least depth filter
2022	22323B_C	Raster – MBES	2022-09-20	2022-12-15	2x2m, unknown	

*The track distance was provided in the meta-data provided by NLHO, looking at the data points itself in QGIS showed that this track distance is the approximate minimum. Most of the tracks are closer to each other than the track distance, but some tracks (especially the surveys before 1999) show a larger track distance than stated in the meta-data (in the order of 10 metres).

The start and end date of the survey campaigns from Table A.1 have been displayed in the following figure. Most of the surveys in the study area start in the end of February/beginning of March.

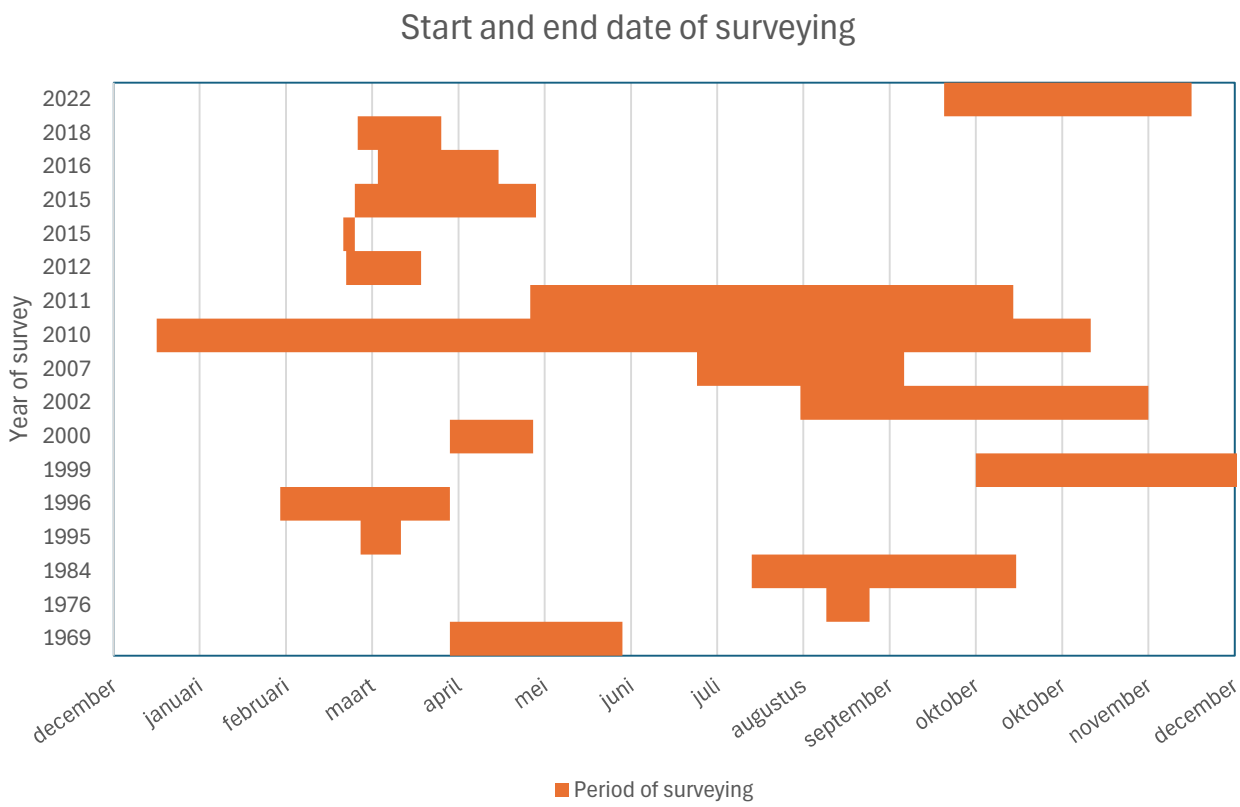

Figure A.1: Start and end date of surveying according to metadata retrieved via NLHO

A.2. Processing survey data from Hydrographic Service repository

The surveys of the NLHO repository, which meet the same criteria as discussed in Methodology, are from 2007, 2011, 2012 and 2016. These survey campaigns were executed with MBES so do not need to be transformed from points to raster. However, they do differ in grid resolution, coordinate system and orientation compared to the surveys obtained via the Deltares OPeNDAP repository.

Firstly, the surveys obtained via NLHO are reprojected from a gradient coordinate system to the same coordinate system as Deltares OPeNDAP (EPSG:25831 - ETRS89 / UTM zone 31N) in QGIS 3.36. Secondly, to account for differences in grid resolution and orientation, the surveys have been resampled with QGIS 3.36 to a 5x5m raster grid by applying an averaging method. Specifically, for each 5x5m grid cell in the new raster, the average value of all original 3x5m grid cells that overlap with the area is calculated. This 5x5m grid is then used for different purposes and down-sampled by mean to a 50m, 25m and 10 m resolution grid for answering parts of the second research question. The 25m resolution grid has also been used for comparing the different repositories.

A.3. Grid Resampling NLHO repository

For changing the grid origin, the surveys of NLHO have been reprojected in the average observed migration direction obtained via the OPeNDAP repository. This was done by averaging the aspect map created along the process of WaterProof's method for establishing the NMRL within Cable Section 2; the outcome was 21.9 degrees. The origin of the OPeNDAP repository had been relocated by 12.5m in this direction. From this origin, a 25x25m grid was constructed. The depth per raster cell was determined by averaging the original 3x5m/2x2m resolution depths that overlap with the area. This assures that the grid is relocated and sampled to a 25x25m resolution. Figure 34 shows one peak of a sand wave with the original grid and the relocated grid.

B. NUMBER OF SURVEYS CONSIDERED TO BE USEFUL PER REPOSITORY

After excluding surveys as discussed in the Methodology (Section 3.1), the number of surveys within the area of interest per repository are displayed in this appendix. The following figures illustrate the number of surveys considered to be useful.

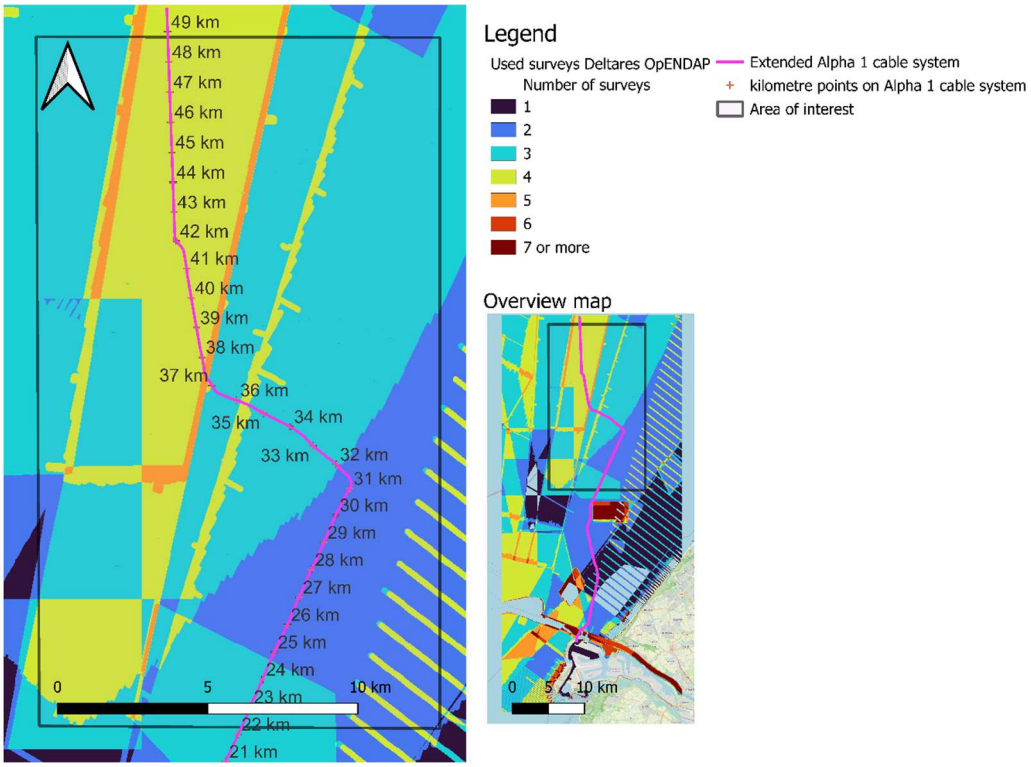

Figure B.1: Number of surveys considered to be useful in the Deltares OPeNDAP repository

Note that in the EMODnet repository, the 1999 survey was not available.

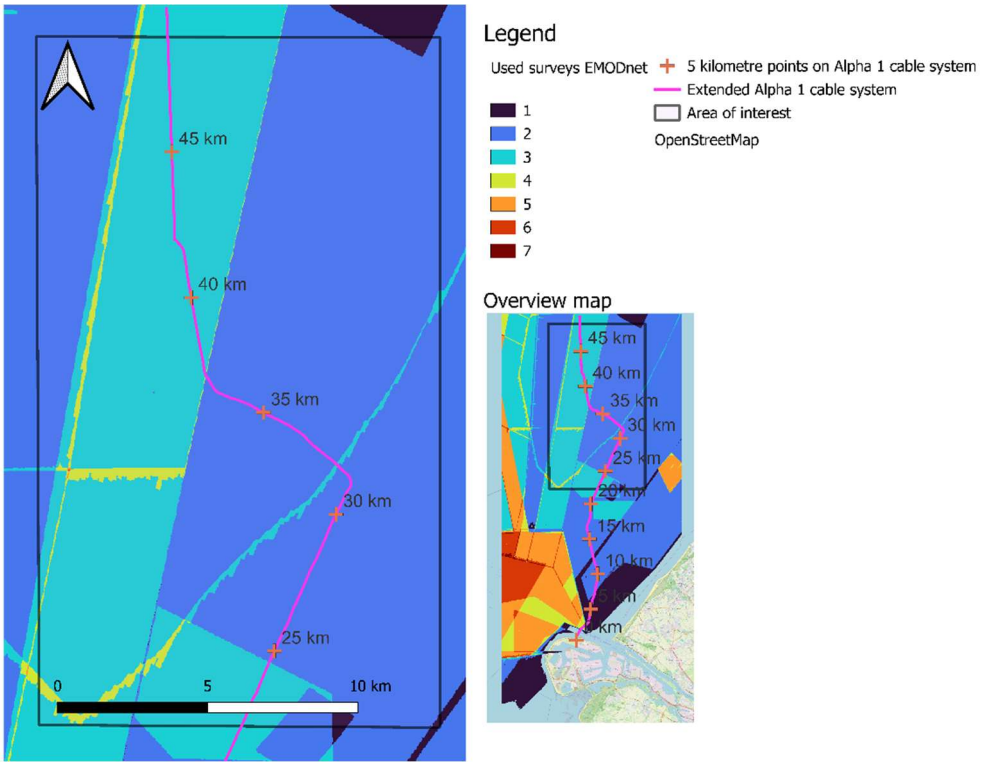

Figure B.2: Number of surveys considered to be useful in the EMODnet repository

Note that for the NLHO repository, the 2022 survey are included whereas the 1999 was not obtained.

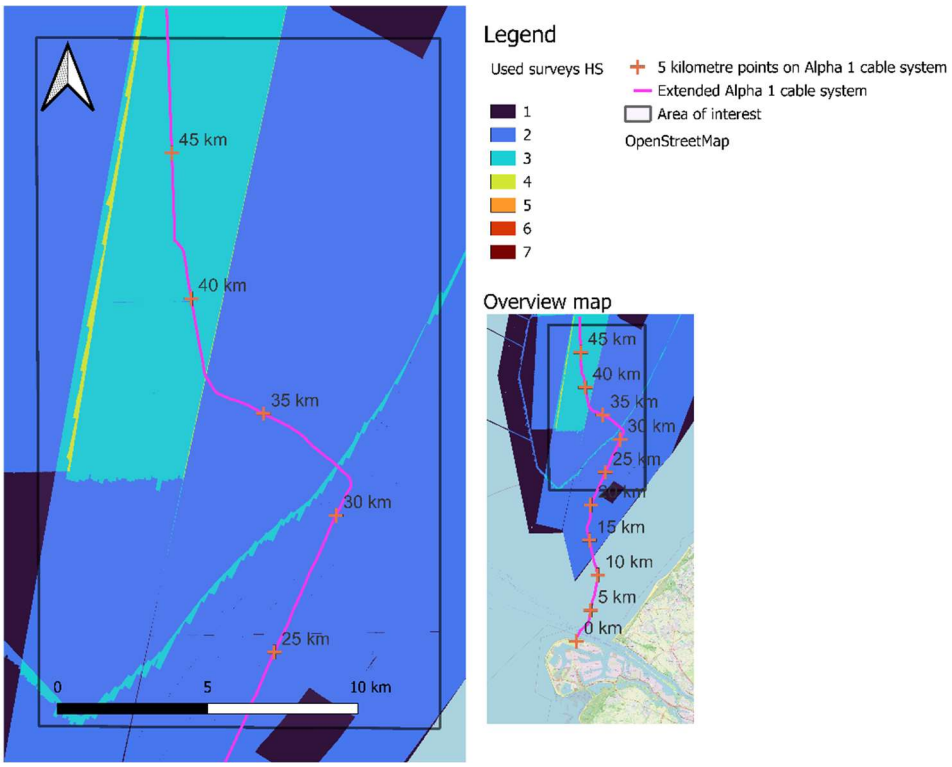

Figure B.3: Number of surveys considered to be useful in the NLHO repository

C. SURVEY DATA IN DELTARES OPENDAP REPOSITORY

In Figure C.1, the spread in survey data before 1999 can be seen, this data is already interpolated by Deltares with Inverse Distance Weight interpolation with a 100 m search radius. The data in the area of interest consists often out lines in sailing direction of the vessel.

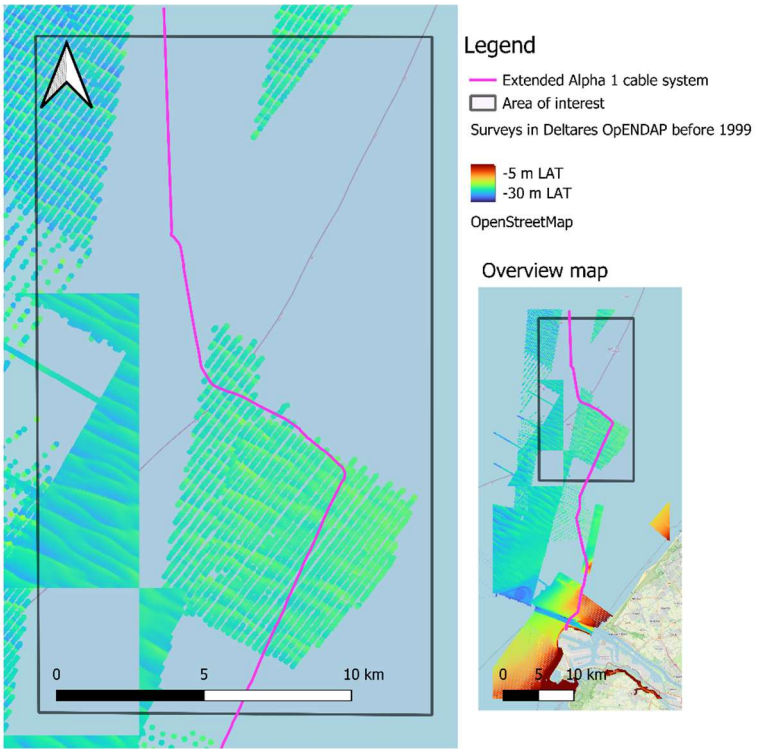

Figure C.1: MRSL of datasets before 1999 in Deltares OPeNDAP repository in area of interest

In Figure C.2, the surveys of 2011 and 2012 in the Deltares OPeNDAP repository can be seen. The survey of 2011 slightly overlaps Section 2 of the Alpha 1 extended cable route.

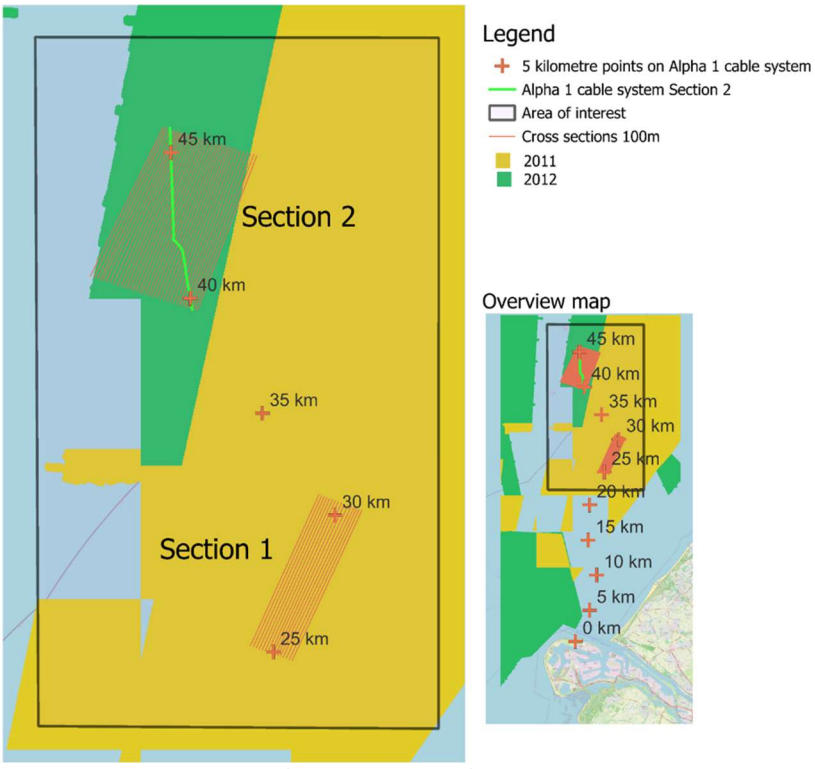

Figure C.2: 2011 and 2012 survey in Deltares OPeNDAP repository

D. SURVEY DATA IN EMODNET REPOSITORY

D.1. Processing survey data from EMODnet repository

Firstly, the surveys obtained via NLHO are reprojected from a gradient coordinate system to the same coordinate system as Deltares OPeNDAP (EPSG:25831 - ETRS89 / UTM zone 31N). Secondly, to account for the difference in grid resolution (EMODnet is on a 20 m resolution grid), the surveys have been resampled using QGIS 3.36 to a 25x25m raster grid by applying an averaging method, taking into account the overlapping areas of the original and new grid.

E. SURVEY DATA FROM TENNET

In the following figure, the survey executed post the cable installation on the Alpha 1 and Alpha 2 cable is shown (November 2021). The trench and thus location of the cables are clearly visible and approximately 20 m wide. The width of the survey campaign is approximately 100 m per cable.

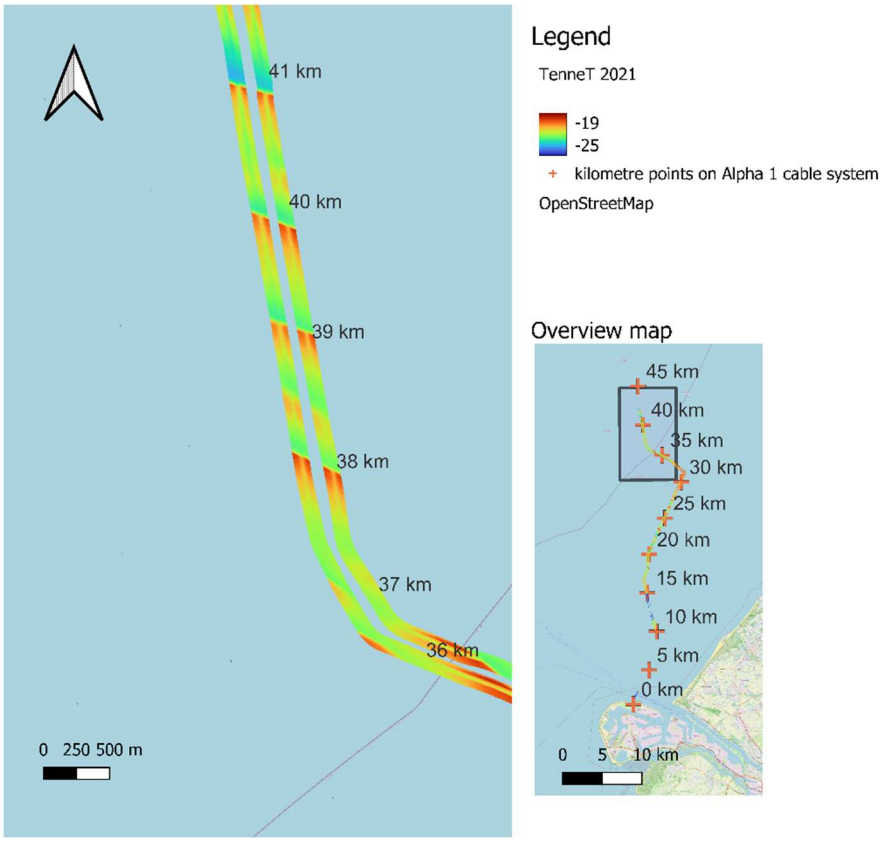

Figure E.1: Post installation of Alpha 1 and 2 cable survey of TenneT

F. DIFFERENCE BETWEEN REPOSITORIES

There are differences between the three repositories that were used. As mentioned in Section 3.1, the assumption has been made that these differences are constant. To compare the different repositories, they need to be corrected. Firstly, the average depth per repository has been looked at. Since the repositories include different survey campaigns and some differ in coverage, the average depth per survey cannot be used for correction. Therefore, Sections 1 and 2 on the extended cable have been used. Two rectangular polygons had been drawn in Figure F.1 around the 5.5km cross-sections that overlay all different surveys, and the areas are in the direction of the migration direction of sand waves.

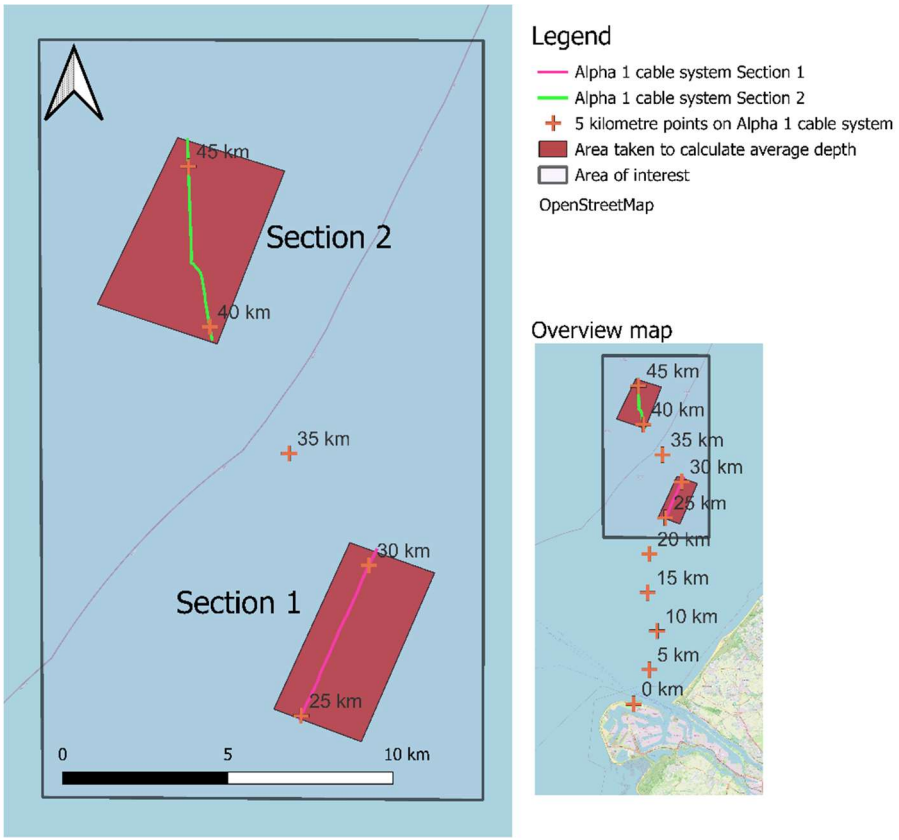

Figure F.1: Area taken to calculate average depth per survey

The average depth for the surveys presented in multiple repositories was calculated and is displayed in the following table. The difference is not consistent between surveys; for example, the EMODnet 2007 survey is 14 cm above the OPeNDAP 2007 survey, whereas the EMODnet 2016 survey is 11 cm below the OPeNDAP 2016 survey.

Table F.1: Average depth for different surveys for two areas

	Average depth Section 1 (m LAT)		**Average depth Section 2 (m LAT)**		
Year	2011	2022	2007	2012	2016
OPeNDAP	-20.68	-	-22.00	-22.02	-22.05
EMODnet	-20.79	-20.40	-21.85	-21.96	-22.10
NLHO	-20.71	-20.80	-22.00	-22.08	-22.26
	The absolute difference between repository and OPeNDAP (cm)				
EMODnet	-11.45	-	14.31	6.89	-5.28
NLHO	-3.88	-	-0.06	-5.41	-21.00

Subtracting these absolute differences of the surveys in the EMODnet and NLHO repository can be seen as levelling the surveys to the same reference level. The result can be seen in the following figure.

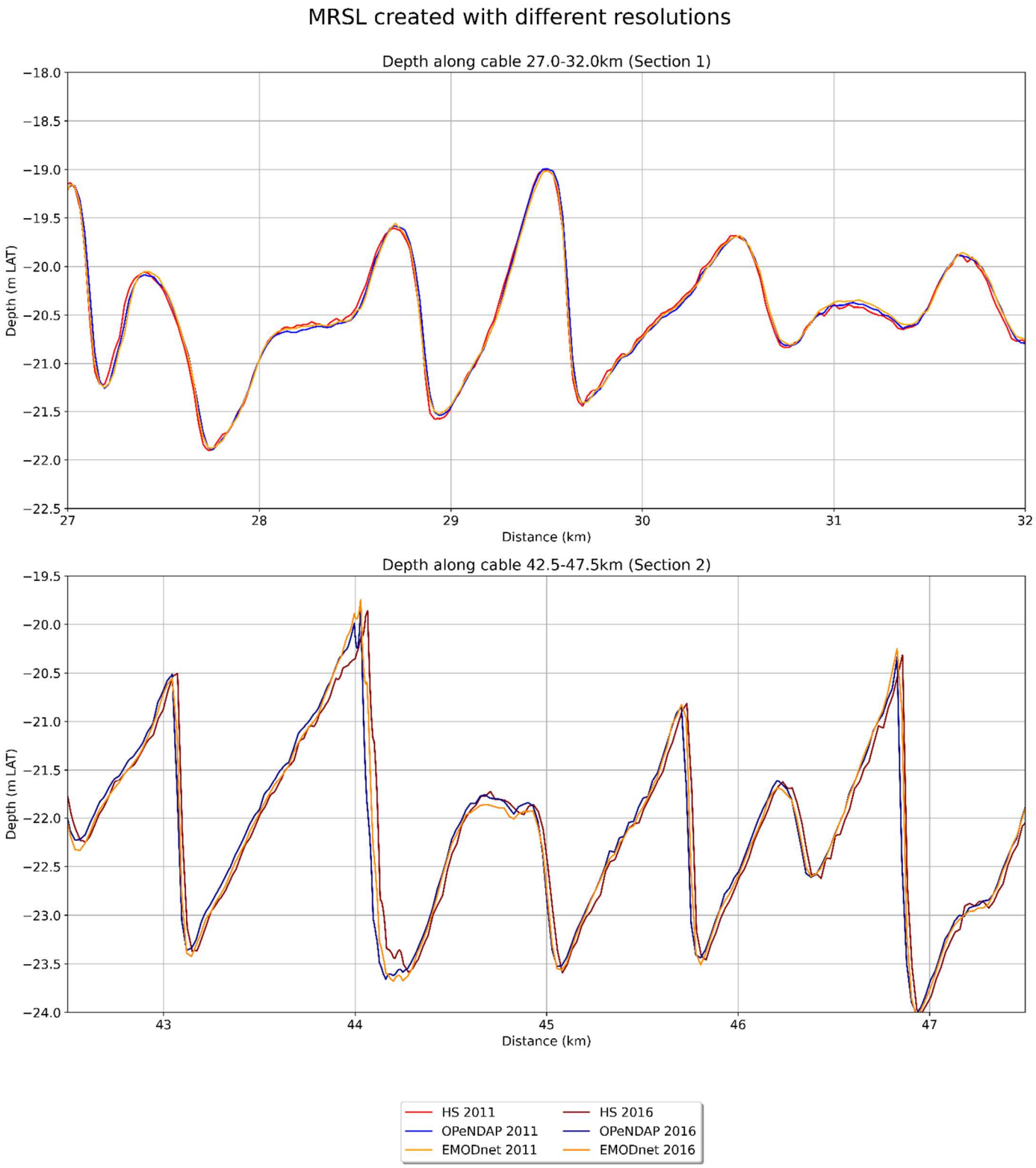

Figure F.2: MRSL from the different repositories corrected by mean depth, depth profile for whole Cable Section 1 and 2

In Cable Section 2, it looks like there is a spatial shift between the different surveys. The lag has been estimated by calculating the spatial cross-correlation for different spatial shifts. The lag corresponding with the highest cross-correlation is the observed lag between the OPeNDAP repository and the other repositories. For the surveys as shown in Figure F.2, the lag can be seen in the following table.

Table F.2: Lag observed between OPeNDAP and other repositories

Repository	Lag 2011 (in m) for Section 1	Lag in 2016 (in m) for Section 2
NLHO	-2	-29
EMODnet	-1	-13

Correcting the 2016 surveys for the lag results in the following depth profile.

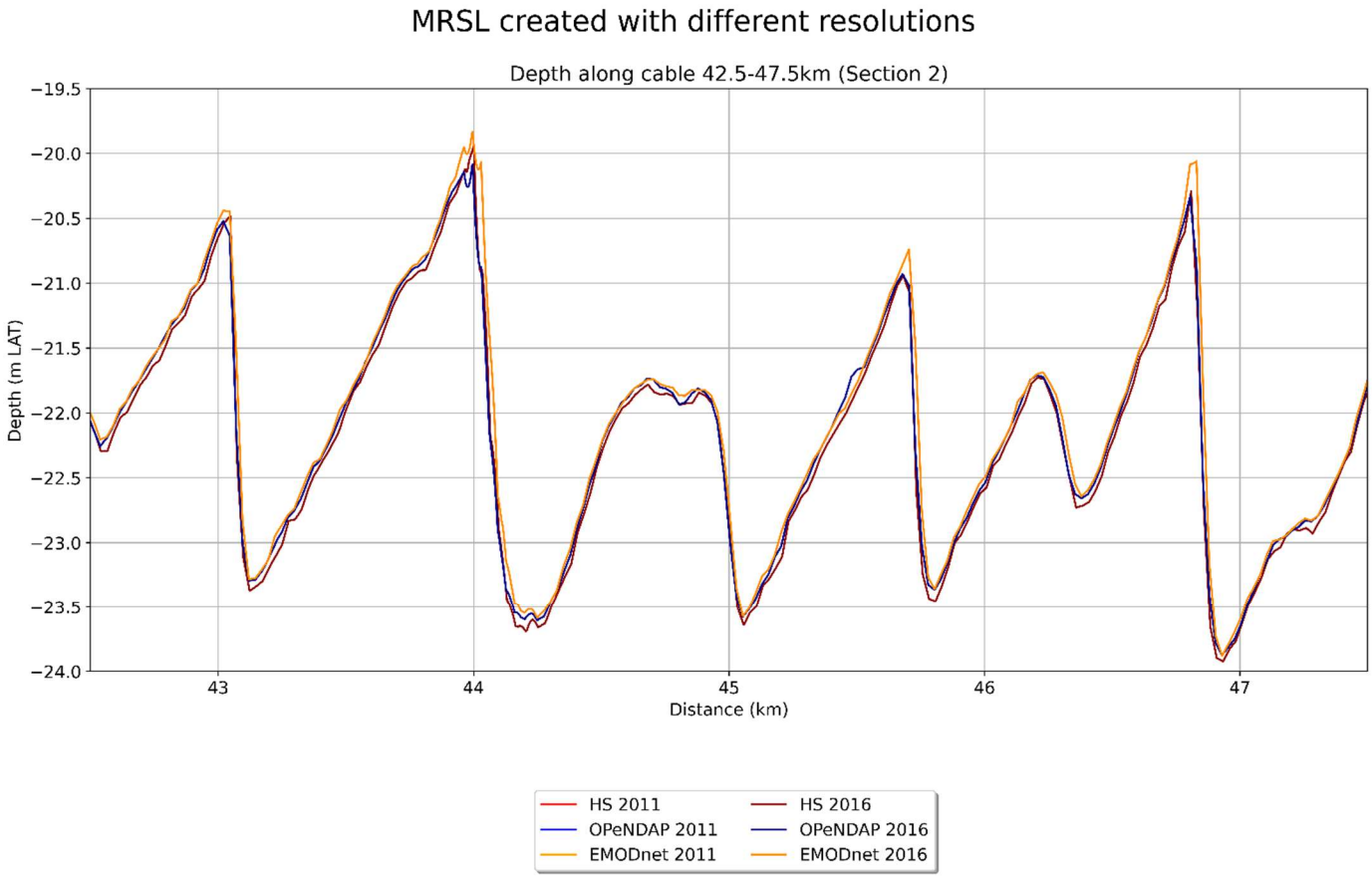

Figure F.3: MRSL from the different repositories corrected by mean depth, depth profile for whole Cable Section 2

G. RESULTS RESEARCH QUESTION 1.

G.1. Percentile

In Figure G.1, the NMRLs projected on the Cable Route of all tested percentiles can be seen.

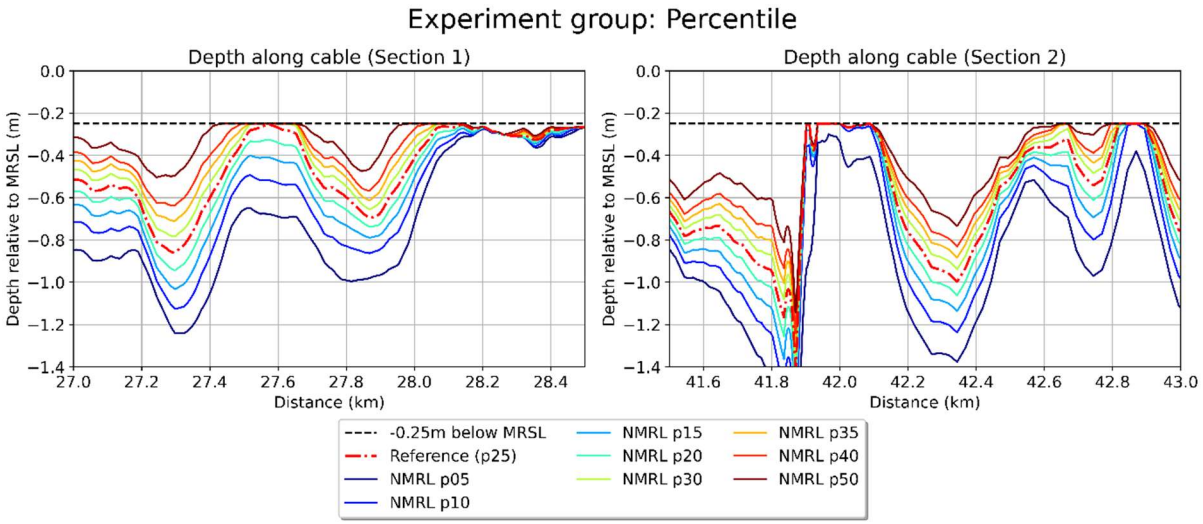

Figure G.1: NMRL on extended Alpha 1 cable system relative to the MRSL for different percentiles

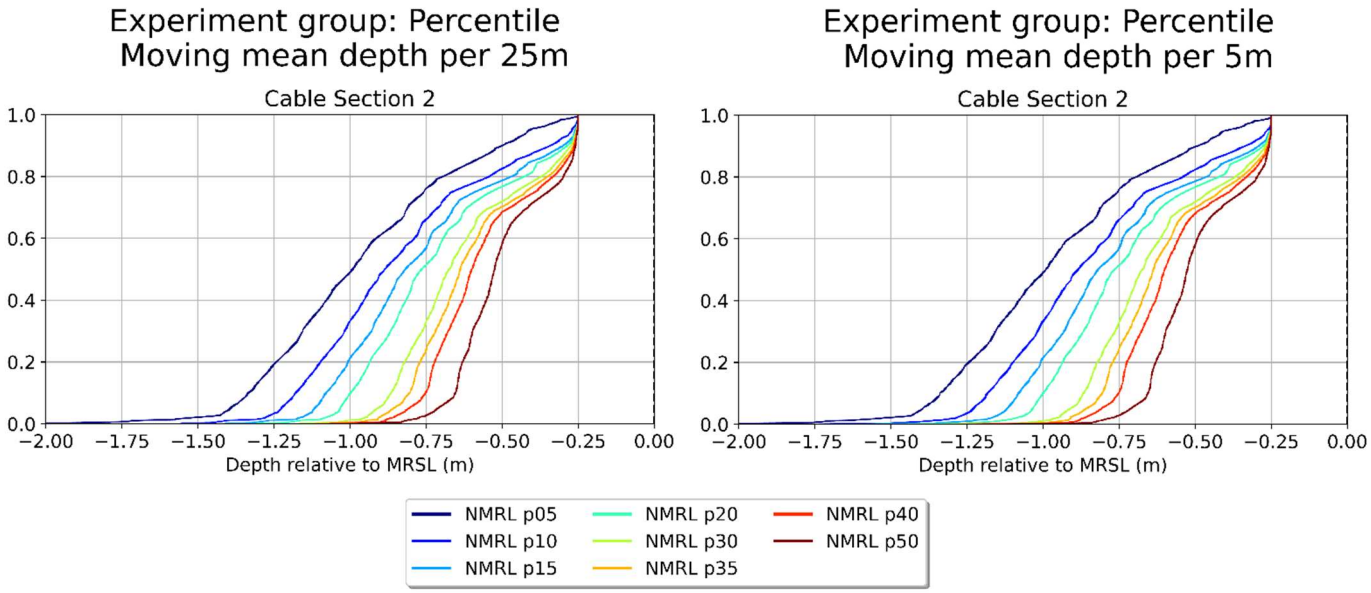

Figure G.2: Moving mean depth of the NMRL for a 25m (left) and 5m (right) cable length relative to the MRSL for the full sections (5km). The NMRL is shown for various Experiment Cases with different percentiles

Table G.1 shows the difference between the median depth per Experiment Case relative to the MRSL in Cable Section 2 per 5 and 25m cable. The difference (5m mean minus 25m mean) in medians is below 0.3% for all cases compared to the median. Note that the medians are provided with unrealistic accuracy; they should be in cm accuracy. However, no difference would then be seen between the 5 and 25m. The local difference between the 5 and 25m mean was determined by subtracting the 5m from the 25m mean. Taking the 99th percentile of the absolute difference results in the local maximum absolute difference. The highest difference is seen in the p05 case, with 6 cm. Deeper located NMRLs relative to the MRSL show a higher maximum local difference between the 5m and 25m mean averaged NMRL. Further investigation showed that the largest deviations are seen at the lee sides of the sand waves right before the throughs.

Table G.1: Median depth relative to the Reference Case in Cable Section 2, per 25m or 5m cable and the difference between these.

Case	Median 25m mean rel. to MRSL in Cable Section 2 (in cm)	Median 5m mean rel. to MRSL in Cable Section 2 (in cm)	Difference (5m mean-25m mean) (in cm)	Difference (5m mean-25m mean) (%)	Maximum difference of 99th percentile (in cm)
p05	-98.99	-99.00	-0.00	0.00	6
p10	-88.39	-88.46	-0.06	0.07	6
p15	-81.74	-81.87	-0.13	0.16	5
p20	-76.27	-76.46	-0.19	0.25	5
p30	-67.29	-67.26	0.02	-0.03	4
p35	-63.67	-63.63	0.04	-0.07	4
p40	-59.82	-59.96	-0.14	0.23	4
p50	-52.40	-52.46	-0.06	0.11	4

G.2. Distance between Cross-Sections

In the following figure, the PDF estimation created from the observations can be seen. This is an overall PDF per cross-section, thus all observations found per cable section were used to establish these PDFs. The PDFs from the experiment where the distance between the cross-section is 400 m differs the most from the other PDFs. Most significant is the bump visible in the growth rate of the trough at -0.03 m/year for the 400 m distance.

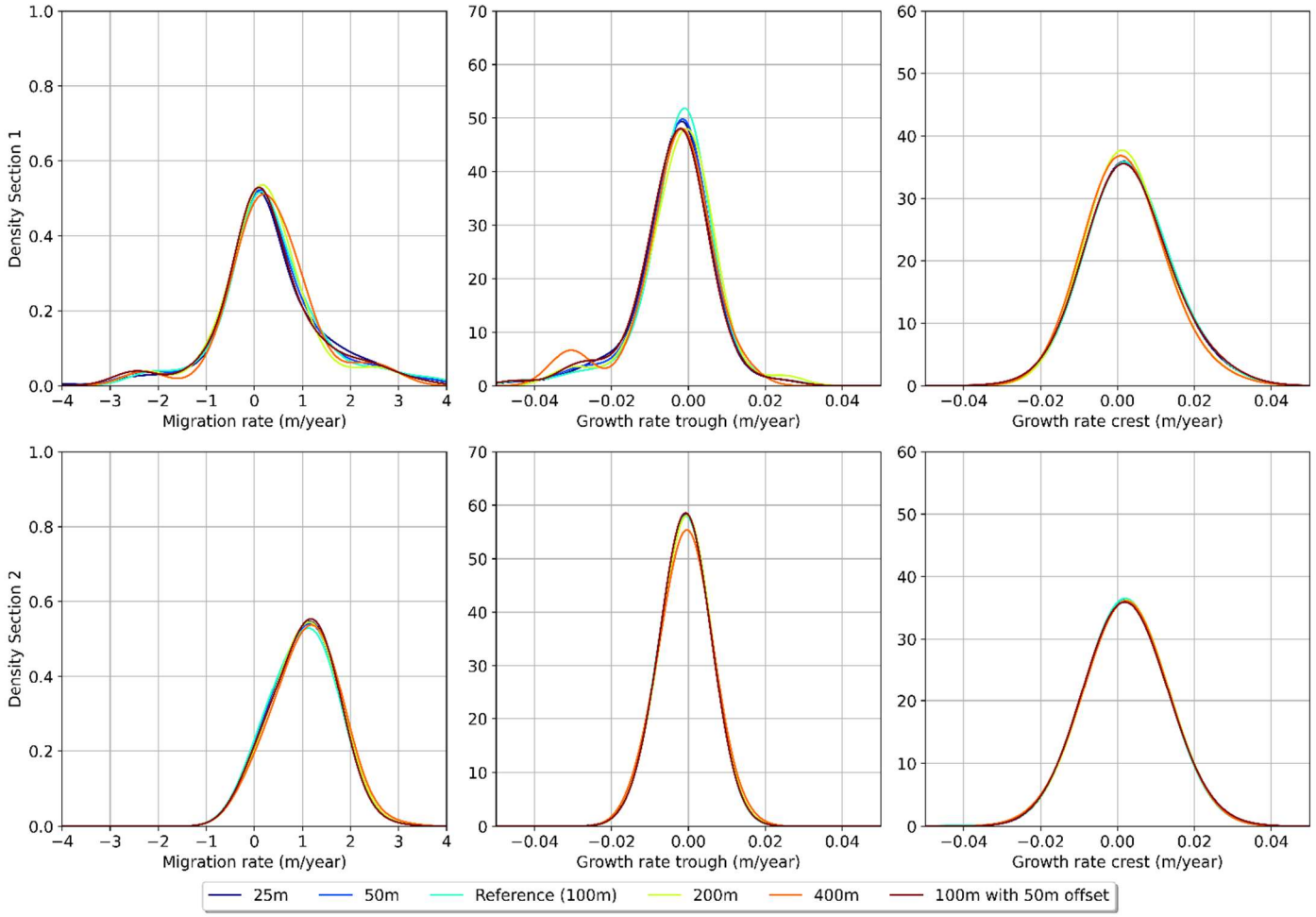

Figure G.3: Average PDF estimation per cable section.

G.3. Including intermediate data sets

The different overall PDF estimations per Cable Section are displayed for the migration rate and the growth rates in Figure G.4. With overall PDF, the PDF created on only the unique observations is meant. This means that the PDFs, as displayed below, are not used for creating the NMRL as the PDFs used for the NMRL are created per individual cross-section.

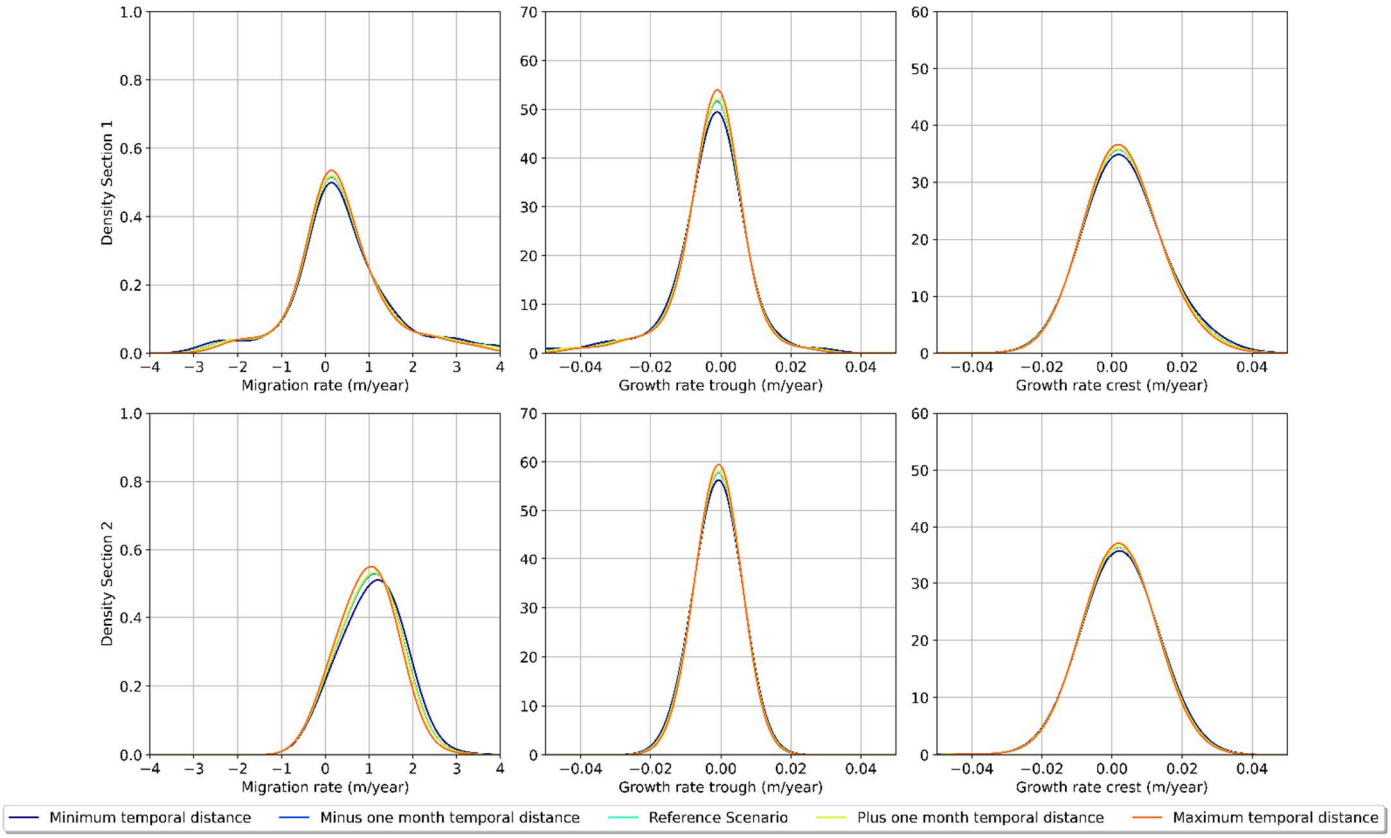

Figure G.4: PDF estimations for the migration and growth rates for different temporal distances (period between surveys) per Cable Section

Form the PDF estimation of the migration rate as shown in Figure G.4, the Interquartile Range (IQR) was determined. For both Cable Sections, the IQR and percentual difference with the Reference Case are displayed in the following table. An increasement in period between surveys leads to a decrease in IQR of up to 5%. Decreasing the period between surveys leads, overall, to an increase in IQR of up to 4%. For Cable Section 1, the difference for minus one month case is negative where an increasement was expected.

Table G.2: Median depth relative to the Reference Case in Cable Section 2, per 25m or 5m cable and the difference between these.

Case	Interquartile range of migration rate PDF in Figure G.4 on Cable Section 1 (m/year)	Percentual difference with Reference Case	Interquartile range of migration rate PDF in Figure G.4 on Cable Section 2 (m/year)	Percentual difference with Reference Case
Minimum period	1.17	3.3%	1.06	4.2%
Minus one month period	1.12	-0.5%	1.02	0.3%
Reference Case	1.13	-	1.02	-
Plus one month period	1.12	-1.2%	1.02	-0.3%
Maximum period	1.07	-4.9%	0.98	-3.6%

The NMRL per case relative to the Reference Case is displayed in Figure G.5 for the two Cable Sections. The difference stays within plus 5 centimetres and minus 3 cm relative to the NMRL of the Reference Case.

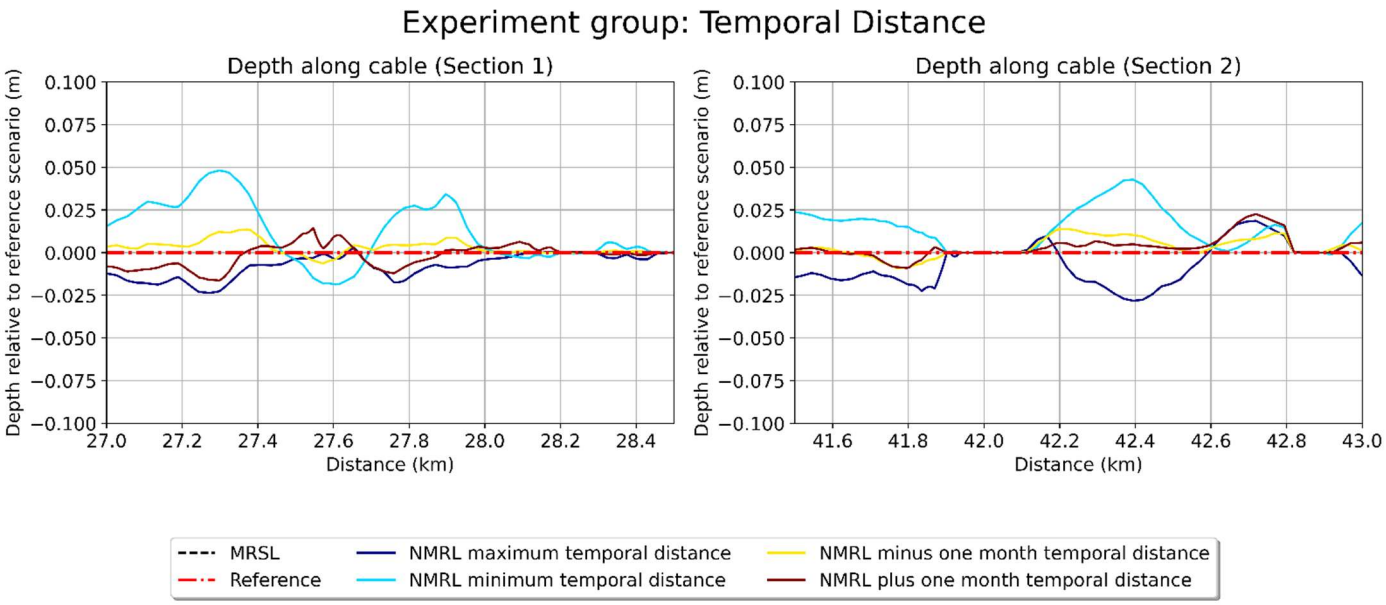

Figure G.5: NMRLs on extended Alpha 1 cable system relative to the NMRL of the Reference Case for different temporal distances (period between surveys).

H. RESULTS RQ2. INPUT

H.1. Repositories

For the NLHO repository, two extra (not real) Cable Sections have been introduced since more areas were available outside the area of interest. For the other two sections, the NMRL has been created and the PDFs have been established.

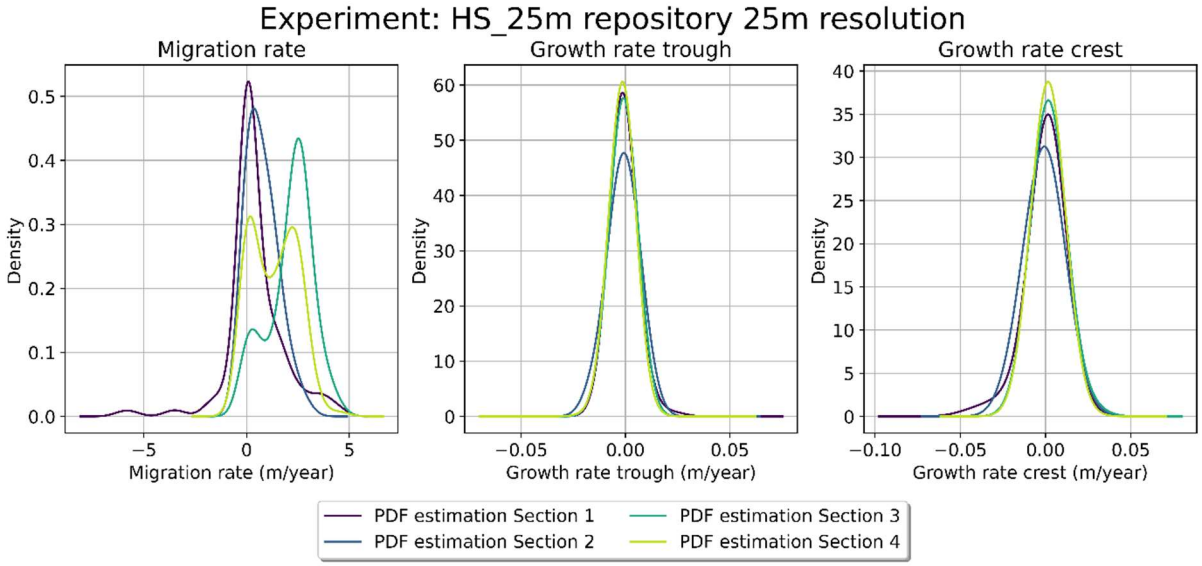

H.1: PDF estimations for migration and growth rates on the imaginary cable route for NLHO repository.

UNIVERSITY OF TWENTE
Drienerlolaan 5
7522 NB Enschede

P.O. Box 217
7500 AE Enschede

P +31 (0)53 489 9111

info@utwente.nl
www.utwente.nl